Linking Structure and Function for the DNA Repair Complex Mre11-Rad50-Nbs1

De samenhang tussen de structuur en functie van het Mre11-Rad50-Nbs1 DNA reparatie complex

Eri Kinoshita

ISBN: 978-94-6182-386-1

The work presented in this thesis was performed at the department of Cell Biology & Genetics at the Erasmus Medical Center (Erasmus MC) in Rotterdam.

Cover design / layout: Off Page, Amsterdam

Printing: Off Page, Amsterdam

Linking Structure and Function for the DNA Repair Complex Mre11-Rad50-Nbs1

De samenhang tussen de structuur en functie van het Mre11-Rad50-Nbs1 DNA reparatie complex

Proefschrift

ter verkrijging van de graad van doctor aan de Erasmus Universiteit Rotterdam op gezag van de rector magnificus

Prof.dr. H.A.P. Pols

en volgens besluit van het College voor Promoties.

De openbare verdediging zal plaatsvinden op

Dinsdag 28 Januari 2014 om 13:30 uur

Eri Kinoshita
geboren te Kawasaki, Japan

PROMOTIECOMMISIE

Promotoren:	Prof.dr. C. Wyman
	Prof.dr. R. Kanaar
Overige leden:	Dr.ir. S.J.T. van Noort
	Prof.dr. C.P. Verrijzer
	Dr. W. Vermeulen

TABLE OF CONTENTS

AIM AND SCOPE OF THE THESIS

Deoxyribonucleic acid (DNA) is, simply put, the molecule used to encode all the genetic information required by the living organism to maintain its life functions. Therefore, its stability and integrity is of absolute importance. DNA is actually not a “full-protected” static substance – it is a chemical entity composed of nucleotides attached to a sugar-phosphate backbone. Such a structure can be damaged by environmental factors such as irradiation, chemicals, and ultraviolet rays (UV). The DNA can also undergo oxidative damage by free radicals, which are byproducts of metabolism. One serious result of these chemical changes in DNA can be double-strand breaks (DSBs) in the chromosome. Be it environmental or internal, DNA damage must be repaired as the accumulation of unrepaired DNA can lead to aging and disease. Organisms have developed various processes to detect and repair DNA breaks. There are two main double-strand break (DSB) repair pathways: homologous recombination (HR) and non-homologous end joining (NHEJ). One protein complex, the Mre11-Rad50-Nbs1 (MRN), has diverse roles in both HR and NHEJ. Each protein component of this versatile complex contributes to the overall structure and functions.

The aim of this thesis is understand how the organization of the MRN components in the complex contribute to and control its known functions such as DNA binding and DNA tethering. MRN is a versatile protein complex that has been referred to as the “primary damage sensor” due to its early appearance at sites of DSBs. Changes in the structure of the complex upon DNA binding are likely responsible for its role in DNA tethering and damage signaling. The individual components have some remarkable structural features. The Rad50 component has a long coiled-coil region which has been well characterized in scanning force microscopy (SFM) studies. These studies have shown that the coiled coils can take part in both intra- and intercomplex associations. Inter-complex associations allow the protein complex to tether DNA chains as far as 120 nM apart. Interestingly, while there have been various studies using MR and MRN complexes as well as Mre11 alone, very little is known about the biochemical activities of Rad50 by itself. The various studies on Mre11 have indicated this protein can bind DNA and that it has nuclease acitivty. This observation has led to the assumption that Mre11 is the central component of the MR or MRN complex responsible for DNA binding and regulating DNA tethering. However, a study of purified yeast Rad50 protein indicated that this protein can also bind DNA. As for the remaining protein complex component, Nbs1 has no known DNA binding activities. However, the successful purification of different specific protein complexes such as MR, MRN, MN and RN suggest that Nbs1 has multiple binding sites to Mre11 and Rad50, which contribute to different stoichiometries. It is also clear that the arrangements of the protein components within the complex can vary and

that this affects function. The clearest example is the binding of ATP to the two Rad50 ATPase domains. ATP binding causes the Rad50 head to become a compact homodimer and the reorientation with respect to Mre11 makes the Mre11 nuclease site inaccessible to DNA. Evidence also suggests that DNA binding, one of the most basic functions of this protein complex, can be affected by disrupting specific protein complex interfaces involved with Mre11 dimerization. These observations suggest many possibilities for structural changes regulating function and emphasize that there are still unanswered questions regarding this versatile complex. Elucidating the connection between the protein complex structure and function will reveal details of how this protein machinery changes to preforms multiple roles early in DNA break repair.

Does human RAD50 bind to DNA? If so, is it structurally similar to the MR and MRN complex? Is Mre11 necessary for DNA binding and tethering? Does Nbs1 contribute to differences in protein complex structure and function? How do the specific protein complex interfaces change in the different complex structures and/or function? The five chapters of this thesis aim to answer such questions. Chapter 1 discusses the homologous recombination (HR) and non-homologous end joining (NHEJ) pathway and reviews what is known about the role of Mre11, Rad50 and Nbs1. The chapter further explains the conformational changes induced by ATP binding as well as some standing questions regarding the dynamics and stoichiometry of this protein complex. The thesis goes on to analyze the biochemical activites of human Rad50 alone (Chapter 2) and provides evidence that Mre11 is not necessary to maintain DNA binding and tethering activities (Chapter 3). However, it becomes clear that specific interactions within the complex affect these activities (Chapter 4) and (before that) ATP binding contributes to increased DNA binding which may promote additional DNA tethering activities (Chapter 5).

CHAPTER 1

RAD50, an SMC family member with multiple roles in DNA break repair: how does ATP affect function?

Eri Kinoshita[1], Eddy van der Linden[1],
Humberto Sanchez[1] and Claire Wyman[1, 2]

[1]Department of Cell Biology & Genetics, Cancer Genomics Center and [2]Department of Radiation Oncology, Erasmus MC, PO Box 2040, 3000 CA Rotterdam, The Netherlands

Modified and updated from:
Chromosome Research 2009 *17(2)*, 277-288.

ABSTRACT

The protein complex including Mre11, Rad50, and Nbs1 (MRN) functions in DNA double-strand break repair to recognize and process DNA ends as well as signal for cell cycle arrest. Amino acid sequence similarity and overall architecture make Rad50 a member of the structural maintenance of chromosome (SMC) protein family. Like SMC proteins, Rad50 function depends on ATP binding and hydrolysis. Current evidence indicates that ATP binding and hydrolysis cause architectural rearrangements in eukaryotic Mre11-Rad50 (MR) complexes that may have important implications for their functions. In this review we update what is currently known about the roles of each component in the protein complex, the ATP-dependent activities as well as recent implications of structure revealed by SAXS and X-ray crystallography.

INTRODUCTION

The structural maintenance of chromosome (SMC) proteins, as their name implies, are involved in organizing DNA to assure proper function of chromosomes. SMC family proteins also have important roles organizing DNA for repair. DNA damage, such as double-strand breaks (DSBs), can disrupt chromosome architecture. DNA damage repair, especially repair of DSBs, is an essential element of maintaining or re-establishing proper DNA arrangement in chromosomes. The SMC family member Rad50, in complex with Mre11 and Nbs1, is a required component of DSB repair. Here we introduce the DNA repair functions of Rad50-containing complexes. ATP binding and hydrolysis are important for all of these protein complexes. We review what is known about the molecular architectural effects and functional significance of the ATPase activity for these proteins. We also update the MR architecture corresponding to the ATP-free and ATP-bound state considering recent SAXS and X-ray crystallography studies.

Double-strand break repair

DNA double-strand breaks (DSBs) are one of the most damaging occurrences for an organism. All organisms, therefore, have evolved intricate pathways to efficiently and systematically repair these breaks. Unrepaired DSBs can cause cell-cycle checkpoint arrest, ultimately leading to cell death. Improper repair can cause genome rearrangements, which in multicellular organisms are a common precursor to cancer. Eukaryotes have two main DSB DNA repair mechanisms: non-homologous end joining and homologous recombination (Figure 1). Non-homologous end joining rejoins DNA breaks with little or no homology, often resulting in deletions and insertions in the genome. Some breaks are directly ligated or joined after minimal processing. These sequences are aligned and the remaining DNA is removed via a nuclease or filled in by a DNA polymerase and then re-ligated (Weterings & van Gent, 2004). Homologous recombination, in contrast, is an error-free, 'accurate' genetic recombination pathway that predominates in the S and G_2 phases as it uses the undamaged homologous duplex as a template for repair synthesis (Wyman et al., 2004).

Homologous recombination requires DNA processing by architectural, structural and enzymatic factors. This pathway begins with the recognition of the DSB followed by 5′ to 3′ nuclease processing which yields 3′ single-stranded DNA (ssDNA). This 3′-ssDNA is covered by RPA (replication protein A), which is subsequently displaced by the DNA strand exchange protein Rad51. Assembly of Rad51 onto properly processed ssDNA is aided by recombination mediators such as Rad54, Rad54B, Rad50/Mre11, the Rad51 paralogues (XRCC2, XRCC3, Rad51B, Rad51C, and Rad51D), and BRCA2 (Symington et al., 2002; Wyman et al., 2004; Wyman & Kanaar, 2006). Rad51 forms a nucleoprotein filament on ssDNA that invades homologous DNA segments for eventual

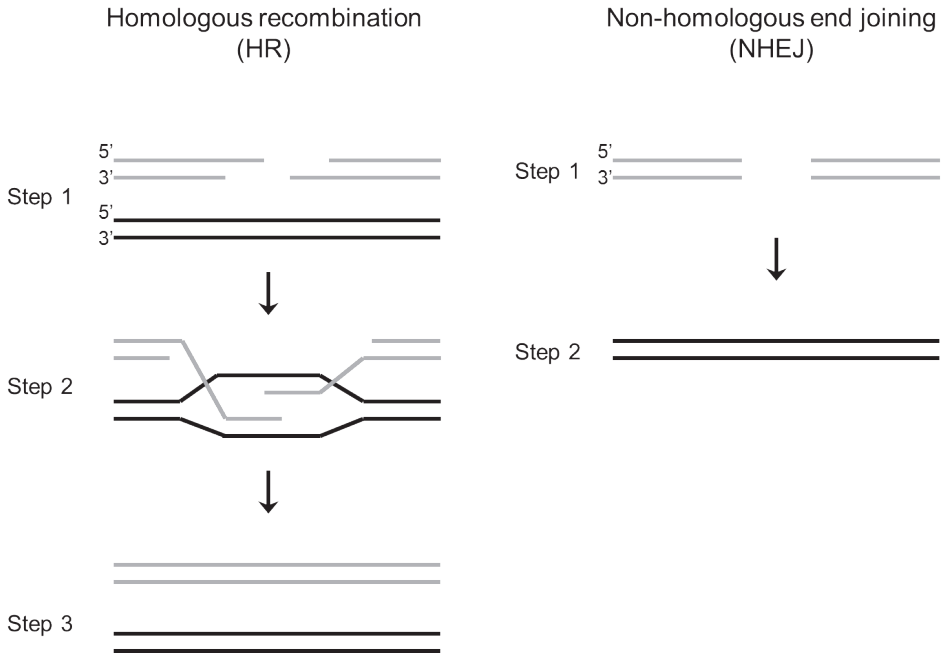

Figure 1. Schematic diagram of the steps in homologous recombination (HR) and non-homologous end joining (NHEJ). A double-strand break (DSB) containing DNA molecule is shown in light gray and the intact DNA is shown in black. (A) Homologous recombination of a double-strand break (DSB) is an error-free DNA repair pathway that uses an undamaged homologous duplex as a template for repair synthesis. The DNA ends at a DSB are processed to yield 3'- single-stranded overhangs (Step 1) which invade a homologous template DNA molecule (black) by strand displacement, resulting in the the formation of D-loops (Step 2). The 3'- ends are extended and subsequently undergo strand resolution and ligation (Step 3). (B) Non-homologous end joining (NHEJ) is a DNA repair pathway that directly joins a pair of DNA ends. The DSB ends are put through no or minimal processing (Step 1) and ligated (Step 2).

polymerase-mediated extension (West, 2003). The process is then completed with strand resolution and ligation. DSB repair pathways are closely linked to cell-cycle checkpoint signaling via the ATM checkpoint kinase (D'Amours & Jackson, 2002; Assenmacher & Hopfner, 2004). ATM activation causes cell-cycle arrest until the DNA breaks are repaired or cells undergo apoptosis (Khanna & Jackson, 2001).

Multiple roles of the MRN complex in DSB repair

The MRN complex is involved at several distinct steps in DSB repair including break recognition, DNA end processing, and signaling for cell cycle arrest. The MRN complex

is a primary damage sensor involved in the early steps of DSB repair in both human and yeast cells (D'Amours & Jackson, 2002). The importance of Rad50, Mre11, and Nbs1 genes in mammals is indicated by the resulting cell non-viability or embryonic lethality when any of these three genes is disrupted (Xiao & Weaver, 1997; Luo et al., 1999; Zhu et al., 2001). In humans, mutations in Nbs1 cause Nijmegen breakage syndrome (NBS). NBS patients show radiation sensitivity, immune system deficiency, and a high rate of malignancy (Shiloh et al., 1997). NBS patients show phenotypes similar to ataxia-telangiectasia (A-T), a related radiation sensitivity disorder. A-T is caused by mutations in the A-T mutated gene (ATM), which encodes a large protein kinase that initiates DNA damage signalling in response to DSBs. A connection between MRN and ATM arose with the identification of two families with A-T-like disorder (ATLD), clinically identical to A-T but caused by mutations in Mre11 (Stewart et al., 1999).

Structure and function of MRN components

All DSB repair functions of MRN involve interactions with DNA that require at least Rad50 and Mre11. Homologues of Rad50 and Mre11 exist in archaea, fission and budding yeasts, as well as higher metazoans (Hopfner et al., 2000a; D'Amours & Jackson, 2002). The Mre11-Rad50 (MR) complex has essential functions early in DSB repair, based both on time of accumulation at breaks in cells and its biochemical activities (Assenmacher & Hopfner, 2004; Lisby et al., 2004). The associated Nbs1 (also known as nibrin) or Xrs2 proteins (MRN or MRX complexes), in mammalian and yeast cells, respectively, link the Mre11-Rad50 complex to cell-cycle checkpoint activation (Assenmacher & Hopfner, 2004).

Rad50

Rad50 is approximately 150 kDa and resembles the SMC proteins involved in chromosome cohesion and chromatin condensation (Aravind et al., 1999; Strunnikov & Jessberger, 1999). SMC proteins all contain Walker A and B nucleotide (NTP)-binding motifs at their amino- and carboxy-terminal ends, respectively. These motifs are separated by long stretches of amino acids that form an extended coiled-coil structure. The Rad50 coiled coil folds back on itself to form the intramolecular association of the ATPase domains at one end and the "hook" or hinge domain at the other end of an elongated structure (Figure 2A). The conserved hook domain contains two invariant cysteines (CXXC), which coordinates a zinc ion to form inter-complex interactions (de Jager et al., 2001b; Hopfner et al., 2002). These structural elements and their architectural arrangement are exploited for various functions of Rad50 and related proteins.

The core Rad50 complex is a heterotetramer of Mre11 and Rad50 (M_2R_2) with two Mre11 and two Rad50 nucleotide binding domains (NBDs) which make the globular

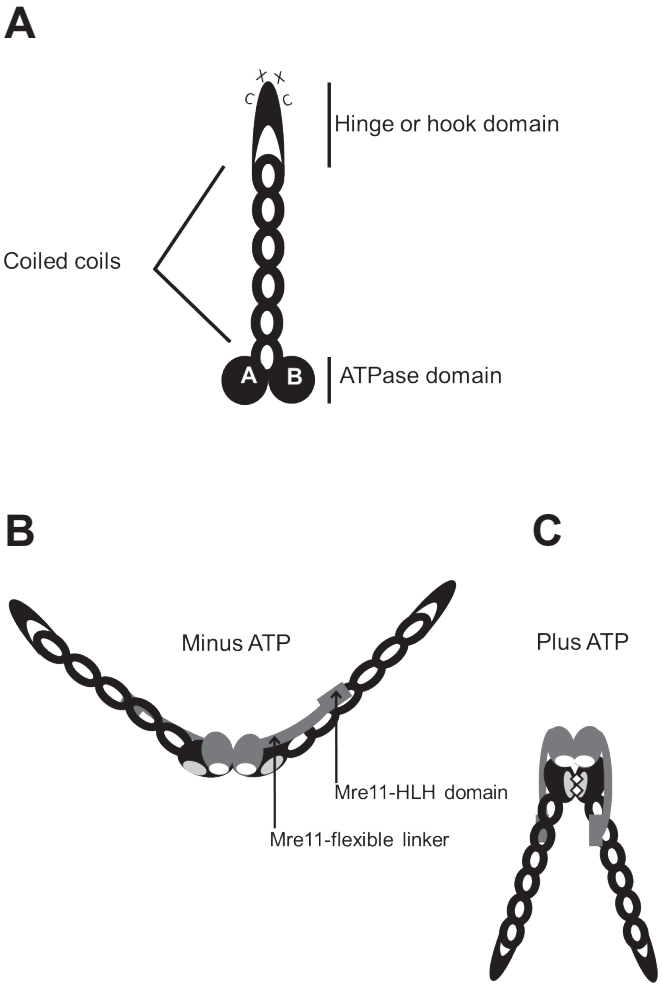

Figure 2. Schematic diagrams of MR. Rad50 is shown in black, the Rad50 ATP-binding sites are shown in light gray, Mre11 is shown in dark gray, the Mre11 DNA-binding domains are shown in white and ATP is shown as a diamond. (A) The arrangement of Rad50 in an intramolecular coiled coil results in juxtaposing the ATPase Walker A and Walker B domains from the N- and C-terminus to make the catalytic head domain. The coiled coil folds back on itself and extends outwards from the head domain. (B) MR without ATP has a conformation in which the Mre11 dimer is placed between the two Rad50 molecules with the Mre11 HLH domains bound to the base of the Rad50 coiled coils. The Rad50 ATP binding sites are facing outwards and away from each other in this ATP-free “open” complex. (C) MR with ATP bound in a dramatically different arrangement. The Mre11 dimer is now positioned adjacent to the Rad50 dimer with its flexible linker and HLH domains lying adjacent to the Rad50 coiled coils. The Rad50 coiled coils reorient to take a V shape as a result of the dimerization of the Rad50 ATP-binding sites, resulting in the ATP-bound “closed” complex.

"catalytic head" domain. The DNA-binding sites on the Mre11 dimer is close to the two Rad50 ATPase domains (de Jager et al., 2001b; Hopfner et al., 2001) with the flexible coiled coils extending from it (de Jager et al., 2001b; van Noort et al., 2003; Moreno-Herrero et al., 2005) (Figure 2B). The coiled coils are important for biological function as mutant complexes with shortened or truncated coiled coils showed defects in both homologous recombination and NHEJ (Hohl et al., 2011). The importance of the hook domain was demonstrated by a hook mutation that disrupted the interactions between Mre11 and Rad50 and increased radiation sensitivity (Hopfner et al., 2002). Mutants that have the hook domain removed *in vivo* after the expression of TEV protease showed defects in homologous recombination and NHEJ (Hohl et al., 2011). These results indicate that the coiled coils and the hook domains are important for biological functions and are involved in conformational "cross-talk" between the hook, coiled coils and the Rad50 globular domain, which regulates function.

The Rad50 coiled coils can be joined via intra- and inter- complex associations (de Jager et al., 2001b; Hopfner et al., 2002; Moreno-Herrero et al., 2005; van Noort et al., 2003). Intracomplex associations presumably help keep the components (M_2R_2) together and would also limit the arrangement of Mre11 and Rad50 heads. One M_2R_2 DNA binding head can potentially connect short-range DNA ends while the zinc-dependent octameric $(M_2R_2)_2$ interactions can tether DNA chains up to 120 nM apart (Hopfner et al., 2002; Moreno-Herrero et al., 2005). DNA is an allosteric effector of the MRN complex and its binding causes the RAD50 coiled coils to assume a parallel conformation that favors the inter-complex (hook-hook) interactions which presumably promotes DNA tethering and organizing DNA for eventual repair (Moreno-Herrero et al., 2005).

Mre11

Mre11 is a 70 - 90 kDa protein with a phosphoesterase domain (Hopkins & Paull, 2008) at the N-terminus and two DNA-binding domains at the C-terminus (D'Amours & Jackson, 2002; Williams et al., 2008). Mre11 exists as a functional dimer with an elongated crescent shape. The Mre11 dimer interface consists of a hydrophobic 4-helix bundle that extends outwards into the capping domains (Figure 3A and 3B; Figure 3A is from Figure 3D in Williams et al., 2008). Mre11 binds ss-, ds- and forked DNAs (de Jager et al., 2001; Paull & Gellert, 1999; Wen et al., 2008) and has 3′→5′ dsDNA exonuclease and ssDNA and dsDNA endonuclease activities (Paull & Gellert, 1998; Paull & Gellert, 1999) and DNA end bridging activities (Williams et al., 2008). The exonuclease and hairpin opening activities of Mre11 are stimulated by Rad50 and ATP. Mre11 dimer is capable of manipulating the DNA into a specific shape dependent on the type of substrate (Williams et al., 2008). This suggests that blunt DNAs could be aligned while forked DNAs would

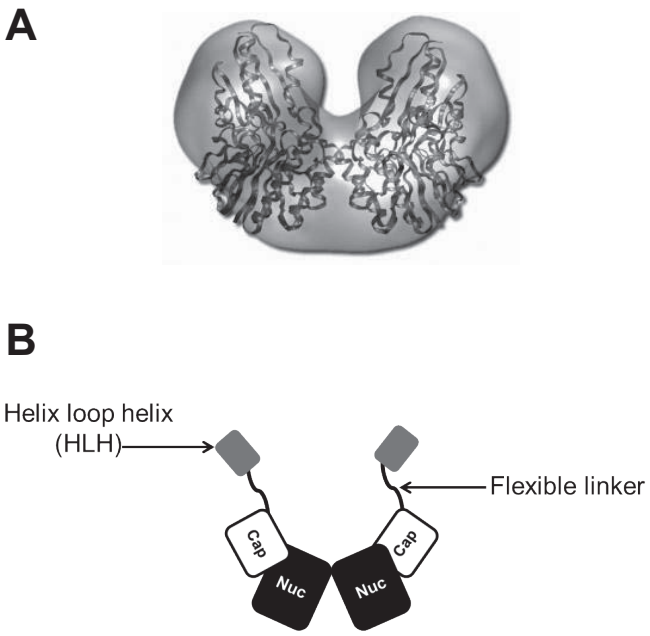

Figure 3. The structure of Mre11. Mre11 is a functional dimer with an elongated crescent shape with the hydrophobic 4-helix bundle extending outwards into the capping domains, flexible linker and HLH domains. (A) The *P. furiosus* Mre11 small-angle X-ray solution scattering (SAXS) structure (transparent gray envelope) is overlapped with the crystallographic structure (dark gray ribbons). From: Williams et al. (2008). Mre11 dimers coordinate DNA end bridging and nuclease processing in double-strand-break repair. (B) A schematic representation of the *P. furiosus* Mre11 dimer with the nuclease domains (Nuc), capping domains (Cap), flexible linker and helix-loop-helix (HLH) domains.

be positioned to undergo nucleolytic processing in one strand when bound to Mre11. The existence of two varying DNA-bound forms indicates that additional DNA-binding modes may exist, which may be the mechanistic basis of the versatile functions of Mre11 such as endo- and exonuclease activities as well as end-bridging activities.

Mre11 has four highly conserved nuclease domains in the N-terminus with the third domain (motif III) being necessary for the nuclease activity (Stracker et al., 2004). Mutating the invariant histidine (H125) in motif III of *S. cerevisiae* showed a relatively mild phenotype compared to Mre11 null strains that have severe radiation hypersensitivity, defective DSB repair and shortened telomeres (Bressan et al., 1998; Krogh et al., 2005; Lewis et al., 2004; Moreau et al., 1999). Despite the mild phenotypes observed in yeast, the nuclease activity of Mre11 is essential for maintaining genomic integrity in mammals (Buis et al., 2008). Conditional mouse cell lines lacking Mre11 or expressing only nuclease-deficient

Mre11 (H125S) had growth defects and chromosomal irregularities and showed sensitivity to DNA-damaging agents. The nuclease-deficient Mre11 in the MRN complex is not required for ATM activation but is required for repairing DSBs after ionizing radiation (IR) and stress during replication. In *S. pombe*, nuclease-deficient Mre11 (H134S) has a strong sensitivity to DNA-damaging agents (Williams et al., 2008). Interestingly, while the nuclease activities of Mre11 participate in both homologous recombination and NHEJ, the intrinsic 3′→5′ exonuclease activities of Mre11 is not the correct polarity to generate 3'- ssDNA overhangs required for homologous recombination. Both yeast and mammals have 5′→3′ exonucleases which can create 3′ overhangs (Farah et al., 2009; Hopkins & Paull, 2008), suggesting that MRN functions cooperatively with other proteins to generate the 3'- ssDNA overhangs required for homologous recombination (reviewed in Mimitou & Symington, 2009). In agreement with this implication, a recent study using purified human proteins have shown that MRN does indeed cooperate with other proteins to allow more efficient DNA end resection (Nimonkar et al., 2011).

Nbs1

The third component in the MRN complex, Nbs1 (or Xrs2 in *Saccharomyces cerevisiae*) is a 65 - 75 kDa protein that does not have any known enzymatic functions but is required for cell cycle checkpoint signaling (D'Amours & Jackson, 2002; Stracker et al., 2004). X-ray crystallography of Nbs1 from *S. pombe* reveals an elongated cylindrical structure with an FHA domain and tandem BRCT (BRCT1 and BRCT2) domains at the N-terminus that are connected by a flexible linker to the C-terminus. Adjacent to the flexible linker domain are binding sites for Mre11 and ATM (Figure 4A) (Williams et al., 2010). Both the FHA and BRCT domains typically bind to phosphorylated proteins (Durocher et al., 2000; Manke et al., 2003; Yu et al., 2003). Proteins phosphorylated during the DNA damage response that interact with the FHA/BRCT domains of Nbs1 include CtIP (Lloyd et al., 2009; Williams et al., 2009), MDC1 (Hari et al., 2010; Lloyd et al, 2009; Spycher et al., 2008), ATR (Olsen et al., 2007) and the WRN helicase (Kobayashi et al., 2010). The interaction between Nbs1 and ATM is required for ATM activation and its recruitment to DSBs (Falck et al., 2005; You et al., 2005). These results suggest that Nbs1 participates in cell cycle signaling by interacting with phospho-proteins that directly or indirectly activate ATM.

The recently published crystal structure of the *S. pombe* Mre11 catalytic domain together with Nbs1 indicates that two Nbs1 subunits bind to Mre11 (Figure 4B). The two Nbs1 molecules are not together and bind to the phosphodiesterase domains at either end of the elongated Mre11 dimer. Interestingly, only one of the two Nbs1 subunits binds fully to the Mre11 dimer interface via the highly conserved NFKxFxK motif. This

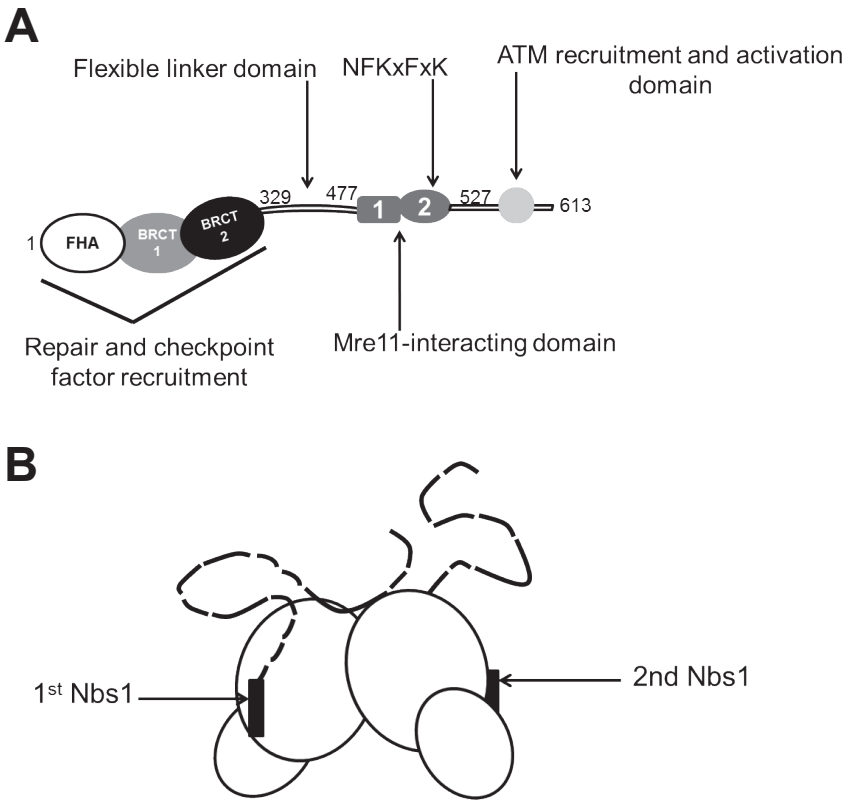

Figure 4. Structure of Nbs1 Mre11-interacting region ($Nbs1_{mir}$) and Mre11 catalytic domain ($Mre11_{cd}$). (A) Schematic representation of the domains and motifs of *S. pombe* Nbs1. (B) Schematic diagram showing the interacting domains from two Nbs1 molecules (black) bound to the Mre11 dimer (white). The Mre11-interacting domain 1 of Nbs1 binds outside the two Mre11 phosphodiesterase domains. One of the two Nbs1 molecules also binds across the Mre11 dimer interface with Mre11-interacting domain 2.

asymmetric binding of one Nbs1 to the Mre11 dimer interface sterically hinders the second Nbs1 from doing the same (Figure 4A) (Schiller et al., 2012). The successful purification of Mre11-Rad50-Nbs1 (MRN), Mre11-Nbs1 (MN) and Rad50-Nbs1 (RN) (Paull & Gellert et al., 1999; van der Linden et al., 2009), however, suggests that Nbs1 has multiple binding sites contributing to varying stoichiometries to comprise the MRN, MN or RN complex. SFM-based single particle volume analysis and ultracentrifugation suggest at least two stoichiometries of NBS1 in purified protein preparations (Lee et al., 2003; van der Linden et al., 2009) but the arrangement of NBS1 in the whole complex at high resolution has yet to be defined.

Roles of ATP

ATP binding and hydrolysis cause architectural rearrangements in SMC proteins. A functional ATPase is formed in the characteristic SMC structure when intramolecular antiparallel coiled-coil interactions bring the N-terminal Walker A and C-terminal Walker B nucleotide-binding domains together (de Jager et al., 2001b; Haering et al., 2002; Hopfner et al., 2002). These nucleotide-binding domains place SMC proteins in the conserved family of ATP-binding cassette (ABC) ATPases (Hopfner & Tainer, 2003; Ye et al., 2004). Although proteins in this family have diverse functions, their ATPase modules share structural and mechanistic properties. ATP binds at a dimer interface whereby the Walker A and B nucleotide-binding domains contact a highly conserved signature motif (C motif) from a second protein (Figure 5) (Hopfner et al., 2000b).

The role of ATP in DNA binding by Rad50 complexes

Various studies suggest that ATP binding or hydrolysis is important for MR(N) function. ATP likely acts as a structural switch that changes the conformation of MR(N). The addition of ATP, and more so AMP-PNP, increased the preference of purified human MR for forming large oligomers on DNA substrates with 3′-overhangs compared to blunt ends and 5′-overhangs (de Jager et al., 2002). Based on X-ray crystallography of isolated ATPase domains, ATP binding causes two major structural rearrangements to the ATPase domain of Rad50. Firstly, there is a 30° rotation of the C-terminal lobe relative to the N-terminal lobe;

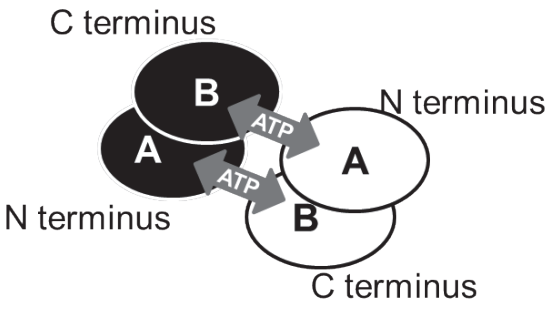

Figure 5. ATP binding sites on Rad50. A schematic representation of the ATP binding sites at the interface of two ABC ATPase monomers. Only the globular ATPase domains of Rad50 are shown. The Walker A and Walker B motifs are located at the N- and C-terminal ends of the protein, respectively. Domains of the same color are from the same protein or polypeptide chain. ATP binds at the dimer interface, whereby the Walker A and B nucleotide-binding domains contact a highly conserved signature motif (C motif) from a second protein. Two ATPs are shown as there are two possible binding sites in the Rad50 dimer. However, it is not known whether two ATPs can or do bind simultaneously.

and secondly, the two ATPase motifs of Rad50 form a compact homodimer (Hopfner et al., 2001). It was proposed that ATP-induced rotation repositions bound DNA with respect to Mre11 (Hopfner et al., 2001).

A specific requirement for ATP in DNA binding by the MR(N) complex has been suggested in several studies, but not observed in others. Rad50 originally purified by itself from *S. cerevisiae* (Raymond & Kleckner, 1993) bound DNA dependent on ATP in a filter-binding assay. Similarly, a protein construct including the N- and C-terminal ATPase domains of *P. furiosus* Rad50 (hereafter referred to as pfRad50cd for catalytic domain) dimerized in the presence of ATP, as determined by dynamic light scattering (Hopfner et al., 2000b). In this same study, an electrophoretic mobility shift assay (EMSA) showed that the same concentrations of pfRad50cd bound more DNA in the presence of ATP. However, purified complexes of human MR or MRN exhibited ATP-independent DNA binding in one study (Paull & Gellert, 1999) but nucleotide and NBS1-dependent DNA binding in another (Lee et al., 2003). Amino acid substitutions in the conserved ATP binding signature motif of human RAD50 abolish DNA binding by the resulting MRN complex (Moncalian et al., 2004), also implying that ATP is required for DNA binding. However substantial DNA binding by human MR complex in the absence of added nucleotides was observed in EMSA assays as well by SFM imaging that demonstrated nucleotide-independent DNA binding, oligomerization, and tethering (de Jager et al., 2001b). A careful look at these different studies shows some important differences that may help clarify the apparently disparate results.

Binding of protein to a substrate, DNA in this case, is characterized by association and dissociation constants related to concentration. Various DNA binding studies, described above, report somewhat different behavior of Rad50-containing complexes. These reported differences may of course be due to varying conditions for the binding reactions and assays. However, any change in the implied affinity of protein for DNA, due to presence or absence of cofactors, would be due to differences in binding constants. The association constants for Rad50, or complexes including Rad50, binding to DNA have not been rigorously determined, and may be difficult to sort out for reasons described below. Nevertheless, apparent DNA-binding activity depends on the concentration of protein and DNA, and these factors differ among the published reports. Nucleotide-independent DNA binding is observed by EMSA and SFM imaging at MR protein concentrations in the range of 10 - 100 nM (de Jager et al., 2001b, de Jager et al., 2002). Varying nucleotide-dependent binding is observed in studies where DNA substrates and protein complex are present in low nanomolar concentrations (Paull & Gellert, 1999; Lee et al., 2003). Comparing these studies indicates that large differences in DNA binding behavior are observed with 2–3-fold changes in protein concentration. This may indicate

that the K_D for MR or MRN binding to DNA is in the range of 10 nM. It is also possible that the purified proteins used in these studies may differ slightly in composition, quality, and specific activity.

In addition to considerations of the amount and quality of protein used, the type of DNA in the different assays may influence apparent binding affinity. EMSA assays typically use relatively short DNA, in the range of 50 - 160 nt or bp in the studies cited above, which would accommodate binding of one or a few MR(N) complex(es). The SFM imaging experiments use longer DNA in the range of 1 - 5 kbp. Binding of MR(N) to longer DNA substrates, on the order of 1 kbp, may involve protein–protein interaction in addition to protein–DNA interaction. SFM imaging shows that the longer DNA is bound by oligomeric assemblies in which protein–DNA complex formation and stability could be influenced by favoring interactions among proteins brought near each other by binding to DNA. The multiple DNA–protein and protein–protein interactions taking place on DNA substrates capable of binding multiple MR(N) complexes make it difficult to determine simple protein–DNA affinities and binding constants.

One way to interpret these reports of ATP-dependent and ATP-independent DNA binding by MR and MRN is that there are different DNA binding sites and that ATP effects access to or assembly of DNA-binding sites. This idea reflects the proposed different DNA binding modes and their control by ATP binding described for *B. subtilis* SMC (Hirano & Hirano, 2006). For the MR complex, different DNA-binding sites are expected as both Mre11 and Rad50 bind DNA (Paull & Gellert, 1998; Raymond & Kleckner, 1993; de Jager et al., 2001a; Hopfner et al., 2000a). Whereas DNA binding by Mre11 is ATP independent, ATP is required for Rad50 alone to bind DNA. Thus the different effects of ATP on DNA binding by MR or MRN complexes may reflect binding to these two different sites. In addition, the access to DNA-binding sites in the protein complex may depend on ATP binding-induced changes in molecular architecture.

By analogy with well-described SMC proteins, it is expected that ATP binding to Rad50 will cause ATPase domains to engage as a dimer and ATP hydrolysis will cause disengagement. X-ray crystallographic studies of pfRad50 catalytic domain reveal a 30° rotation of domains relative to each other induced by ATP binding (Hopfner et al., 2000b). Recent structural studies give additional clues on the role of ATP binding to Rad50. These studies revealed 3 interfaces between Mre11 and Rad50: between 2 Mre11, Mre11-helix loop helix (HLH) to the Rad50 coiled-coil base and the Mre11 capping domain to lobe II of Rad50 (Lammens et al., 2011, Lim et al., 2011, Möckel et al., 2011; Williams et al., 2011). The Mre11 dimer is in the middle with Rad50 on each side bound at the base by Mre11-HLH (Figure 2B). This Rad50-binding Mre11-HLH domain is attached to the rest of Mre11 by a flexible linker suggesting that Mre11 and Rad50

could potentially take dynamic orientations relative to each other. SAXS analysis shows that ATP changes MR from an open-flexible to a closed-compact structure (Figure 2B and 2C). Simultaneously, ATP binding causes a large conformational change to the Rad50 coiled coils (Williams et al., 2011), as well as causing delayed Mre11 nuclease activities compared to the non-ATP bound state (Lim et al., 2011). EMSA assays by Möckel et al. (2011) suggest that ATP-dimerized Rad50 may orient the whole complex to bind specifically to dsDNA. The experimenters incubated the *T. Maritima* HLHMre11-Rad50NBD with AMP-PNP to engage the Rad50NBD domains into a dimer. This dimeric form had a high affinity for dsDNA but showed almost no binding to ssDNA. In contrast, the disulfide bridged closed complex, Mre11-Rad50NBD, bound efficiently to both dsDNA and ssDNA. These results suggest that the Mre11 nuclease and capping domains create an additional ssDNA binding site in the protein complex. It is possible that the ATP-induced dimerization of Rad50 in the protein complex inhibits the Mre11 capping and nuclease domains from binding to dsDNA by physically blocking the Mre11 active sites.

Some biochemical analysis of eukaryotic MR shows enhanced protein–DNA interaction with AMP-PNP (a nonhydrolyzable analogue of ATP) (Lee et al., 2003). These authors reasoned that AMP-PNP binding might block DNA release that is otherwise triggered by ATP hydrolysis. They suggest that the requirement for a nonhydrolyzable ATP analogue implies rapid ATP hydrolysis by MRN. However ATP turnover rates for MR are rather slow, ranging from 0.026 to 0.08 per min per MR complex (de Jager et al., 2002; Bhaskara et al., 2007). For instance, possible effects of DNA binding on MR affinity for and exchange of bound nucleotides has not been determined, nor are the kinetics of ADP release well defined. These mechanistically interesting events are possibly linked to changes in protein complex architecture during the ATPase cycle. In addition, the discussion we present here predicts new aspects of MR(N) function in organizing DNA that could be controlled in the ATPase cycle. These structure–function connections include: (1) the existence of different binding sites or modes in the MR(N) complexes, (2) the importance of protein–protein interactions for controlling DNA binding, and (3) architectural changes in MR(N) that could influence inter- or intra-complex contacts and subsequently control formation of, or access to, DNA-binding sites.

Conversely, DNA is an allosteric effector of MR, which changes the relative orientation of the coiled coils within a complex. Rad50 coiled coils are flexible, allowing their apexes to interact with each other. Because this inter-complex binding between the hook domains is transiently observed in single complexes it appears to be relatively weak (Moreno-Herrero et al., 2005). Remarkably, once bound to DNA, the coiled coils become parallel to each other, an orientation that disfavors intra-complex interactions. In this

way the hook domains of DNA bound MR(N) are poised to interact with those of other DNA bound complexes (Moreno-Herrero et al., 2005). Multiple MR(N) complexes bind to DNA, presenting a dense group of protruding hook domains. These provide multiple weak interacting partners to tether DNA bound by oligomers of MR (de Jager et al., 2001b; Hopfner et al., 2002). In contrast to other SMCs, inter-complex protein–protein interactions play an important role in this aspect of MR(N) function. Because it appears that individual hook–hook interactions are weak but that collectively many such interactions keep bound DNA molecules together, we describe MR as molecular Velcro for DNA.

ATP binding influenced the prevalence of large oligomeric MR complexes on DNAs with different end structures (de Jager et al., 2002). Because Mre11 has DNA end-specific activities, this suggests that ATP binding changes the orientation of the globular domains of the complex, specifically between Rad50 and Mre11. New structural data suggests that ATP binding-associated changes in the complex architecture control access to the DNA binding sites of Mre11. Work with Rad50 alone suggests that a DNA-binding site is created by the dimerization of the ATP-binding domains. Intra-complex ATPase domain dimerization may trap DNA bound to Mre11 or prevent access to DNA binding sites on Mre11. The large conformational changes triggered by ATP binding causes the Rad50 nucleotide-binding domains (NBD) to rotate and face each other, which obstructs the DNA binding sites of Mre11 (Figure 2C). This physical “block” of the Mre11 DNA binding sites by ATP-bound Rad50 may allow Mre11 to accommodate only single-stranded DNA. The nucleotide-triggered conformational changes in MR may also create an additional DNA binding on Rad50 (Figure 6), explaining increased DNA binding after ATP addition. One of the DNA-binding models of Lim et al. (2011) suggests that the ATP-induced rotation of the Rad50 lobe II pushes the Mre11 capping domain, which then partially unwinds the DNA and manipulates it to the Mre11 active site. The conformational change of the Mre11 capping domain and the Mre11 flexible linker in the ATP-bound complex may enable the Mre11 active site to be more accessible, which as a result, accommodates the DNA. Whether different DNA-binding modes exist and whether these different modes trigger the above-mentioned conformational changes still needs to be determined for intact complexes before their cooperation or competition for DNA can be addressed.

DNA binding is only the first step in the multiple activities of the Rad50 complexes that are essential for DNA break repair. The additional functions will inevitably involve changes in molecular architecture to promote new interactions. For instance, DNA tethering requires many protein complexes bound, perhaps cooperatively, to DNA. Thus factors that promote MR complex oligomerization and cooperative DNA binding are expected to be important regulators of this early step in DNA repair. Control of DNA end processing by MR(N) will likely involve modulating the access to Mre11 DNA-binding sites.

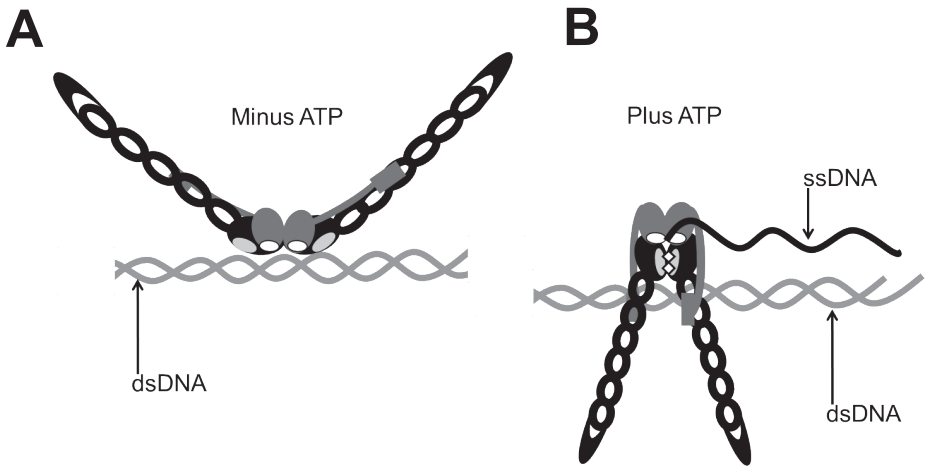

Figure 6. The interaction of MR with DNA. Rad50, Mre11 and ATP are depicted as shown in Figure 2B and 2C. Double-stranded DNA (dsDNA) is shown in light gray and single-stranded DNA is shown in black (ssDNA). (A) In the ATP-free "open" complex, the DNA binding sites of Mre11 (white) are exposed and can bind to dsDNA. The Rad50 ATP-binding sites (light gray) are facing outwards and away from one another, rendering it unlikely to bind DNA. (B) In the ATP-bound "closed" complex, the Rad50 ATP-binding sites (light gray) are dimerized, suggesting that this enables binding of dsDNA (position of DNA binding shown here as one possibility for illustration only), while the Mre11 DNA-binding sites (white) are now possibly limited to binding only ssDNA.

In addition, ATM activation and cell-cycle signaling must require a specific molecular architecture of MRN complexes bound to DNA. We have focused here on details of the role of ATP in DNA binding by MR(N). For this first step there are still important unanswered questions. New information on the nature and control of inter- and intra-complex interactions and the dynamic arrangement of component proteins will provide valuable insight into how the relatively simple MR(N) molecular machine performs its many different jobs in DNA break repair.

REFERENCES

Assenmacher, N., Hopfner, K.P. (2004). MRE11/RAD50/NBS1: Complex activities. Chromosoma *113*, 157-166.

Bhaskara, V., Dupre, A., Lengsfeld, B. et al. (2007). Rad50 adenylate kinase activity regulates DNA tethering by Mre11/Rad50 complexes. Mol Cell *25*, 647-661.

Bressan, D.A., Olivares, H.A., Nelms, B.E., Petrini, J.H. (1998). Alteration of N-terminal phosphoesterase signature motifs inactivates Saccharomyces cerevisiae Mre11. Genetics *150(2)*, 591-600.

D'Amours, D., Jackson, S.P. (2002). The Mre11 complex: at the crossroads of DNA repair and checkpoint signalling. Nat Rev Mol Cell Biol *3*, 317-327.

Durocher, D., Taylor, I.A., Sarbassova, D. et al. (2000). The molecular basis of FHA domain: phosphopeptide binding specificity and implications for phospho-dependent signaling mechanisms. Mol Cell *6*, 1169-1182.

de Jager, M., Dronkert, M.L., Modesti, M., Beerens, C.E., Kanaar, R., van Gent, D.C. (2001a). DNA-binding and strand-annealing activities of human Mre11: implications for its roles in DNA double-strand break repair pathways. Nucleic Acids Res *29*, 1317-1325.

de Jager, M., van Noort, J., van Gent, D.C., Dekker, C., Kanaar, R., Wyman, C. (2001b). Human Rad50/Mre11 is a flexible complex that can tether DNA ends. Mol Cell *8*, 1129-1135.

de Jager, M., Wyman, C., van Gent, D.C., Kanaar, R. (2002). DNA end-binding specificity of human Rad50/Mre11 is influenced by ATP. Nucleic Acids Res *30*, 4425-4431.

Falck, J., Coates, J., Jackson, S.P. (2005). Conserved modes of recruitment of ATM, ATR and DNA-PKcs to sites of DNA damage. Nature *434(7033)*, 605-611.

Farah, J.A., Cromie, G., Steiner, W. W., Smith, G.R. (2005). A novel recombination pathway initiated by the Mre11/Rad50/Nbs1 complex eliminates palindromes during meiosis in *Schizosaccharomyces pombe*. Genetics *169(3)*, 1261-1274.

Haering, C.H., Löwe, J., Hochwagen, A., Nasmyth, K. (2002). Molecular architecture of SMC proteins and the yeast cohesin complex. Mol Cell *9(4)*, 773-788.

Hari, F.J., Spycher, C. Jungmichel, S., Pavic, L., Stucki, M. (2010). A divalent FHA/BRCT-binding mechanism couples the MRE11-RAD50-NBS1 complex to damaged chromatin. EMBO Rep *11(5)*, 387-392.

Hirano, M., Hirano, T. (2006). Opening closed arms: long-distance activation of SMC ATPase by hinge-DNA interactions. Mol Cell *21(2)*, 175-186.

Hohl, M., Kwon, Y., Galvan, S.M., Sue, X., Tous, C., Aguilera, A. Sung, P., Petrini, J.H. (2011). The Rad50 coiled-coil domain is indispensable for Mre11 complex functions. Nat Struc Mol Biol *18(10)*, 1124-1131.

Hopfner, K.P., Karcher, A., Craig, L., Woo, T.T., Carney, J.P., Tainer, J.A. (2001). Structural biochemistry and interaction architecture of the DNA double-strand break repair Mre11 nuclease and Rad50-ATPase. Cell *105*, 473-485

Hopfner, K.P., Karcher, A., Shin, D., Fairley, C., Tainer, J.A., Carney, J.P. (2000a). Mre11 and Rad50 from *Pyrococcus furiosus*: Cloning and biochemical characterization reveal an evolutionarily conserved multiprotein machine. J Bacteriol *182*, 6036-6041.

Hopfner, K.P., Karcher, A., Shin, D.S. et al. (2000b). Structural biology of Rad50 ATPase: ATP-driven conformational control in DNA double-strand break repair and the ABC ATPase superfamily. Cell *101*, 789-800.

Hopfner, K.P., Craig, L., Moncalian, G. et al. (2002). The Rad50 zinc-hook is a structure joining Mre11 complexes in DNA recombination and repair. Nature *418*, 562-566.

Hopkins, B.B., Paull, T.T. (2008). The P. furiosus mre11/rad50 complex promotes 5' strand resection at a DNA double-strand break. Cell *35(2)*, 250-260.

Khanna, K.K., Jackson, S.P. (2001). DNA double-strand breaks: Signaling, repair and the cancer connection. Nat Genet *27*, 247-254.

Kobayashi, J., Okui, M., Asaithamby, A., Burma, S., Chen, B.P., Tanimoto, K., Matsuura, S., Komatsu, K., Chen, D.J. (2010). WRN participates in translesion synthesis pathway through interaction with NBS1. Mech Ageing Dev *131(6)*, 436-444.

Krough, B.O., Llorente, B., Lam, A., Symington, L.S. (2005). Mutations in Mre11 phosphoesterase motif I that impair *Saccharomyces cerevisiae* Mre11-Rad50-Xrs2 complex stability in addition to nuclease activity. Genetics *171(4)*, 1561-1570.

Lammens, K., Bemeleit, D.J., Möckel, C. et al. (2011). The Mre11:Rad50 structure shows an ATP-dependent molecular clamp in DNA double-strand break repair. Cell *145(1)*, 54-66.

Lee, J.H., Ghirlando, R., Bhaskara, V., Hoffmeyer, M.R., Gu, J., Paull, T.T. (2003). Regulation of Mre11/Rad50 by Nbs1: effects on nucleotide-dependent DNA binding and association with ataxia-telangiectasia-like disorder mutant complexes. J Biol Chem *278*, 45171-45181.

Lewis, L.K., Storici, F., van Komen, S., Calero, S., Sung, P., Resnick, M.A. (2004). Role of the nuclease activity of *Saccharomyces cerevisiae* Mre11 in repair of DNA double-strand breaks in mitotic cells. Genetics *166(4)*, 1701-1713.

Lim, H.S., Kim, J.S., Park, Y.B., Gwon, G.H., Cho, Y. (2011). Crystal structure of the Mre11-Rad50-ATPγS complex: understanding the interplay between Mre11 and Rad50. Genes Dev *25(10)*, 1091-1104.

Lisby, M., Barlow, J.H., Burgess, R.C., Rothstein, R. (2004). Choreography of the DNA damage response: Spatiotemporal relationships among checkpoint and repair proteins. Cell *118*, 699-713.

Lloyd, J., Chapman, J.R., Clapperton, J.A. et al. (2009). A supramodular FHA/BRCT-repeat architecture mediates Nbs1 adaptor function in response to DNA damage. Cell *139*, 100-111.

Luo, G., Yao, M.S., Bender, C.F. et al. (1999). Disruption of mRad50 causes embryonic stem cell lethality, abnormal embryonic development, sensitivity to ionizing radiation. Proc Natl Acad Sci USA *96*, 7376-7381.

Manke, I.A., Lowery, D.M., Nguyen, A., Yaffe, M.B. (2003). BRCT repeats as phosphopeptide-binding modules involved in protein targeting. Science *302*, 636-639.

Mimitou, E.P., Symington, L.S. (2009). DNA end resection: many nucleases make light work. DNA Repair (Amst) *8(9)*, 983-995.

Möckel, C., Lammens, K., Schele, A., Hopfner, K.P. (2011). ATP driven structural changes of the bacterial Mre11:Rad50 catalytic head complex. Nucleic Acids Res *40(2)*, 914-927.

Moncalian, G., Lengsfeld, B., Bhaskara, V. et al. (2004). The Rad50 signature motif: essential to ATP binding and biological function. J Mol Biol *335*, 937-951.

Moreau, S., Ferguson, J.R., Symington, L.S. (1999). The nuclease activity of Mre11 is required for meiosis but not for mating type switching, end joining, or telomere maintenance. Mol Cell Biol *19(1)*, 556-566.

Moreno-Herrero, F., de Jager, M., Dekker, N.H., Kanaar, R., Wyman, C., Dekker, C. (2005). Mesoscale conformational changes in the DNA-repair complex Rad50/Mre11/Nbs1 upon binding DNA. Nature *437*, 440-443.

Nimonkar, A.V., Genschel, J., Kinoshita, E. et al. (2011). BLM-DNA2-RPA-MRN and EXO1-BLM-RPA-MRN constitute two DNA end resection machineries for human DNA break repair. Genes Dev *25(4)*, 350-362.

Olson, E., Nievera, C.J., Lee, A.Y., Chen, L., Wu, X. (2007). The Mre11-Rad50-Nbs1 complex acts both upstream and downstream of ataxia telangiectasia mutated and Rad3-related protein (ATR) to regulate the S-phase checkpoint following UV treatment. J Biol Chem *282*, 22939-22952.

Paull, T.T., Gellert, M. (1998). The 3' to 5' exonuclease activity of Mre11 facilitates repair of DNA double-strand breaks. Mol Cell *1*, 969-979.

Paull, T.T., Gellert, M. (1999). Nbs1 potentiates ATP-driven DNA unwinding and endonuclease cleavage by the Mre11/Rad50 complex. Genes Dev *13*, 1276-1288.

Paull, T.T., Lee, J. H. (2005). The Mre11/Rad50/Nbs1 complex and its role as a DNA double-strand break sensor for ATM. Cell Cycle *4*, 737-740.

Raymond, W.E., Kleckner, N. (1993). RAD50 protein of *S. cerevisiae* exhibits ATP-dependent DNA binding. Nucleic Acids Res *21*, 3851-3856.

Schiller, C.B., Lammens, K., Guerini, I. et al. (2012). Structure of Mre11-Nbs1 complex yields insights into ataxia-telangiectasia-like disease mutations and DNA damage signaling. Nat Struct Mol Biol *19(7)*, 693-700.

Spycher, C., Miller, E.X., Townsend, K. et al. (2008). Constitutive phosphorylation of MDC1 physically links the MRE11-RAD50-NBS1 complex to damaged chromatin. J Cell Biol *181(2)*, 227-240.

Shiloh, Y. et al. (1997). Ataxia-telangiectasia and the Nijmegen breakage syndrome: related disorders but genes apart. Annu Rev Genet *31*, 635-662.

Stewart, G.S., Maser, R.S., Stankovic, T. et al. (1999). The DNA double strand break repair gene hMRE11 is mutated in individuals with an ataxia-telangiectasia-like disorder. Cell *99*, 577 -587.

Symington, L.S. (2002). Role of RAD52 epistasis group genes in homologous recombination and double-strand break repair. Microbiol Mol Biol Rev *66*, 630-670.

van der Linden, E. Sanchez, H., Kinoshita, E., Kanaar, R., Wyman, C. (2009). RAD50 and NBS1 form a stable complex functional in DNA binding and tethering. Nucleic Acids Res *37*, 1580-1588.

van Noort, J., van der Heijden, T., de Jager, M., Wyman, C., Kanaar, R., Dekker, C. (2003). The coiled-coil of the human Rad50 DNA repair protein contains specific segments of increased flexibility. Proc Natl Acad Sci USA *100*, 7581-7586.

Wen, Q., Scorah, J., Phear, G., Rodgers, G., Rodgers, S., Meuth, M. (2008). A mutant allele of MRE11 found in mismatch repair-deficient tumor cells suppresses the cellular response to DNA replication fork stress in a dominant negative manner. Mol Biol Cell *19(4)*, 1693-705.

Weterings, E., van Gent, D.C. (2004). The mechanism of non-homologous end-joining: a synopsis of synapsis. DNA Repair (Amst) *3*, 1425-1435.

Williams, R.S., Dodson, G.E., Limbo, O. et al. (2009). Nbs1 flexibly tethers Ctp1 and Mre11-Rad50 to coordinate DNA double-strand break processing and repair. Cell *139(1)*, 87-99.

Williams, R.S., Moncalian, G., Williams, J.S. et al. (2008). Mre11 dimers coordinate DNA end bridging and nuclease processing in double-strand-break repair. Cell *135(1)*, 97-109.

Williams, G.J., Lees-Miller, S.P., Tainer, J.A. (2010). Mre11-Rad50-Nbs1 conformations and the control of sensing, signaling, and effector responses at DNA double-strand breaks. DNA Repair (Amst) *9(12)*, 1299-1306.

Williams, G.J, Williams, R.S., Williams, J.S. et al. (2011). ABC ATPase signature helices in Rad50 link nucleotide state to Mre11 interface for DNA repair. Nat Struc Mol Biol *18(4)*, 423-431.

Wyman, C., Kanaar, R. (2006). DNA double-strand break repair: All's well that ends well. Annu Rev Genet *40*, 363-383.

Wyman, C., Ristic, D., Kanaar, R. (2004). Homologous recombination-mediated double-strand break repair. DNA Repair (Amst) *3*, 827-833.

Xiao, Y., Weaver, D.T. (1997). Conditional gene targeted deletion by Cre recombinase demonstrates the requirement for the double-strand break repair Mre11 protein in murine embryonic stem cells. Nucleic Acids Res *25*, 2985-2991.

Ye, J., Osborne, A.R., Groll, M., Rapoport, T.A. (2004). RecA-like motor ATPases--lessons from structures. Biochim Biophys Acta *1659(1)*, 1-18.

You, Z., Chahwan, C., Bailis, J., Hunter, T., Russell, P. (2005). ATM activation and its recruitment to damaged DNA require binding to the C terminus of Nbs1. Mol Cell Biol *25*, 5363-5379.

Yu, X., Chini, C.C., He, M., Mer, G., Chen, J. (2003). The BRCT domain is a phospho-protein binding domain. Science *302*, 639-642.

Zhu, J., Petersen, S., Tessarollo, L., Nussenzweig, A. (2001). Targeted disruption of the Nijmegen breakage syndrome gene NBS1 leads to early embryonic lethality in mice. Curr Biol *11*, 105-109.

CHAPTER 2

Human RAD50 makes a functional complex that can bind to DNA

Eri Kinoshita[1], Sari van Rossum-Fikkert[1], Humberto Sanchez[1], Aryandi Kertokalio[1] and Claire Wyman[1,2]

[1]Department of Cell Biology & Genetics, Cancer Genomics Center and [2]Department of Radiation Oncology, Erasmus MC, PO Box 2040, 3000 CA Rotterdam, The Netherlands

ABSTRACT

The MRE11-RAD50-NBS1 (MRN) complex has various functions in DNA repair and has roles in both non-homologous end joining (NHEJ) and homologous recombination (HR), two mechanistically distinct double-strand break repair pathways. While the ATP-dependent activities of MR(N) have been well characterized, there is no information regarding the biochemistry of isolated RAD50. We obtained purified human RAD50 and observed that it binds ATP, undergoes ATP-dependent conformational changes as well as having ATPase activities. SFM analysis clearly showed that human RAD50 binds DNA although not as oligomers. Neither human RAD50 nor MRE11 alone was functional in tethering DNA molecules. ATP increased formation of globular shaped multimers without any visible RAD50 coiled coils in contrast to the MRE11-RAD50 complex where ATP induced oligomers have obvious coiled coils protruding from a central accumulation. These results suggest that MRE11 is important in maintaining structural integrity of the protein complex and perhaps has a role in reinforcing proper alignment of the coiled coils in the ATP-bound state.

INTRODUCTION

The MRE11-RAD50-NBS1 (MRN) is a multi-protein complex with diverse roles in both NHEJ and HR (Krough & Symington, 2004). MRE11 and RAD50 are well conserved between organisms while NBS1 (Xrs2 in yeast) is less conserved. Electron microscopy and SFM analysis have shown that NBS1/Xrs2 is not necessary for the protein complex to maintain its basic structure which consists of a catalytic DNA binding head (2 molecules of RAD50 and 2 molecules of MRE11) with the elongated coiled coils of RAD50 extending away (de Jager et al., 2001; Hopfner et al., 2001).

Mre11 alone forms dimers that can be purified and have several well defined biochemical activities such as DNA binding (Hopfner et al., 2001; Williams et al., 2008). Mre11 has phosphodiesterase motifs with manganese-dependent endo- and exonuclease (3' → 5' directionality) activities as well as DNA hairpin opening activity (Furuse et al., 1998; Hopfner et al., 2000a; Paull & Gellert, 1998; Trujillo et al., 1998; Usui et al., 1998). Rad50, on the other hand, consists of ATP-binding motifs, the Walker A and Walker B domains at the N- and C- terminus, respectively (Hopfner et al., 2000a). A functional ATPase catalytic site is formed by juxtaposition of the N- and C- termini at the end of a long (up to 900 amino acids and 50 nm) intramolecular coiled-coil structure that joins them. The catalytic domain of *P. furiosus* Rad50 (artificially joined N- and C-terminal regions of Rad50) undergo ATP-dependent dimerization and DNA binding (Hopfner et al., 2000a). The full-length Rad50, purified in the absence of Mre11, from *S. cerevisiae* similarly showed ATP-dependent DNA binding (Raymond & Kleckner, 1993). The conformational changes to MR after ATP binding is such that Rad50 physically obscures the DNA binding sites of Mre11 (Lammens et al., 2011; Lim et al., 2011; Williams et al., 2011). This structural information together with the observation that the complex binds DNA in the presence of ATP suggests that Rad50 also has DNA binding sites that are accessible in the ATP-bound MR complex. It is therefore important to assess Rad50 DNA binding activities without Mre11 and see if there are changes in the complex organization and architecture compared with MR complexes.

We show that the human RAD50 binds ATP and maintains ATPase activities. Our SFM imaging shows that the human RAD50 predominantly has a dimeric conformation with the coiled coils extending outwards as previously seen in MR complexes (de Jager et al., 2001; de Jager et al., 2002; Moreno-Herrero et al., 2005; van der Linden et al., 2009). Interestingly, ATP binding did not cause RAD50 to oligomerize in the same way as MR but induces formation of globular multimers without discernible coiled coils. This suggests that although RAD50 can bind DNA, MRE11 has an important role in maintaining the arrangement of the coiled coils, which is likely important for DNA tethering and other biological functions. We have previously hypothesized that DNA tethering is a function mediated by multiple weak interactions between the flexible coiled

coils which enable two broken DNA molecules to be kept in close vicinity (de Jager et al., 2001). We propose that without MRE11, RAD50 cannot maintain the extended coiled-coil conformation and thus DNA tethering activity is perturbed.

MATERIALS & METHODS

Protein expression and purification

Human RAD50 and MR were produced by infection of Sf9 cells in suspension culture with a baculovirus dual expression construct producing both C-terminally 6-histidine tagged RAD50 and untagged MRE11. Cells were harvested after 72 hours. The purification procedure was based on methods described by van der Linden et al. (2009). Briefly, infected cells were collected and flash frozen in liquid nitrogen. They were subsequently thawed on ice and resuspended in 100 ml of ice-cold buffer (50 mM Tris-HCl pH 8.0; 10% glycerol, 500 mM NaCl, 10 mM β-mercaptoethanol) and two tablets of Complete, EDTA-free protease inhibitor cocktail tablets (Roche). The cells were disrupted by 20 strokes of a type B pestle in a Dounce homogenizer and centrifuged for 1 hour at 100,000 g at 4°C. The soluble fraction was loaded onto 5 ml of Ni-NTA agarose beads (Qiagen) equilibrated with buffer (50 mM Tris-HCl pH 8.0; 10% glycerol, 500 mM NaCl, 1mM DTT). The column was washed with 10 column volumes of Buffer A (50 mM Tris-HCl pH 8.0; 10% glycerol, 300 mM NaCl, 1 mM DTT) with 10 mM imidazole and then with 10 column volumes of Buffer A with 40 mM imidazole. Proteins were eluted by 1 column volume of Buffer A with 130 mM and then 1 column volume of Buffer A with 200 mM imidazole. Fractions containing MR were pooled, diluted two fold to lower the salt concentration to 150 mM NaCl and loaded onto a 1 ml HitrapQ column (GE Healthcare) equilibrated with Buffer A (50 mM Tris-HCl pH 8.0; 10% glycerol, 100 mM NaCl, 1 mM DTT). After washing the column with 5 column volumes, the proteins were eluted with a salt step of 600 mM NaCl in Buffer A. Relevant fractions were pooled and loaded on a Superose 6 size exclusion column (GE Healthcare) equilibrated with Buffer A (200 mM NaCl). Relevant fractions were pooled and loaded onto a MonoQ column equilibrated with Buffer A. The column was washed with 5 column volumes of Buffer A and the proteins were eluted with a salt gradient from 100 mM to 600 mM NaCl. During this final purification step, fractions containing only RAD50 were separated from those with MR. Protein concentrations were determined by comparison to standards on a polyacrylamide gel (using BSA) stained with Coomassie Brilliant Blue. The protein preparations were aliquoted, flash frozen in liquid nitrogen and stored at -80°C until further use.

DNA substrates

The 66 bp double-stranded DNA (dsDNA66) was made by annealing the oligos: 5' - AF532 - AGA AAC TGG GCA TGT GGA GAC AGA GAA GAC TCT TGG GTT TCT GAT AGG

CAC TGA CTC TCT CTG CCT-3' and its complement 5'-AGG CAG AGA GAG TCA GTG CCT ATC AGA AAC CCA AGA GTC TTC TCT GTC TCC ACA TGC CCA GTT TCT - 3' (both synthesized by Eurogenetec) in buffer containing 50 mM Tris-HCl, pH 8.0; 100 mM NaCl; 10 mM $MgCl_2$ and 1 mM DTT at 95°C for 10 minutes which was then left to slowly cool overnight.

The 3 kb linear dsDNA with a 3'- overhang was created by digestion of pUC19 with *PstI* and subsequently purified by standard phenol:chloroform extraction and ethanol precipitation.

Immunoblotting

RAD50 (R_2), MR (M_2R_2) or MRE11 (M_2), calculated as a 60 nM dimer in binding buffer, (50 mM Tris-HCl, pH 8.0, 5% glycerol, 100 mM NaCl, 5 mM $MgCl_2$ and 1 mM DTT) with or without incubation including ATP as described below, were loaded and run on a 4% non-denaturing polyacrylamide gel (pre-run at 50 V for 1 hour) in 0.5 x TG at 75 V for 3 hours. The protein was transferred from the gel to a nitrocellulose membrane (Whatman) at 100 V for 1 hour using the BioRad Mini Protean 3 Western transblot system. The blot was incubated with a RAD50 antibody GTX70228 (Genetex) after blocking for 1 hour with 0.2% milk solution and detected with an anti-mouse secondary antibody, HRP conjugate (Jackson ImmunoResearch).

ATP binding assay

RAD50 (R_2) or MR (M_2R_2), calculated as a 60 nM dimer, were mixed with 1.5 µM ATP supplemented with radiolabeled [γ^{32}P]ATP (1 mCi/mL) in 10 µl of ATPase buffer (50 mM Tris-HCl, pH 8.0, 5% glycerol, 100 mM NaCl, 5 mM $MgCl_2$ and 1 mM DTT). The reaction was incubated for 5 minutes at room temperature. Samples were loaded onto a 4% non-denaturing polyacrylamide gel in 0.5 x TG run at 75 V for 3 hours and dried onto a Whatman filter paper. The dried gel was exposed overnight to a phosphor image plate (Molecular Diagnostics) and visualized by phosphorimaging using a Typhoon 9200 image analyzer.

ATPase assay

RAD50 calculated as a 60 nM dimer, were mixed with 1.5 µM ATP supplemented with radiolabeled [γ^{32}P]ATP (1 mCi/mL) in 10 µl of ATPase buffer (50 mM Tris-HCl, pH 8.0, 5% glycerol, 100 mM NaCl, 5 mM $MgCl_2$ and 1 mM DTT). The reaction was incubated for 120 minutes at 37°C. Samples of 2.5 µl were removed at 0, 60 and 120 minutes and the reaction stopped by adding EDTA to a final concentration of 125 mM. Samples were analyzed by thin layer chromatography (Merck TLC plates) run in 0.7 M K_2HPO_4, 0.4 M Boric acid, exposed to a phosphor image plate (Molecular Diagnostics) for 1 hour and imaged using a Typhoon 9200 analyzer.

Scanning force microscopy (SFM)

Sample preparation; proteins ± nucleotides ± DNA

RAD50 (R_2) or MR (M_2R_2), calculated as a 12 nM dimer, was incubated in 20 µl of protein storage buffer (50 mM Tris–HCl, pH 8.0, 10% glycerol, 300 mM NaCl, 1 mM DTT) for 1 minute at room temperature. Where indicated nucleotide was added to 1 mM ATP or AMP-PNP, DNA was added to 1 nM (fragment) 3 kb linear dsDNA in 20 µl and incubated, or both nucleotide and DNA were added. All binding reactions were incubated for 1 minute at room temperature. After incubation, the sample was diluted 5-fold by adding 80 µl of deposition buffer (10 mM HEPES, pH8.0, 20 mM $MgCl_2$) and 50 µl was deposited onto freshly cleaved mica for 1 minute, washed 3 times with MilliQ and dried with filtered air.

All samples were imaged in air at room temperature and humidity by tapping mode SFM using a Nanoscope IV (Digital Instruments). Silicon Nanotips were from Digital Instruments (Nanoprobes). Images were collected at 2.5 µm x 2.5 µm and processed by flattening to remove background slope.

RESULTS

RAD50 isolated during protein purification

Although both MRE11 and RAD50 were expressed together for purification of the complex, during the final purification step (MonoQ column) of the human MRE11-RAD50 (MR) complex, there were fractions containing only RAD50 (Figure 1A, Lane 2). Immunoblotting analysis with a RAD50 antibody GTX70229 (Genetex) and an MRE11 antibody #2244 (Erasmus MC) confirmed that the RAD50 fraction contained only RAD50 while the MR fractions contained both MRE11 and RAD50 (data not shown).

Human RAD50 can bind and hydrolyze ATP

We investigated the biochemical activities of this RAD50 preparation to see which functions are maintained in the absence of MRE11. RAD50 belongs to the family of SMC proteins and contains ATP-binding Walker A and Walker B domains (Hopfner et al., 2000a). We developed a gel assay to test for ATP binding by detecting radiolabeled ATP migrating at the same position as the protein. After incubating 60 nM of RAD50 (R_2) or MR (M_2R_2) with 1 µM ATP in 10 µl, we ran the reaction mix in a 4% non-denaturing polyacrylamide gel and did an immunoblotting analysis with a RAD50 antibody GTX70228 (GeneTex) to determine the running pattern of RAD50, alone and in the MR complex. We confirmed the presence of RAD50 in both RAD50 and MR preparations (Figure 2A, Lanes 2 and 3, respectively). To determine whether ATP binds to the protein, we similarly made reactions with 60 nM of RAD50 (R_2) or MR (M_2R_2) with radiolabelled [γ^{32}P]ATP. Radiolabeled ATP comigrates with RAD50

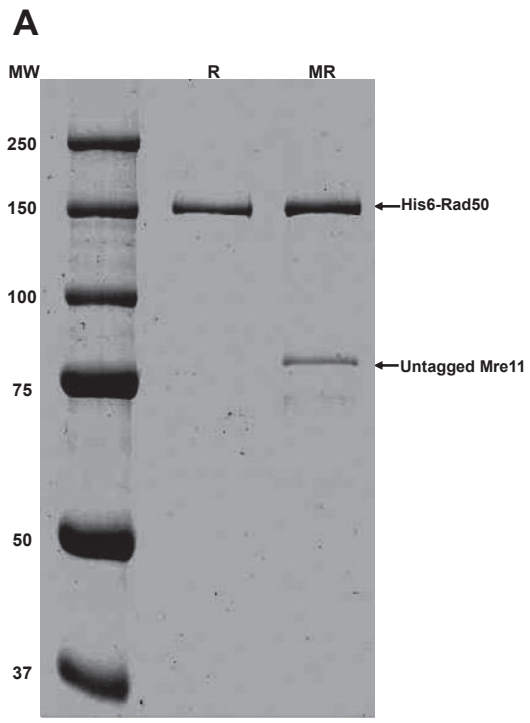

Figure 1. Purification of RAD50 and MR. Coomassie stained SDS-PAGE gel (8%) of purified protein preparations. Lane 1, molecular weight marker (MW; molecular mass indicated in kiloDaltons); Lane 2, RAD50 (R); Lane 3, MRE11-RAD50 (MR).

in both the RAD50 and MR preparations (Figure 2B, Lanes 2 and 3, respectively) indicating ATP binding in both samples although MR binds more ATP than RAD50. Additionally, the human RAD50 has a detectable ATPase activity, although it is lower than MR at the two time points (Figure 2C). We conclude that human RAD50 maintains ATP binding and hydrolysis activities in the absence of MRE11.

Human RAD50 is arranged similar to MR but does not oligomerize

The MR and MRN complexes have a distinct architectural arrangement and show nucleotide induced oligomerization in SFM analysis. The preparations including RAD50 only had clearly discernible coiled coils protruding from the globular head domain that is similar to MR (compare Figures 3B and 3E). Similar to our previous study (de Jager et al., 2002), we observed small multimeric MR complexes (defined as multimers up to 8 coiled-coil arms protruding from a central globular accumulation) and much larger oligomeric MR complexes

(compare Figures 3F and 3G). Adding ATP to MR caused a notable increase in oligomers. Interestingly, both ATP and AMP-PNP increased multimeric structures of RAD50 (Figure 3C), however, these globular accumulations had no distinguishable coiled coils protruding, as if the coiled coils were collapsed close to the globular domains.

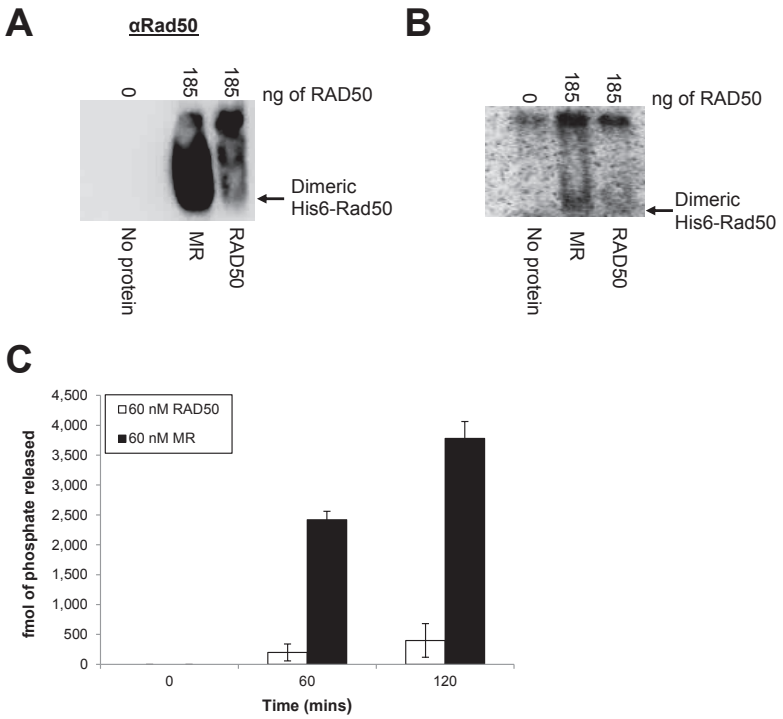

Figure 2. ATP binding and hydrolysis by RAD50. Native gel assay for ATP binding; (A) Immunoblot of 4% non-denaturing polyacrylamide gel, in which all samples were incubated with 1.5 μM ATP, and probed with a RAD50 antibody GTX70228 (GeneTex). Lane 1, no protein; Lane 2, 60 nM MR; Lane 3, 60nM RAD50. The concentrations of RAD50 (R_2) and MR (M_2R_2) were adjusted so that 185 ng of RAD50 was loaded onto the gel for both protein complexes. (B) Detection of [γ^{32}P]ATP from a native gel run in conditions identical to the one blotted in A, here all samples were incubated with radiolabelled [γ^{32}P] ATP (1 mCi/mL) supplemented with unlabeled ATP to make a final concentration of 1.5 μM; no protein (Lane 1), 60 nM MR (Lane 2) and 60 nM RAD50 (Lane 3). The [γ^{32}P]ATP runs out of the lane in the no protein control (Lane 1). There is some background signal in the well of all lanes but clearly more for MR (Lane 2) and RAD50 (Lane 3), suggesting that this is caused by multimeric protein complexes. The position of RAD50 was determined by overlaying the immunoblot with the native gel. The concentrations of RAD50 (R_2) and MR (M_2R_2) were adjusted so that 185 ng of RAD50 was loaded onto the gel for both protein complexes. (C) ATPase activity expressed as fmol of phosphate released by 60 nM of MR or RAD50 (R) at 0, 60 and 120 minutes. The concentration of RAD50 (R_2) and MR (M_2R_2) were both calculated as a 60 nM dimer. Error bars indicate SEM of independent triplicate experiments.

Our typical preparations of MR consist predominantly of dimers with respect to having two RAD50 coiled coils, and include also forms such as monomers, multimers as well as larger oligomeric complexes (de Jager et al., 2001; van der Linden et al., 2009). We similarly observed here that MR consisted mostly of dimeric forms, which were 67% of the total population while monomers and multimers/oligomers were 13% and 20%, respectively. When counting the MR molecules, we included multimers and oligomers in the same category. In comparison to MR, the RAD50 preparation consisted almost entirely of dimeric complexes, 97% of the population, while monomers and multimers without coiled coils were 1% and 2%, respectively. The multimeric structures of RAD50 were entirely the globular structures without obvious coiled coils (Figure 3C). MRE11, which has no ATP binding activity, is not expected to change to the oligomeric form with added nucleotide and is taken along as a control here (data not shown). We did not observe any oligomerization in RAD50 or MRE11 alone in response to ATP. We therefore conclude that the increased oligomerization of MR in response to ATP is not maintained when either RAD50 or MRE11 are separated from the MR complex.

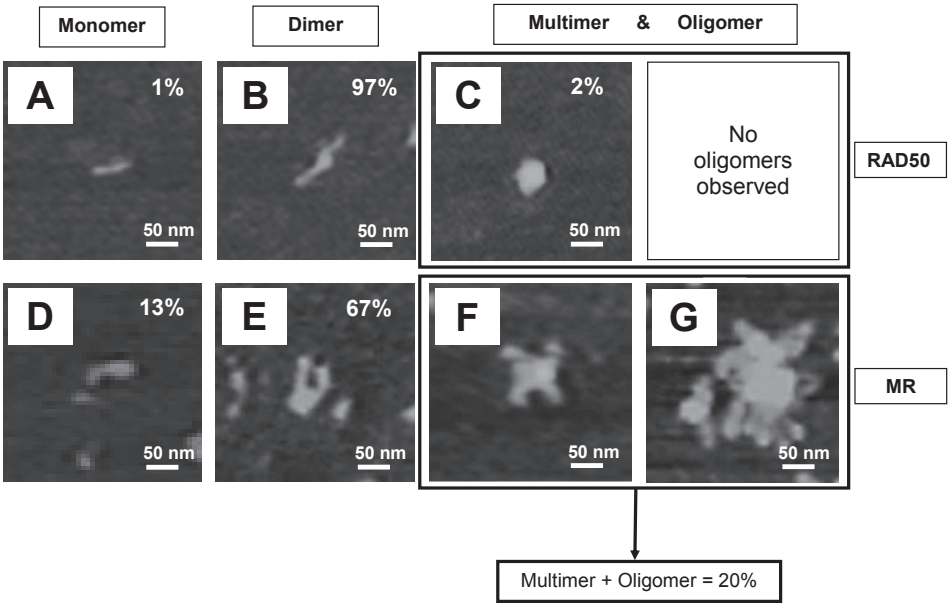

Figure 3. SFM analysis of RAD50 and MR compexes. (A to F) Representative SFM images of protein complexes in different conformations. The percentage of complexes in the different conformations is indicated in each panel (223 molecules were analyzed for RAD50, 170 molecules were analyzed for MR). The scale bar is 50 nm. Color represents height from 0 to 3 nm (dark to light).

Human RAD50 binds DNA with a different conformation compared to MR

Several studies have indicated that RAD50 (or parts of RAD50) have ATP-dependent DNA binding activities (Hopfner et al., 2000a; Raymond & Kleckner, 1993). We initially did electrophoretic mobility shift assays (EMSAs) using an Alexa Fluor 532 labeled 66 bp dsDNA to compare the DNA binding of RAD50 and MR (data not shown). We observed that while RAD50 did bind DNA, there was a much lower affinity compared to MR, making it difficult to quantify the DNA binding with this assay. We used SFM imaging to study DNA binding because in this relatively small amounts of concentrated proteins can be used and would more likely identify differences in how RAD50 and MR bound to DNA. We observed both RAD50 and MR clearly bound to DNA (Figures 4A and 4B; Figures 4C, 4D and 4E, respectively). As expected, MR bound to DNA via the globular head with the coiled coils extending away from the DNA (Figures 4C and 4D). In addition, we observed that MR was involved in typical DNA tethering complexes with MR oligomers and multiple DNA molecules (Figure 4E) as described previously (de Jager et al., 2001; de Jager et al., 2002; van der Linden et al., 2009). Adding ATP did not dramatically change the percentage of DNA bound by RAD50. However, of the DNA-bound RAD50, more appeared to be collapsed RAD50

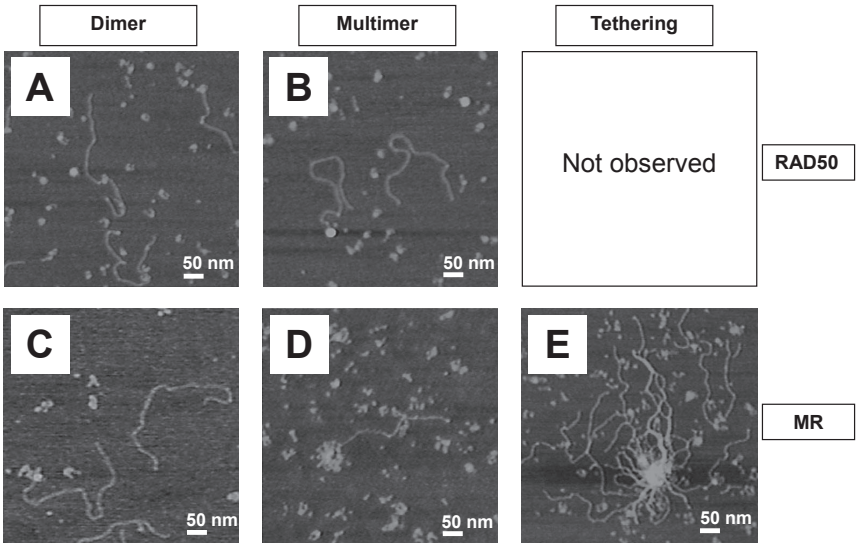

Figure 4. SFM analysis of RAD50- and MR-DNA complexes. (A to E) Representative SFM images of protein-DNA complexes as indicated. The scale bar is 50 nm. Color represents height from 0 to 3 nm (dark to light).

structures without visible coiled coils in the presence of ATP. Focusing solely on RAD50 bound to DNA, the collapsed RAD50 structures without discernible coiled coils increased from 17% to 41% when ATP was present. MR, on the other hand, bound to DNA as dimers or multimers (Figures 4C and 4D, respectively) and tethered DNA molecules (Figure 4E). In the presence of ATP, the percentage of DNA bound by oligomeric MR complexes increased from 5% to 7% and the percentage of DNA involved in tethering complexes increased from 4 to 6%. No DNA was bound by oligomeric complexes nor involved in DNA tethering for RAD50 or MRE11 alone.

DISCUSSION

We have purified and characterized human RAD50 alone, lacking detectable MRE11. This was achieved by purifying it as a by-product of cells that expressed the MR complex. Previous attempts to express RAD50 alone in our laboratory have failed to produce soluble proteins (Unpublished results from C. Wyman, R. Kanaar, & M. de Jager). Our previous *in vivo* experiments have also indicated that MRE11 siRNA knockdown in U2OS cells results in significant reduction of RAD50 protein levels (Unpublished results from E. Kinoshita). Defining the biochemical activities of RAD50 provides insight into which activities are maintained in the absence of MRE11. This analysis also indicates which of the known activities, necessary for biological function, are modulated by MRE11. We confirmed that RAD50 binds and hydrolyzes ATP (Figures 2A, 2B and 2C) although our ATPase assay indicated that RAD50 alone is less active as an ATPase compared to RAD50 in the context of the MR complex. We additionally observed that RAD50 binds DNA (Figures 4A and 4B) and in the presence of ATP, DNA binding is increased due to the multimeric forms induced. Although our sensitive SFM imaging assay does reveal DNA binding in the absence of ATP, our results are consistent with a previous study showing that *S. cerevisiae* Rad50 binds DNA in an ATP-dependent manner (Raymond & Kleckner, 1993). Thus it appears that, as also implied by others, RAD50 has DNA binding sites indicating that DNA binding in the MR(N) complex is a combination of, and potential competition between, interactions of DNA with multiple sites in the protein complex. The availability of the RAD50, as well as MRE11 and NBS1 separately enable characterization of component-specific functions.

It is clear that ATP binding brings together the ATPase domains of Rad50 causing dramatic conformational changes in MR complexes (Lammens et al., 2011, Lim et al., 2011, Williams et al., 2011). We observe that dimeric RAD50 had a globular DNA binding head with coiled coils extending from it (Figure 3B), similar to that observed for MR (Figure 3E), where the ATPase domains of two RAD50s are in close proximity. The orientation and association of these specific domains of the two RAD50 molecules are

not determined from these images. The decreased ATPase activity of RAD50 compared to MR indicates that association with MRE11 organizes RAD50 in the MR complex such that the association of the ATPase domains is more efficient for catalysis. What was striking was the lack of extending coiled coils in the multimeric forms of RAD50, as extended coiled coils are always observed in our SFM images of MR(N) (de Jager et al., 2001; de Jager et al., 2002; van der Linden et al., 2009).

Oligomerization correlates with DNA binding in some assays. We observe weak binding by RAD50 in EMSA assays which is similar to EMSA results with MR complexes at very low concentrations. This suggests that the DNA binding detected in EMSAs is largely due to the oligomeric forms which are stable enough to be detected. Thus and at lower MR concentrations and on shorter DNA substrates there would be fewer oligomeric forms leading to less (stable) DNA binding. It was clear from the SFM images that RAD50 multimers are less abundant than those of MR and RAD50 does not make oligomers nor does it tether DNA. In addition, the lack of extended coiled coils in RAD50 multimers bound to DNA indicates that MRE11 has an important role in organizing RAD50 so that the coiled coils can function in DNA tethering and possibly other roles.

Our results suggest that MRE11 has an important role in maintaining the functional architectural arrangement of the MR protein complex. SFM imaging reveals that in the absence of MRE11 the arrangement of the long RAD50 coiled coils is dramatically different, specifically they disappear into a globular structure and are no longer extended when ATP is present and bound. A plausible explanation could be that the RAD50 coiled coils collapse or get entangled during ATP-induced protein reorientations if MRE11 is not associated to prevent this. The crystal structures of MR show that Mre11 binds to RAD50 via a helix-loop-helix (HLH) contacting the RAD50 coiled coils near their base (Lammens et al., 2011; Lim et al., 2011; Williams et al., 2011). Notably, in the absence of bound ATP the two Rad50 ATPase domains are separated on opposite sides of the Mre11 dimer more than 100 Å apart (Lammens et al., 2011; Lim et al., 2011; Williams et al., 2011; Wyman et al.,2011). Although ATP binding triggers a dramatic conformational change in MR that brings together the Rad50 ATPase domains, the Mre11 HLH domain is still bound at the base of the RAD50 coiled coils via a flexible linker domain of Mre11 (which connects the MRE11 HLH domain with the MRE11 nuclease domains). It is possible that the Mre11 HLH domains and the Mre11 flexible linker that lies along and outside the Rad50 coiled coils may support proper coiled coil conformations after ATP binding.

An important result of DNA binding by MR is the reorganization of the complex so that the coiled coils adopt a conformation that is effective for DNA tethering (Moreno-Herrero et al., 2005). Structural data on MR complexes (with shortened or truncated coiled coils) indicated that ATP-binding results in reorientation of Rad50 relative to Mre11 obscuring

some DNA binding sites and likely changing the orientation of the coiled coils (Lammens et al., 2011; Lim et al., 2011; Williams et al., 2011). DNA tethering likely involves inter-molecular interactions of human MR coiled coils (de Jager et al., 2002; Hofner et al., 2002; Hohl et al., 2011). The ATP induced increase in oligomeric MR together with the conformational change in the coiled coils caused by DNA would both contribute to efficient DNA tethering. This DNA tethering could play important roles in both HR and NHEJ. During HR, for example, the MR complex could tether the broken end and the intact sister chromatid. During NHEJ, on the other hand, the MR complex could tether the ends of the same sister chromatid.

REFERENCES

de Jager, M., van Noort, J., van Gent, D.C., Dekker, C., Kanaar, R., Wyman, C. (2001b). Human Rad50/Mre11 is a flexible complex that can tether DNA ends. Mol Cell *8*, 1129-1135.

de Jager, M., Wyman, C., van Gent, D.C., Kanaar, R. (2002). DNA end-binding specificity of human Rad50/Mre11 is influenced by ATP. Nucleic Acids Res *30*, 4425-4431.

Furuse, M., Nagase, Y., Tsubouchi, H., Murakami-Murofushi, K., Shibata, T., Ohta, K. (1998). Distinct roles of two separable in vitro activities of yeast Mre11 in mitotic and meiotic recombination. EMBO J *17(21)*, 6412-6425.

Hohl, M., Kwon, Y., Galvan, S.M., Sue, X., Tous, C., Aguilera, A., Sung, P., Petrini, J.H. (2011). The Rad50 coiled-coil domain is indispensable for Mre11 complex functions. Nat Struc Mol Biol *18(10)*, 1124-1131.

Hopfner, K.P., Karcher, A., Craig, L., Woo, T.T., Carney, J.P., Tainer, J.A. (2001). Structural biochemistry and interaction architecture of the DNA double-strand break repair Mre11 nuclease and Rad50-ATPase. Cell *105*, 473-485.

Hopfner, K.P., Karcher, A., Shin, D., Fairley, C., Tainer, J. A., Carney, J.P. (2000a). Mre11 and Rad50 from *Pyrococcus furiosus*: Cloning and biochemical characterization reveal an evolutionarily conserved multiprotein machine. J Bacteriol *182*, 6036-6041.

Hopfner, K.P., Karcher, A., Shin, D.S. et al. (2000b). Structural biology of Rad50 ATPase: ATP-driven conformational control in DNA double-strand break repair and the ABC ATPase superfamily. Cell *101*, 789-800.

Hopfner, K.P., Craig, L., Moncalian, G. et al. (2002). The Rad50 zinc-hook is a structure joining Mre11 complexes in DNA recombination and repair. Nature *418*, 562-566.

Krough, B.O., Llorente, B., Lam, A., Symington, L.S. (2005). Mutations in Mre11 phosphoesterase motif I that impair *Saccharomyces cerevisiae* Mre11-Rad50-Xrs2 complex stability in addition to nuclease activity. Genetics *171(4)*, 1561-1570.

Lammens, K., Bemeleit, D.J., Möckel, C. et al. (2011). The Mre11:Rad50 structure shows an ATP-dependent molecular clamp in DNA double-strand break repair. Cell *145(1)*, 54-66.

Lee, J.H., Ghirlando, R., Bhaskara, V., Hoffmeyer, M.R., Gu, J., Paull, T.T. (2003). Regulation of Mre11/Rad50 by Nbs1: effects on nucleotide-dependent DNA binding and association with ataxia-telangiectasia-like disorder mutant complexes. J Biol Chem *278*, 45171-45181.

Lim, H.S., Kim, J.S., Park, Y.B., Gwon, G.H., Cho, Y. (2011). Crystal structure of the Mre11-Rad50-ATPγS complex: understanding the interplay between Mre11 and Rad50. Genes Dev *25(10)*, 1091-1104.

Moreno-Herrero, F., de Jager, M., Dekker, N.H., Kanaar, R., Wyman, C., Dekker, C. (2005). Mesoscale conformational changes in the DNA-repair complex Rad50/Mre11/Nbs1 upon binding DNA. Nature *437*, 440-443.

Paull, T.T., Gellert, M. (1998). The 3' to 5' exonuclease activity of Mre11 facilitates repair of DNA double-strand breaks. Mol Cell *1*, 969-979.

Raymond, W.E., Kleckner, N. (1993). RAD50 protein of *S. cerevisiae* exhibits ATP-dependent DNA binding. Nucleic Acids Res *21*, 3851-3856.

Trujillo, K.M., Yuan, S.S., Lee, E.Y., Sung, P. (1998). Nuclease activities in a complex of human recombination and DNA repair factors Rad50, Mre11, and p95. J Biol Chem *273*, 21447-21450.

Usui, T., Ohta, T., Oshiumi, H. et al. (1998). Complex formation and functional versatility of Mre11 of budding yeast in recombination. Cell *95(5)*, 705-716.

van der Linden, E., Sanchez, H., Kinoshita, E., Kanaar, R., Wyman, C. (2009). RAD50 and NBS1 form a stable complex functional in DNA binding and tethering. Nucleic Acids Res *37*, 1580-1588.

Williams, R.S., Moncalian, G., Williams, J.S. et al. (2008). Mre11 dimers coordinate DNA end bridging and nuclease processing in double-strand-break repair. Cell *135(1)*, 97-109.

Williams, G.J., Williams, R.S., Williams, J.S. et al. (2011). ABC ATPase signature helices in Rad50 link nucleotide state to Mre11 interface for DNA repair. Nat Struc Mol Biol *18(4)*, 423-431.

Wyman, C., Lebbink, J., Kanaar, R. (2011). Mre11-Rad50 complex crystals suggest molecular calisthenics. DNA Repair (Amst) *10(10)*, 1066-1070.

CHAPTER 3

RAD50 and NBS1 form a stable complex functional in DNA binding and tethering

Eddy van der Linden[1], Humberto Sanchez[1], Eri Kinoshita[1], Roland Kanaar[1,2] and Claire Wyman[1,2]

[1]Department of Cell Biology & Genetics, Cancer Genomics Center and [2]Department of Radiation Oncology, Erasmus MC, PO Box 2040, 3000 CA Rotterdam, The Netherlands

Published in: Nucleic Acids Research 2009 *37(5)*, 1580-1588.

ABSTRACT

The RAD50/MRE11/NBS1 protein complex (RMN) plays an essential role during the early steps of DNA double-strand break (DSB) repair by homologous recombination. Previous data suggest that one important role for RMN in DSB repair is to provide a link between DNA ends. The striking architecture of the complex, a globular domain from which two extended coiled coils protrude, is essential for this function. Due to its DNA-binding activity, ability to form dimers and interact with both RAD50 and NBS1, MRE11 is considered to be crucial for formation and function of RMN. Here, we show the successful expression and purification of a stable complex containing only RAD50 and NBS1 (RN). The characteristic architecture of the complex was not affected by absence of MRE11. Although MRE11 is a DNA-binding protein it was not required for DNA binding *per se* or DNA-tethering activity of the complex. The stoichiometry of NBS1 in RMN and RN complexes was estimated by SFM-based volume analysis. These data show that *in vitro*, R, M and N form a variety of stable complexes with variable subunit composition and stoichiometry, which may be physiologically relevant in different aspects of RMN function.

INTRODUCTION

DNA double-strand breaks (DSBs) can be caused by endogenous or exogenous DNA-damaging agents. Unrepaired DSBs can be lethal, whereas misrepaired DSBs can cause chromosomal fragmentation, translocations and deletions. The resulting genome instability is a common precursor to carcinogenesis and therefore, effective repair of DSBs is of great importance (Su et al., 2006). DSB repair involves several processes including recognition of DNA breaks, activation of cell-cycle checkpoints and eventual restoration of intact chromosomes. In eukaryotic cells DSB repair can occur by one of two distinct mechanisms, non-homologous end joining (NHEJ) and homologous recombination (HR) (Khanna & Jackson, 2001; Valerie & Povirk, 2003; van Gent et al., 2001). The RAD50/MRE11/NBS1 (RMN) protein complex is a required component during the early steps of HR (Borde et al., 2004; Lisby et al., 2004). The essential role of RMN is underscored by the fact that null mutations in genes encoding any of the three subunits are embryonic lethal in mice (Luo et al., 1999; Xiao & Weaver, 1997; Zhu et al., 2001). Similarly, both budding and fission yeast cells deleted for RMN subunits have severe DNA-damage sensitivity phenotypes (Chahwan et al., 2003; D'Amours & Jackson, 2002, Paques & Haber, 1999). In humans, hypomorphic mutations in the genes encoding RMN components cause genetic disorders characterized by marked cancer predisposition. The NBS1 gene gets its name from the human autosomal recessive disorder Nijmegen Breakage syndrome (NBS) (Varon et al., 1998). Mutations in MRE11 cause ataxia-telangiectasia-like disorder (ATLD), constituting a subset of the phenotype of patients with NBS (Stewart et al., 1999).

The RMN complex has a striking architecture that is crucial for its function (de Jager et al., 2001). The well-defined RM complex is a heterotetrameric assembly of two RAD50 and two MRE11 molecules (R_2M_2) (Hopfner et al., 2001). The RAD50 amino acid sequence has a long region predicted to form a coiled-coil domain separating the Walker A- and B-amino-acid motifs of an ATPase domain. The RAD50 polypeptide folds back on itself forming a 50-nm coiled coil, which juxtaposes the N- and C-termini to constitute a functional ATP binding and hydrolyzing head (de Jager et al., 2001a; Hopfner et al., 2001). The role of ATP binding and hydrolysis in RM function has not been entirely defined. The distinct 50-nm-long coiled coil is a notably flexible structure (van Noort et al., 2003). The coiled-coil apex consists of a pair of cysteine residues that can coordinate a Zn ion and pair with two analogous cysteines from another RAD50 apex (Hopfner et al., 2002; Wiltzius et al., 2005; Cahill & Carney, 2007). In the complex, MRE11 interacts with itself and with the RAD50 coiled coils near the connection to the ATPase domain, forming a stable heterotetramer (Hopfner et al., 2001; Wiltzius et al., 2005). Several DNA-processing activities of MRE11 have been demonstrated *in vitro* including, DNA binding, DNA annealing, Mn^{2+}-dependent 3′ to 5′ dsDNA exonuclease, ssDNA endonuclease and DNA duplex unwinding (D'Amours

& Jackson, 2002; Carney et al., 1998; Moncalian et al., 2004; Paull & Gellert, 1998; Paull & Gellert, 1999; de Jager et al., 2001b; Hopfner et al., 2001; Furuse et al., 1998; Trujillo et al., 1999). In some *in vitro* situations these activities are influenced by association with RAD50 and NBS1 (D'Amours & Jackson, 2002; Carney et al., 1998; Moncalian et al., 2004; Paull & Gellert, 1998; Paull & Gellert, 1999). Recently, MRE11 has been shown to be crucial for initiation and coordination of DNA end-processing during DSB repair (Williams et al., 2008; Buis et al., 2008; Hopkins & Paull, 2008; Zhu et al., 2008; Mimitou & Symington, 2008). MRE11 is also expected to be crucial for NBS1 association with the complex, based on a reduced association of NBS1 in the presence of an MRE11 allele associated with ATLD (ATLD¾) (Lee et al., 2003), and the purification of a stable complex containing only MRE11 and NBS1 (Stewart et al., 1999).

NBS1 is involved in signaling the presence of DNA damage to effect a cell-cycle checkpoint (Khanna & Jackson, 2001; D'Amours & Jackson, 2002; Assenmacher & Hopfner, 2004; van den Bosch et al., 2003; You et al., 2005). DSB-repair-associated cell-cycle signaling occurs through NBS1 mediated activation of the ATM kinase (Lee & Paull, 2004; Lee & Paull, 2005). ATM activation is currently thought to involve interaction with NBS1 (Berkovich et al., 2007; Stracker et al., 2007) in the RMN complex bound to DNA at the site of breaks. This interaction is proposed to cause dissociation of inactive ATM dimers, creating kinase active ATM monomers (You et al., 2005; Lee & Paull, 2005). Activated ATM effects on the cell cycle and DNA-damage response occur though phosphorylation of downstream target proteins (Matsuoka et al., 2007). However, the architectural arrangement of protein components that contribute to these NBS1-specific functions has not been determined.

The diverse functions of RMN in DSB repair all involve interaction with DNA, and depend on the specific architecture of this protein complex. DNA is bound by the globular domains that include the RAD50 ATPase active site and MRE11, whereas the RAD50 coiled coils protrude away from DNA (de Jager et al., 2001). On linear double-stranded (ds) DNA, this results in the accumulation of large RMN oligomers that tether DNA molecules via interaction of the RMN coiled coils (de Jager et al., 2001; Hopfner et al., 2002; Wiltzius et al., 2004; Wyman & Kanaar, 2002). DNA is an allosteric effector of the RMN complex as binding DNA at the globular domain induces an ATP-independent reorientation of the RAD50 coiled coils to become parallel to one another (Moreno-Herrero et al., 2005). This latter orientation disables intracomplex association of the coiled-coil apexes, and thus stimulates the intercomplex interactions needed for DNA tethering. These observations all imply an important role for RMN in DSB repair organizing broken DNA strands. The above observations suggest that MRE11 has a crucial role in this process being a central element of the complex involved in

protein architecture and of protein–DNA interaction (Williams et al., 2007). However, Mre11 was not present in Rad50 originally purified from *Saccharomyces cerevisiae*, which nevertheless appears to be a dimeric protein and also binds DNA (Raymond & Kleckner, 1993). The reduced levels of NBS1 in purified RAD50/MRE11-(ATLD¾)/NBS1 preparations are presumably due to altered MRE11–NBS1 interaction. This observation does not exclude the presence of additional NBS1 interaction sites on RAD50.

Here, we show the successful expression and purification of a complex containing only RAD50 and NBS1. Scanning force microscopy (SFM) analysis of purified RN preparations showed that RN, like RM and RMN, formed dimers as well as higher-order multimers. SFM-based volume analysis of different $(RAD50)_2$ complexes further identified RN and RMN to be mixtures of at least two different species with different stoichiometry, the main fractions nicely fitting an R_2N_2 (RN) and $R_2M_2N_2$ (RMN) stoichiometry. In addition, we observed that RN is more active in DNA-binding and -tethering assays than RM and RMN.

MATERIALS & METHODS

Protein expression and purification

Human RM, RMN and RN preparations were produced by co-infection of Sf21 cells (7500 cm^2) in adherent culture with baculoviruses expressing C-terminally 6-histidine tagged RAD50, untagged MRE11 (RM and RMN) and untagged NBS1 (RMN and RN) at an MOI of ~10 (constructs for viruses were a generous gift from T. Paull and M. Gellert). Cells were harvested after 72 h. The purification procedure was based on a method described previously (Lee & Paull, 2006). Briefly, infected cells were collected, washed three times in PBS and frozen in liquid nitrogen. Cells were thawed and re-suspended in 40 ml cold buffer A (50 mM KH_2PO_4, pH 7.0, 0.5 M NaCl, 0.5% Tween 20, 10% glycerol, 20 mM β-mercaptoethanol, 10% glycerol) containing 5 mM imidazole and 1 mM Pefablock (Merck). Then, the cells were disrupted by 30 strokes of a type B pestle in a Dounce homogenizer. After 1 h of centrifugation at 100 000 *g*, the soluble fraction was loaded on a 3-ml Ni^{2+}-NTA agarose column (Qiagen), equilibrated in buffer A containing 5 mM imidazole. The column was washed with 10 vol. of the same buffer and then with 10 vol. of buffer A containing 40 mM imidazole. Bound proteins were eluted in buffer A containing 125 mM imidazole. RAD50 containing fractions were pooled and dialysed against buffer B (20 mM Tris–HCl, pH 8.0, 100 mM NaCl, 10% glycerol, 1 mM DTT). This preparation was loaded on a 1 ml Resource Q column (GE Healthcare) equilibrated in buffer B. After washing the column with 10 column volumes, the proteins were eluted by a 10 ml linear salt gradient from 100 mM to 800 mM NaCl. After addition of Tween 20 (0.1% final concentration), the pooled fractions were loaded

on a Superdex 200 size-exclusion column (GE Healthcare) that was equilibrated in buffer B containing 0.1% Tween 20. (For purification of RMN and RN, buffer B containing 500 mM NaCl was used.) RAD50 complex containing fractions were pooled, aliquoted and frozen in liquid nitrogen. Immunoblotting of RAD50, MRE11 and NBS1 was performed with antibodies MS-RAD10 (GeneTex), PC388 (Oncogene) and sc-8580 (Santa Cruz) respectively, on nitrocellulose transfer membrane (Whatman) using standard immuno-blotting techniques. Protein concentrations were determined by the Bradford method, using BSA as a standard (Bradford, 1976).

SFM analysis

RAD50 stoichiometry

Protein preparations were diluted in protein buffer (20 mM Tris–HCl, pH 8.0, 100 mM NaCl, 10% glycerol, 1 mM DTT, 0.1% Tween 20). Five to 15 ng of protein was deposited on freshly cleaved mica. After ~1 min the mica was rinsed with glass-distilled water (Sigma) and dried with filtered air. Samples were imaged in air at room temperature and humidity by tapping mode SFM using a Nanoscope IV (Digital Instruments). Silicon Nanotips were from Digital Instruments (Nanoprobes). Images were collected at 1 μm × 1 μm, and processed only by flattening to remove background slope. RAD50 stoichiometry was determined by counting the number of 50-nm long coiled coils of individual RAD50 complexes. Relative occurrence of different conformations was determined for all three protein preparations (RM, RMN and RN) from 400–600 individual complexes each.

SFM-based volume analysis

The volume of the globular part of complexes from the three protein preparations was derived from images obtained as described above, but here, only dimeric RAD50 complexes (two coiled coils) were selected. Such dimeric complexes were used for volume analysis of their globular part. Volume analysis was also performed on whole dimeric RM complexes (globular part + coiled coils). Volume determination was performed on images imported into IMAGE SXM 1.69 (National Institutes of Health IMAGE version modified by Steve Barrett, Surface Science Research Centre, University of Liverpool, Liverpool, UK). The average height and area of a manually defined object was used to calculate a volume in arbitrary pixel units. The average volume of three adjacent background regions was then subtracted to determine the volume (Wyman et al., 1997). As RM has a known R_2M_2 stoichiometry (Hopfner et al., 2001; Lee et al., 2003), the volume of this complex was assumed to represent R_2M_2, which was used as a basis for the calculation of mass and stoichiometry of the other RAD50 complexes. For each protein preparation between 258 and 318 complexes were analyzed, and from these data, a Gaussian distribution was calculated using Origin software (OriginLab Corporation,

USA). As an internal control, the mass of RM was also determined as described before (Verhoeven et al., 2002) via comparison of the measured volume for RM with the volume that was determined for the Ku70/80 heterodimer, which has a known mass of 155 kDa.

DNA tethering reactions

EcoRV linearized pBluescript plasmid was incubated at 1.5 nM with 36 nM RAD50 complex (expressed with respect to RAD50) in binding buffer (20 mM Tris–HCl, pH 8.0, 100 mM NaCl, 10% glycerol, 0.1% Tween 20) for 15 min at 25°C in a volume of 80 µl. Reactions were diluted 8-fold in deposition buffer (10 mM HEPES-KOH, pH 8.0, 10 mM $MgCl_2$), deposited and imaged by SFM as described above. DNA tethering was quantified by determining the number of DNA tethers, the volume of each tether, the number of free DNA molecules and the number of DNA molecules involved in tethering from 32 images (8 µm × 8 µm) for each protein preparation. To determine the number of DNA molecules that were tethered, each DNA molecule coming out of a tether that was visible for more than 50% was counted as one whereas shorter pieces were counted as 0.5.

Electrophoretic mobility shift assays (EMSAs)

Aliquots of $dsDNA_{66}$ (5′-AF 532-AGA AAC TGG GCA TGT GGA GAC AGA GAA GAC TCT TGG GTT TCT GAT AGG CAC TGA CTC TCT CTG CCT-3′ annealed to its complementary oligo 5′-AGG CAG AGA GAG TCA GTG CCT ATC AGA AAC CCA AGA GTC TTC TCT GTC TCC ACA TGC CCA GTT TCT-3′ from Eurogentec S.A.) labelled with Alexa Fluor at the 5′ end of the upper strand (1 nM) were incubated with the indicated amounts of protein complex in binding buffer (5% glycerol, 25 mM Tris–HCl, pH 7.5, 100 mM KCl, 5 mM $MgCl_2$, 1 mM DTT and 2% PEG-6000) for 20 min at 25°C, in a final volume of 20 µl. The reactions products were separated on a 5% non-denaturing polyacrylamide gel running in 0.5 × TBE buffer at 4°C. The labelled DNA was visualized by direct scanning of the wet gel with a 532-nm laser using an image analyser (Typhoon 9200). The emission signal was sorted with a 555BP20-nm filter. Quantification of the data was performed with ImageQuant 5.2 software. To check the protein preparations for contaminant nuclease activity, protein (125 ng) was also incubated with DNA (1 nM) as described above and then subjected to an additional incubation at 37°C in the presence or absence of proteinase K (1 mg/ml). Separation and analysis of complexes formed was performed as described above.

RESULTS

During purification of RMN, some preparations included fractions containing mainly RAD50 and NBS1 (Supplementary Figure S1A). Thus, we pursued the possibility that RAD50 and NBS1 might form a stable complex. Native polyacrylamide gel electrophoresis (PAGE)

analysis of such RAD50 and NBS1 containing fractions confirmed that both proteins were indeed part of the same RAD50/NBS1 complex (Supplementary Figure S1B). To see if an RN complex could also be formed in the absence of MRE11, we expressed RN in Sf21 cells that were co-infected with only the baculoviruses expressing C-terminally 6-histidine tagged RAD50, and untagged NBS1. Indeed, we successfully purified RN, showing that in addition to RM and RMN, RN is also a stable protein complex that can be individually expressed and purified (Figure 1A). Immunoblotting analysis confirmed the unambiguous identity of RAD50, MRE11 and NBS1, as expected in the three purified complexes (Figure 1B).

SFM imaging showed that RN looks very similar to RM and RMN with a clear globular domain from which about 50-nm-long coiled coils protrude (Figure 2). Furthermore, RN as well as RM and RMN were all inhomogeneous mixtures of complexes with different amounts of RAD50. By counting the number of coiled coils of individual complexes, they were classified as monomeric, dimeric or multimeric with respect to RAD50. The distribution of complexes with these RAD50 stoichiometries differed among the RMN,

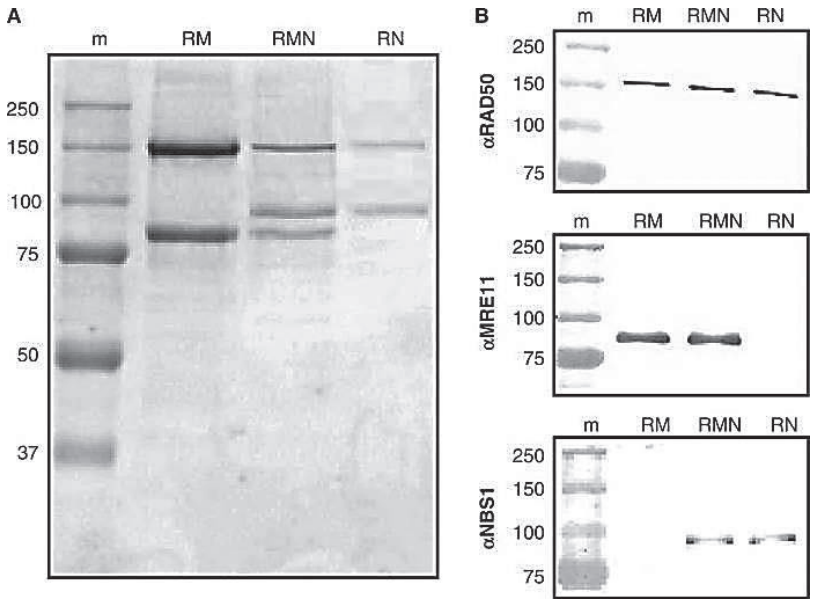

Figure 1. (A) Coomassie stained SDS-PAGE gel of purified protein preparations. Lane 1, molecular size marker (m, molecular mass indicated in kilo Dalton), Lane 2, RAD50/MRE11 complex (RM), Lane 3, RAD50/MRE11/NBS1 complex (RMN), Lane 4, RAD50/NBS1 complex (RN). (B) Immunoblotting analysis of purified proteins. Blots containing purified RM, RMN and RN preparations were probed with antibodies directed against RAD50, MRE11 and NBS1, as indicated.

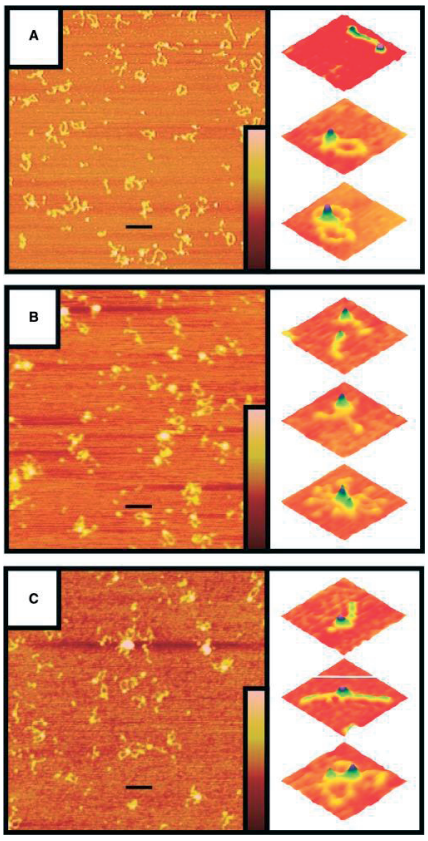

Figure 2. SFM analysis of RM (A), RMN (B) and RN preparations (C). Purified protein was deposited on mica and imaged by tapping mode SFM at 1 μm × 1 μm scale in air (left panels). The scale bars are 100 nm. The color bars represent the height from 0 to 3 nm (brown to pink). The right panels are examples of individual complexes enlarged and presented as surface plots (0.105 μm × 0.105 μm scale) in which RAD50 has a monomeric (I), dimeric (II) or multimeric (III) stoichiometry.

Table 1. Distribution of RAD50 stoichiometry on the different purified protein.

	RAD50 monomers	RAD50 dimers	RAD50 multimers
	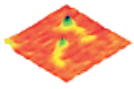	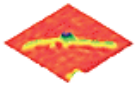	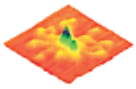
RM (%)	11	86	3
RMN (%)	15	46	39
RN (%)	12	17	71

RM and RN protein preparations (Table 1). For all three preparations, between 11 and 15% of the complexes were monomeric. For RM, the majority of remaining complexes was dimeric (86%). For RMN, on the other hand, dimeric and multimeric complexes were almost equally prevalent, while for RN, the multimeric form was most common. More than 95% of the multimers observed for all preparations was formed via interaction of the globular domains. The above data suggest that the presence of NBS1 as a part of the complex stimulates multimerization via interaction of the globular domains, whereas the presence of MRE11 reduces multimerization.

A heterotetrameric (R_2M_2) complex is formed by the archaeal homolog and this stoichiometry is assumed to be general (Hopfner et al., 2001). Although the above data clearly show the presence of monomeric and multimeric RM complexes, the dimeric RAD50 complex is indeed the most abundant form. In contrast to RM, the stoichiometry of RMN and the newly purified RN complex are not well characterized. We estimated the stoichiometry of RN and RMN, by SFM-based volume analysis on the different protein preparations. Dimeric RAD50 complexes were selected from SFM images of the different purified protein preparations. Such dimeric complexes were used to determine the volume of their globular part. The volume distributions were plotted in histograms and Gaussian distributions were calculated (Figure 3). Volume analysis was also performed on whole dimeric complexes (globular part + coiled coils) to determine the volume of the coiled coils separately, and thus also the volume of the dimeric complexes as a whole. As RM has a known R_2M_2 stoichiometry (Hopfner et al., 2001; Lee et al., 2003), the measured volume for RM (globular part + coiled coils) was assumed to represent R_2M_2 and was used as a basis for calculating the mass and stoichiometry of the other RAD50 complexes (Table 2). To check this assumption, the molecular mass of RM was also calculated by performing a volume determination on the Ku70/80 heterodimer with a known mass of 155 kDa (Supplementary Figure S2). By multiplying the measured number of Ku70/80 equivalents for RM with the size of the Ku70/80 protein, the molecular weight of RM was determined to be 444 kDa, which is close to the 473 kDa as determined by its amino acid sequence, assuming an R_2M_2 stoichiometry.

The distribution of volumes for RMN and RN were best fit by two Gaussians, indicating that both preparations contain two components, low and high molecular weight (Figure 3B and 3C). For RN, the more prevalent, low-molecular-weight complex correlated with an R_2N_2 stoichiometry (R_2N_n, $n = 1.95 \pm 0.16$) while the less abundant high-molecular-weight complex nicely fits a R_2N_4 stoichiometry (R_2N_n, $n = 3.79 \pm 0.20$). For RMN, the determined volume of the low-molecular-weight species corresponds to a molecular mass of 586 ± 22 kDa. This fits a stoichiometry of $R_2(M+N)_n$ with n being 1.65 ± 0.14. For the high-molecular-weight species this mass is 794 ± 34 kDa correlating with a stoichiometry of

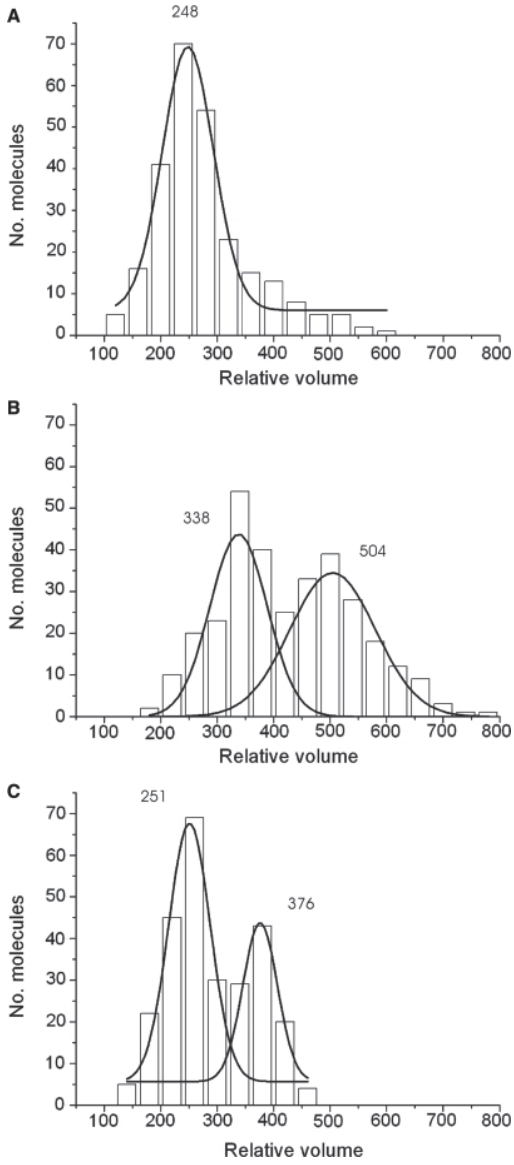

Figure 3. The volume distributions of the globular part for RM (A), RMN (B) and RN (C) are presented in histograms. Purified protein was deposited on mica and imaged by tapping mode SFM at 1 μm × 1 μm scale in air. From such images isolated dimeric RAD50 complexes were selected for volume determination of the globular part. The x-axis is the relative molecular volume obtained from the SFM data, the y-axis is the number of protein molecules in each peak. A Gaussian distribution was calculated for the data and is displayed as a solid black line. The average volumes estimated from the Gaussian distributions are shown above each peak.

Table 2. Estimated mass of different RAD50 complexes measured by SFM-based volume analysis.

Protein / Fraction	SFM-based volume	Mass	Stoichiometry[a]
RM	379 ± 9[b]	473[a]	R_2M_2[a]
RMN (low MW fraction)	469 ± 18	586 ± 22	$R_2(M+N)_n$, n = 1.65 ± 0.14
RMN (high MW fraction)	635 ± 28	794 ± 34	$R_2(M+N)_n$, n = 2.91 ± 0.21
RN (low MW fraction)	382 ± 10	477 ± 13	R_2N_n, n = 1.95 ± 0.16
RN (high MW fraction)	507 ± 13	633 ± 17	R_2N_n, n = 3.79 ± 0.20

[a]RM with its known R2M2 stoichiometry is used as a basis for the calculation of mass and stoichiometry of the other RAD50 complexes. Molecular weight of each polypeptide including C-terminal histidine tag on RAD50 (kDa): RAD50, 155.70; MRE11, 81.03; NBS1, 84.91.

[b]Determined volumes and masses are represented by the mean ± SE.

$R_2(M+N)_n$ with n being 2.91 ± 0.21. Within this method, we are not able to discriminate between MRE11 and NBS1. However, if we assume MRE11 to be present as a dimer in both complexes, the calculated NBS1 stoichiometry in both complexes becomes 1.32 ± 0.26 for the low-molecular-weight complex and 3.77 ± 0.41 for the high-molecular-weight complex.

Due to its ability to form dimers and to interact with both RAD50 and NBS1, MRE11 is considered to be crucial in the formation of stable RMN complexes (Williams et al., 2007). Here, we see that RN also forms a stable dimeric protein complex with an architecture similar to RM and RMN. As MRE11 is able to bind DNA by itself, it is also considered to be an important factor in the DNA-binding and -tethering activities of RMN. To address the role of MRE11 in DNA binding, we performed EMSAs for the different purified preparations in the presence of linear dsDNA using non-denaturing PAGE (Figure 4). The DNA-binding affinity for each complex was determined via quantification of the remaining free DNA after incubation with increasing concentrations of protein complex. Disappearance of the free DNA was not due to contaminant nuclease activity, as for all preparations, treatment with proteinase K led to reappearance of the unbound DNA (Supplementary Figure S3). Surprisingly, we observed that RN is more active in DNA binding than RM and RMN. The amount of RAD50 protein complex needed for binding 50% of the DNA was 58, 32 and 8 ng, corresponding to 6.1, 2.5 and 0.8 nM for RM (R_2M_2), RMN ($R_2M_2N_2$) and RN (R_2N_2), respectively, at 1 nM of DNA. This means that the presence of MRE11 modulates DNA-binding activity of RAD50 containing complexes negatively, whereas NBS1 stimulates this activity.

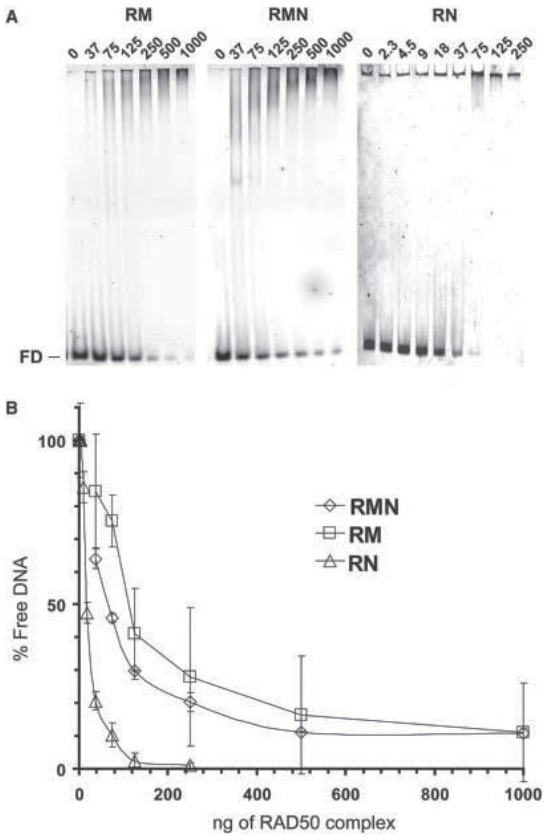

Figure 4. DNA binding by RM, RMN and RN. (A) Alexa Fluor 532 labeled dsDNA66 (1 nM), was incubated with RM (37, 75, 125, 250, 500 and 1000 ng), RMN (idem) or RN (2.3, 4.5, 9, 18, 37, 75, 125 and 250 ng) for 20 min at 25°C in a final volume of 20 µl. Complexes formed were separated by 5% non-denaturing PAGE and visualized by fluorescence scanning. FD, free DNA. (B) Free DNA was quantified and plotted against the amounts of protein added.

We also tested the importance of MRE11 for the DNA-tethering activity of RAD50 complexes by SFM imaging. We incubated the protein with 3 kb linear DNA and deposited it for SFM imaging, where tethering is defined as association of DNA molecules via interaction between bound RAD50 complex multimers. RM and RMN have previously been shown to possess DNA-tethering activity (de Jager et al., 2001; Hopfner et al., 2002; Wiltzius et al., 2005; Wyman & Kanaar, 2002), which we also observe here (Figure 5A and 5B). In addition, we also observed that RN is fully functional in DNA tethering activity (Figure 5C). The RN preparation appeared more active in DNA tethering based on three

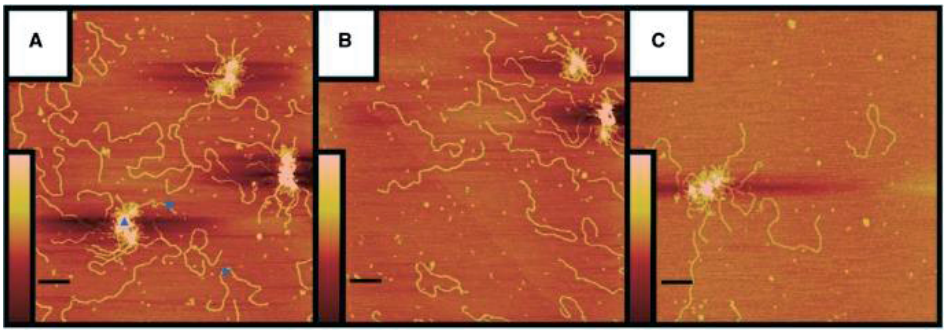

Figure 5. DNA tethering by RM (A), RMN (B) and RN (C). Reaction mixtures containing 15 nM of 3.0-kb linear DNA fragment and 25 nM of purified protein were deposited on mica and imaged by tapping mode SFM. The scale bars are 200 nm. Color represents height from 0 to 3 nm (brown to pink), as shown by the inserts. DNA tethers (triangle), free DNA molecules (star) and DNA molecules involved in DNA tethering (circle) were all quantified as described in 'Materials and Methods' section.

different quantifications from the SFM images, (i) a higher ratio of tethered complexes to free DNA (RN = 1, 9.4, RM = 1, 21.7 and RMN = 1, 17.2), (ii) larger average volume of tethered complexes (RN = 254 000 nm^3, RM = 133 000 nm^3 and RMN = 157 000 nm^3) and (iii) higher percentage of DNA in tethered complexes (RN = 30%, RM = 16% and RMN = 20%). Together, this shows that RAD50 and NBS1 can form a stable complex that maintains its characteristic architecture and that is fully functional in the DNA-binding and the DNA-tethering assays.

DISCUSSION

It is generally accepted that RMN plays an essential role in the early steps of DSB repair. The multiple roles that RMN may have during this process are, however, not yet all clearly defined. Several lines of evidence indicate that one important role for RMN in DSB repair is to link broken DNA ends. Due to its DNA-binding activity and ability to bind RAD50 and NBS1, MRE11 is considered as the central element of the complex involved in protein–protein and protein–DNA interaction. The ability of MRE11 to homodimerize is considered crucial for formation of a functional dimeric RMN complex (Williams et al., 2008).

Here, we show that, in addition to RM and RMN, RN is also a stable protein complex with a similar molecular architecture. This shows that RAD50 is able to directly interact with NBS1. Previous data suggested that NBS1 binding to the complex is linked to MRE11 (Stewart et al., 1999; Lee et al., 2003). However, the presence of NBS1 interaction sites on RAD50 cannot be excluded. It is even possible that MRE11 and NBS1 compete for

binding in the complex, or that RAD50 and MRE11 both contribute to NBS1 interaction. The latter would also explain the reduced yield of protein upon purifying RN compared to MRE11-containing complexes (Figure 1A).

We show that a protein complex with dimeric RAD50 does not depend on the presence of MRE11. This is in line with the observation that purified Rad50 from *S. cerevisiae* was a dimeric protein by itself (Raymond & Kleckner, 1993). In our SFM assay mulitimerization of the protein complex is an important aspect of DNA tethering. In that respect, it is interesting to see that the presence of NBS1 stimulates multimerization, whereas the presence of MRE11 seems to inhibit such globular domain interactions.

A previous sedimentation equilibrium analysis of RMN failed to assign a clear stoichiometry for the components and suggested that this complex may exist as a mixture with different stoichiometries (Lee et al., 2003). Indeed, our SFM-based single-particle volume analysis shows that both RMN and RN are mixtures of at least two complexes with different stoichiometry. For RN, the low- and high-molecular-weight complexes nicely correlate with an R_2N_2 and R_2N_4 stoichiometry. For RMN, we cannot discriminate between MRE11 and NBS1, but assuming that MRE11 is present in both complexes as a dimer, the calculated stoichiometry for the two RMN species is $R_2M_2N_n$ with n being 1.32 for the low-molecular-weight species, and *n* being 3.77 for the high-molecular-weight species. The existence of the latter complex is in line with the relative intensity of Coomassie staining bands on denaturing polyacrylamide gels of purified RMN preparations, where the NBS1 band is up to 1.5 times more intense than the MRE11 band (Figure1A).

Because MRE11 binds DNA by itself, it is also considered centrally important for the DNA-binding and -tethering activity of RMN. Here we see that this is not the case. The RN complex is more active than RMN in both DNA-binding and -tethering activity. Surprisingly, RM appeared to be the least active in DNA binding and tethering. The increased activity for RN in DNA tethering could reflect the increased affinity to bind DNA as well as the preference of RN to form the oligomeric protein complexes required for DNA tethering (de Jager et al., 2001).

These data present a new picture of the RMN complex. Biochemically functional complexes exist with a variety of subunit stoichiometries but all with the same striking architecture. The different components appear to modulate protein oligomerization. This raises the possibility that RAD50 participates in a variety of complexes where dynamic interchange of component parts may modulate biological function. An example of such behaviour is observed at human telomeres where RAD50 and MRE11 are present during interphase, whereas NBS1 is only present during S-phase, and not in G1 or G2 (Verhoeven et al., 2002). Here, the transient recruitment of NBS1 in S-phase is hypothesized to play a role in telomere replication as addition of NBS1 to RM potentiates activities that

could play an important role in the opening of the t-loop facilitating progression of DNA replication to the end of the chromosome. Although MRE11 is clearly an essential protein, it may not contribute to all functions attributed to RMN. For instance, during HR-mediated DSB repair, there might be times where DNA tethering is required but where the nuclease activity contributed by MRE11 is not. The specific role of the different RMN components in biochemical functions can now be addressed.

SUPPLEMENTARY DATA

Supplementary Data are available at NAR Online.

FUNDING

The European Commission (IP 512113 and IP 503259); the Netherlands Genomics Initiative/Netherlands Organization for Scientific Research (NWO); NCI (USA) (SBDR 5PO1CA092584); NWO-Chemical Sciences TOP; and the Dutch Cancer Society (H.S. is a

Marie Currie fellow and C.W. is the recipient of an NWO Vici award). Funding for open access charge: NWO-Chemical Sciences Vici award. Conflict of interest statement. None declared.

REFERENCES

Assenmacher, N., Hopfner, K.P. (2004). MRE11/RAD50/NBS1, complex activities. Chromosoma *113*, 157-166.

Berkovich, E., Monnat, R.J. Jr., Kastan, M.B. (2007). Roles of ATM and NBS1 in chromatin structure modulation and DNA double-strand break repair. Nat Cell Biol *9*, 683-690.

Borde, V., Lin, W., Novikov, E., Petrini, J.H., Lichten, M., Nicolas, A. (2004). Association of Mre11p with double-strand break sites during yeast meiosis. Mol. Cell *13*, 389-401.

Bradford, M.M. (1976). A rapid and sensitive method for the quantification of microgram quantities of protein utilizing the principles of protein-dye binding. Anal Biochem *72*, 248-254.

Buis, J., Wu, Y., Deng, Y., Leddon, J., Westfield, G., Eckersdorff, M., Sekiguchi, J.M., Chang, S., Ferguson, D.O. (2008). Mre11 nuclease activity has essential roles in DNA repair and genomic stability distinct from ATM activation. Cell *135*, 85-96.

Cahill, D., Carney, J.P. (2007). Dimerization of the Rad50 protein is independent of the conserved hook domain. Mutagenesis *22*, 269-274.

Carney, J.P., Maser, R.S., Olivares. H., Davis, E.M., Le Beau, M., Yates, J.R., Hays, L., Morgan, W.F., Petrini, J.H.J. (1998). The hMre11/hRad50 protein complex and Nijmegen breakage syndrome, linkage of double-strand break repair to the cellular DNA damage response. Cell *93*, 477-486.

Chahwan, C., Nakamura, T.M., Sivakumar, S., Russell, P., Rhind, N. (2003). The fission yeast Rad32 (Mre11)-Rad50-Nbs1 complex is required for the S-phase DNA damage checkpoint. Mol Cell Biol *23*, 6564-6573.

D'Amours, D., Jackson, S.P. (2002). The MRE11 complex, at the crossroads of DNA repair and checkpoint signalling. Nat Rev Mol Cell Biol *3*, 317-327.

de Jager, M., Dronkert, M.L.G., Modesti, M., Beerens, C.E.M.T., Kanaar, R., van Gent, D.C. (2001a). DNA-binding and strand-annealing activities of human Mre11, implications for its roles in DNA double-strand break repair pathways. Nucleic Acids Res *29*, 1317-1325.

de Jager, M., van Noort, J., van Gent, D., Dekker, C., Kanaar, R., Wyman, C. (2001b). Human Rad50/Mre11 is a flexible complex that can tether DNA ends. Mol. Cell *8*, 1129-1135.

Furuse, M., Nagase, Y., Tsubouchi, H., Murakami-Murofushi, K., Shibata, T., Ohta, K. (1998). Distinct roles of two separable in vitro activities of yeast Mre11 in mitotic and meiotic recombination. EMBO J *17*, 6412-6425.

Hopfner, K.P., Karcher, A., Craig, L., Woo, T.T., Carney, J.P., Tainer, J.A. (2001). Structural biochemistry and interaction architecture of the DNA double-strand break repair Mre11 nuclease and Rad50-ATPase. Cell *105*, 473-485.

Hopfner, K.P., Craig, L., Moncalian, G., Zinkel, R.A., Usui, T., Owen, B.A.L., Karcher, A., Henderson, B., Bodmer, J.L., McMurray, C.T., et al. (2002). The Rad50 zinc-hook is a structure joining Mre11 complexes in DNA recombination and repair. Nature *418*, 562-566.

Hopfner, K.P., Karcher, A., Shin, D.S., Craig, L., Arthur, L.M., Carney, J.P., Tainer, J.A. (2000). Structural biology of Rad50 ATPase, ATP-driven conformational control in DNA double-strand break repair and the ABC-ATPase superfamily. Cell *101*, 789-800.

Hopfner, K.P., Karcher, A., Shin, D.S., Fairley, C., Tainer, J.A., Carney, J.P. (2000). Mre11 and Rad50 from Pyrococcus furiosus, Cloning and biochemical characterization reveal an evolutionarily conserved multiprotein machine. J Bacteriol *182*, 6036-6041.

Hopkins, B.B., Paull, T.T. (2008). The P. furiosus Mre11/Rad50 complex promotes 5' strand resection at a DNA double-strand break. Cell *135*, 250-260.

Khanna, K.K., Jackson, S.P. (2001). DNA double-strand breaks, signalling, repair and the cancer connection. Nat Gen *27*, 247-254.

Lee, J.H., Ghirlando, R., Bhaskara, V., Hoffmeyer, M.R., Gu, J., Paull, T.T. (2003). Regulation of Mre11/Rad50 by Nbs1. J Biol Chem *278*, 45171-45181.

Lee, J.H., Paull, T.T. (2004). Direct activation of the ATM protein kinase by the Mre11/Rad50/Nbs1 complex. Science *304*, 93-96.

Lee, J.H., Paull, T.T. (2005). ATM activation by DNA double-strand breaks through the Mre11-Rad50-Nbs1 complex. Science *308*, 551-554.

Lee, J.H., Paull, T.T. (2006). Purification and biochemical characterization of ataxia-telangiectasia mutated and Mre11/Rad50/Nbs1. Methods Enzymol *408*, 529-539.

Lisby, M., Barlow, J.H., Burgess, R.C., Rothstein, R. (2004). Choreography of the DNA damage response, spatiotemporal relationships among checkpoint and repair proteins. Cell *118*, 666-668.

Luo, G., Yao, M.S., Bender, C.F., Mills, M., Bladl, A.R., Bradley, A., Petrini, J.H.J. (1999). Disruption of mRad50 causes embryonic stem cell lethality, abnormal embryonic development, and sensitivity to ionizing radiation. Proc Natl Acad Sci USA *96*, 7376-7381.

Matsuoka, S., Ballif, B.A., Smogorzewska, A., McDonald, E.R. III, Hurov, K.E., Corey, J.L., Bakalarski, C.E., Zhao, Z., Solimini, N., Lerenthal, Y., et al. (2007). ATM and ATR substrate analysis reveals extensive protein networks responsive to the DNA damage. Science *316*, 1160-1166.

Mimitou, E.P., Symington, L.S. (2008). Sae2, Exo1 and Sgs1 collaborate in DNA double-strand break processing. Nature *455*, 770-774.

Moncalian, G., Lengsfeld, B., Bhaskara, V., Hopfner, K.P., Karcher, A., Alden, E., Tainer, J.A., Paull, T.T. (2004). The Rad50 signature motif, Essential to ATP binding and biological function. J Mol Biol *335*, 937-951.

Moreno-Herrero, F., de Jager, M., Dekker, N.H., Kanaar, R., Wyman, C., Dekker, C. (2005). Mesoscale conformational changes in the DNA-repair complex Rad50/Mre11/Nbs1 upon binding DNA. Nature *437*, 440-443.

Paull, T.T., Gellert, M. (1998). The 3′ to 5′ exonuclease activity of Mre11 facilitates repair of DNA double-strand breaks. Mol Cell *1*, 969-979.

Paull, T.T., Gellert, M. (1999). Nbs1 potentiates ATP-driven DNA unwinding and endonuclease cleavage by the Mre11/Rad50 complex. Genes Dev *13*, 1276-1288.

Pâques, F., Haber, J.E. (1999). Multiple pathways of recombination induced by double-strand breaks in Saccharomyces cerevisiae. Microbiol Mol Biol Rev *63*, 349-404.

Raymond, W.E., Kleckner, N. (1993). RAD50 protein of S. cerevisiae exhibits ATP-dependent DNA binding. Nucleic Acids Res *21*, 3851-3856.

Stewart, G.S., Maser, R.S., Stankovic, T., Bressan, D.A., Kaplan, M.I., Jaspers, N.G.J, Raams, A., Byrd, P.J., Petrini, J.H.J, Taylor, A.M. (1999). The DNA double-strand break repair gene hMRE11 is mutated in individuals with an Ataxia-Telangiectasia-like disorder. Cell *99*, 577-587.

Stracker, T.H., Morales, M., Couto, S.S., Hussein, H., Petrini, J.H.J. (2007). The carboxy terminus of NBS1 is required for induction of apoptosis by the MRE11 complex. Nature *447*, 218-221.

Su, T.T. (2006). Cellular responses to DNA damage, one signal, multiple choices. Ann Rev Genet *40*, 187-208.

Trujillo, K.M., Yuan, S.F., Lee, E.Y.H.P., Sung, P. (1998). Nuclease activities in a complex of human recombination and DNA repair factors Rad50, Mre11, and p95. J Biol Chem *273*, 21447-21450.

Valerie, K., Povirk, L.F. (2003). Regulation and mechanisms of mammalian double-strand break repair. Oncogene *22*, 5792-5812.

van den Bosch, M., Bree, R.T., Lowndes, N.F. (2003). The MRN complex, coordinating and mediating the response to broken chromosomes. EMBO Rep *4*, 844-849.

van Gent, D.C., Hoeijmakers, J.H.J., Kanaar, R. (2001). Chromosomal stability and the DNA double-stranded break connection. Nat Rev Genet *2*, 196-206.

van Noort, J., van der Heijden, T., de Jager, M., Wyman, C., Kanaar, R., Dekker, C. (2003). The coiled-coil of the human Rad50 DNA repair protein contains specific segments of increased flexibility. Proc Natl Acad Sci USA *100*, 7581-7586.

Varon, R., Viussinga, C., Platzer, M., Cerosaletti, K.M., Chrzanowska, K.H., Saar, K., Beckmann, G., Seemanová, E., Cooper, P.R., Nowak, N.J., et al. (1998). Nibrin, a novel DNA double-strand break repair protein, is mutated in Nijmegen breakage syndrome. Cell *93*, 467-476.

Verhoeven, E.E.A., Wyman, C., Moolenaar, G.F., Goosen, N. (2002). The presence of two UvrB subunits in the UvrAB complex ensures damage detection in both DNA strands. EMBO J *21*, 4196-4205.

Williams, R.S., Moncalian, G., Williams, J.S., Yamada, Y., Limbo. O., Shin, D.S., Groocock, L.N., Cahill, D., Hitomi, C., Guenther, G., et al. (2008). Mre11 dimers coordinate DNA end bridging and nuclease processing in double-strand-break repair. Cell *135*, 97-109.

Williams, R.S., Williams, J.S., Tainer, J.A. (2007). Mre11-Rad50-Nbs1 is a keystone complex connecting DNA repair machinery, double-strand break signaling, and the chromatin template. Biochem. Cell Biol *85*, 509-520.

Wyman, C., Rombel, I., North, A.K., Bustamente, C., Kustu, S. (1997). Unusual oligomerization required for activity of NtrC, a bacterial enhancer-binding protein. Science *275*, 1658-1661.

Wyman C, Kanaar, R. (2002). Chromosome orginization, reaching out to embrace new models. Curr Biol *12*, R446-R448.

Wiltzius, J.J.W., Hohl, M., Fleming, J.C., Petrini, J.H.J. (2005). The Rad50 hook domain is a critical determinant of Mre11 complex functions. Nat Struct Mol Biol *12*, 403-407.

Xiao, Y., Weaver, D.T. (1997). Conditional gene targeted deletion by Cre recombinase demonstrates the requirement for the double-strand break repair Mre11 protein in murine embryonic stem cells. Nucleic Acids Res *25*, 2985-2991.

You, Z., Chahwan, C., Bailis, J., Hunter, T., Russell, P. (2005). ATM activation and its recruitment to damaged DNA require binding to the C terminus of Nbs1. Mol Cell Biol *25*, 5363-5379.

Zhu, Z., Chung, W., Shim, E.Y., Lee, S.E., Ira, G. (2008). Sgs1 helicase and two nucleases Dna2 and Exo1 resect DNA double-strand break ends. Cell *134*, 981-994.

Zhu, X.D., Küster, B., Mann, M., Petrini, J.H.J., de Lange, T. (2000). Cell-cycle-regulated association of RAD50/MRE11/NBS1 with TRF2 and human telomeres. Nat Genet *25*, 347-352.

Zhu, J., Petersen, S., Tessarollo, L., Nussenzweig, A. (2001). Targeted disruption of the Nijmegen breakage syndrome gene NBS1 leads to early embryonic lethality in mice. Curr Biol *11*, 105-109.

CHAPTER 4

Specific protein interfaces differentially influence MR(N) complex architecture, oligomerization and interactions with DNA

Eri Kinoshita[1], Rajashree Deshpande[2], Dejan Ristic[1], Tanya T. Paull[2] and Claire Wyman[1, 3]

[1]The Department of Cell Biology & Genetics, Cancer Genomics Center, Erasmus MC, PO Box 2040, 3000 CA Rotterdam, The Netherlands. [2] The Howard Hughes Medical Institute, The Department of Molecular Genetics and Microbiology, and the Institute for Cellular and Molecular Biology, The University of Texas at Austin, Austin, TX 78712, USA and [3] The Department of Radiation Oncology, Erasmus MC, PO Box 2040, 3000 CA Rotterdam, The Netherlands

ABSTRACT

The Mre11-Rad50-Nbs1 (MRN) complex is involved in DNA double-strand break (DSB) repair by both homologous recombination (HR) and non-homologous end joining (NHEJ). The various functions such as DSB recognition, DNA end processing and DSB-induced cell cycle checkpoint signaling, suggest that different protein architecture or arrangements of components in the complex may have different functions. To explore the role of specific protein interfaces in architecture of the complex we used point mutations that aimed to disrupt specific interfaces; MRE11 dimerization (L72K), RAD50 zinc hook dimerization (C2G) or a stable RAD50 ATP-bound state (L1211W). Scanning force microscopy (SFM) showed that complex architecture is affected by disrupting specific interfaces. Protein function (i.e. DNA binding) is also affected, indicating specific functional roles for MRE11 dimerization, RAD50 zinc hooks and ATP-dependent RAD50 dimerization in defining protein complex activities during DSB repair.

INTRODUCTION

DNA double-strand breaks (DSBs) occur continually in all organisms due to internal (e.g. metabolic by products, replication errors) and external (e.g. ionizing radiation, mutagenetic chemicals) factors and will eventually lead to cell death if left unrepaired. The Mre11-Rad50-Nbs1 (Xrs2 in *S. cerevisiae*) (MRN/MRX) complex plays an important role in DSB repair and acts in DSB recognition, DNA end processing and DSB-induced cell cycle checkpoint signaling in both HR and NHEJ (Lamarche et al., 2010; Stracker & Petrini, 2011). While Mre11 and Rad50 are conserved among the animal kingdoms, Nbs1 (Xrs2) is so far only found in eukaryotes.

The MR complex is a heterotetramer including two Mre11 and two Rad50. Their association into a complex depends on interactions between Mre11's and between Mre11 and Rad50. Separately Mre11 is a globular dimer. Mre11 has manganese-dependent endonuclease and exonuclease activities (Paull & Gellert 1998; Truijllo et al., 1998) important for processing DNA during repair (Mimitou & Symington, 2009). Rad50 is an asymmetric protein with a globular ATPase domain at one end of a very long (50 nm) coiled coil and a Zn hook self-interaction domain at the other end. Mre11 associates along the lower region of the Rad50 coiled coils near the globular ATPase domains (de Jager et al., 2001; Hopfer et al., 2001). Two Rad50 are included in the complex but, in the absence of bound ATP, their globular domains are separated from each other because they are bound at opposite sides of the Mre11 dimer (Lim et al., 2012). Rad50 can also dimerize when bound to ATP by association of two ATP binding sites formed where the Walker A and Walker B motifs from one protein associate with the signature motif from a second Rad50 protein (Hopfner et al., 2000a). The conserved C-X-X-C motif of the coiled-coil apex coordinates a zinc ion to interact with another such motif (referred to as "zinc hooks") to make dimeric bridges extending up to 120 nm (Hopfner et al., 2002). Nbs1(Xrs2) itself does not have any known enzymatic activities but its C-terminus interacts with ATM (Tel1). This interaction recruits ATM to DSBs where it is subsequently autophosphorylated and activated (Falck et al., 2005; You et al., 2005). The successful purification of sub-complexes consisting of Mre11-Nbs1 (MN) (Paull & Gellert, 1999) and Rad50-Nbs1 (RN) (van der Linden et al., 2009) suggests that Nbs1 may have multiple binding sites with potentially varying stoichiometries to comprise the MRN (or RN) complex. SFM-based single particle volume analysis and ultracentrifugation detected at least two stoichimetries of Nbs1 in MRN and RN in the purified protein preparations (van der Linden et al., 2009; Lee et al., 2003).

The arrangement of the protein components in the complex can vary and has important effects on function. The Rad50 coiled coils take a parallel conformation after DNA binding which prevents intra-complex zinc hook interactions and promotes

inter-complex interactions needed for DNA tethering. While ATP binding causes the association of two Rad50 ATPase domains into a compact homodimer. The MRN complex is an intricate protein machine in which binding to ligands, specifically DNA and ATP, affects the functional conformation of domains up to 50 nm away. Rad50 is part of the structural maintenance of chromosome (SMC) protein family named for their roles in chromosome cohesion and chromatin condensation (Connelly et al., 1998). All SMC proteins contain Walker A and B nucleotide (NTP)-binding motifs at the N- and C- terminus, respectively, and have ATPase activity. The importance of the dynamic interface at the ATPase domain of the MR complex is evident from a variety of *in vivo* and *in vitro* data. The Rad50 ATPase activity is required *in vivo* as mutating the conserved lysine in the Walker A motif to alanine, glutamate or arginine in *S. cerevisiae* cause increased DNA damage sensitivity as well as defects in HR and NHEJ (Chen et al., 2005). Purified MRX with the same Walker A mutations are defective in ATPase activity, ATP-dependent DNA unwinding and ATP-dependent endonuclease activities (Chen et al., 2005). Mutating the conserved serine to arginine in the signature motif which interacts with the ATP gamma phosphate, also shows DNA damage sensitivity while the purified human MRN with the same mutation shows decreased ATP-dependent endonuclease activity (Moncalian et al., 2004).

The protein complex can undergo dramatic conformational changes upon nucleotide binding. Crystal structures of the *P. furiosus* Rad50 catalytic domain (residues 1 - 152 and residues 735 - 882) show that nucleotide binding induces dimerization of the active site forming a compact homodimer (Hopfer et al., 2001). Recent structural analyses of Mre11-Rad50 complexes show nucleotides induce reorientation of Rad50 relative to the Mre11 dimer such that the nuclease sites of Mre11 are largely inaccessible (Lammens et al., 2011, Lim et al., 2011, Williams et al., 2011). This may explain why the ATP-bound and ATP-free MR conformations differ in Mre11 nuclease activities (Maijka et al., 2012).

There is additional evidence indicating that architectural arrangement of the components affects MR complex function such as DNA binding. Mutations disrupting the Mre11 dimerization interface show increased DNA damage sensitivity in *S. pombe* as well as reduced DNA binding affinity (Williams et al., 2008). Deleting the zinc hook similarly causes increased DNA damage sensitivity in yeast (Wiltzius et al., 2001). Changing the conserved second cysteine to glycine in the zinc hook disrupts interactions between Mre11 and Rad50 as well as showing increased DNA damage sensitivity (Hopfner et al., 2002). Considering that the zinc hook is at a distance of approximately 50 nm from the globular ATPase domain, the abolished Mre11 and Rad50 interaction at the distant head domain indicates that the overall complex architecture is intricately linked and that the zinc hook is important in maintaining complex integrity. Truncated coiled-coil mutants as

well as a hook deletion mutant indicate that both these structures are required for proper HR and NHEJ functions *in vivo* (Hohl et al., 2011).

It is clear that the Rad50 ATPase function is important and that nucleotide binding can induce large changes in the arrangement of protein domains within the complex. However, the relationship between nucleotide binding (and hydrolysis) and the resulting conformational changes observed in crystallized sub-complexes or truncated proteins have not been linked with functions of the complete complex. Here we use SFM analysis to compare wild-type MR(N) and point mutations aimed to disrupt specific complex interfaces (i.e. Mre11 dimerization, Rad50 hook) or impose a stable ATP-bound state (i.e. Rad50 dimerization). SFM imaging revealed differences correlated with the disrupted protein interfaces in; protein stoichiometry, coiled-coil arrangement, protein oligomerization, DNA binding, DNA tethering and DNA bound by protein oligomers. The MR(N) complexes observed by SFM can be classified with respect to Rad50 as monomers, globular-domain associated dimers (head dimers), coiled-coil apex associated dimers (hook dimers) and multimers. Adding Nbs1 or nucleotides to MR increased protein oligomerization although the presence of both Nbs1 and nucleotides are not mutually enhancing. Adding nucleotide substrate increased the amount of DNA bound by MR(N) and the amount of DNA in tethered associations. These results imply that intact dimerization interfaces (Mre11 dimerization, hook dimerization) and a stable ATP-bound state have specific functional roles controlling MR(N) activity in DSB repair.

MATERIALS & METHODS

Expression constructs

The human Mre11 gene was modified with a C-terminal FLAG tag (Sigma) by PCR from pTP17 (Paull & Gellert, 1998) to make pTP813. This was used to make a recombinant bacmid, pTP814, to generate baculoviruses following the manufacturer's instructions. The human Nbs1 gene was similarly modified with a C-terminal FLAG tag to make pTP288. This construct was used to make bacmid pTP289 to generate baculoviruses following the manufacturer's instructions. Point mutations were made using the Quik Change Site-Directed Mutagenesis Kit (Stratagene). The mutations were confirmed by sequencing the complete open reading frame of the DNA.

Protein expression and purification

Human MR was expressed by infecting Sf21 with pTP814 and pTP11 as previously described (Paull & Gellert, 1998) with some modifications. Briefly, the desired proteins were eluted from a Ni-NTA column (Qiagen) in Buffer NiB (50 mM sodium phosphate (pH 7.0), 10% glycerol, 50 mM KCl, 20 mM β-mercaptoethanol, 150 mM imidazole). Fractions with human

MR were subsequently loaded onto a 1 ml anti-FLAG M2 agarose resin column (Sigma) and washed with Buffer A (20 mM Tris pH 8.0, 10% glycerol, 100 mM NaCl, 1 mM DTT) and eluted with Buffer A containing 200 g/ml of FLAG peptide (Sigma). The FLAG purified protein was loaded onto a Superose 6 10/300GL column collecting 0.5 ml fractions. Proteins eluting at a 10.5 ml volume were used for SFM experiments and all mentioned biochemical studies. Human NBS1 was expressed by infecting Sf21 with pTP289. NBS1 was first bound to SP resin in Buffer A and eluted with 600 mM NaCl in Buffer A. The protein was subsequently loaded onto an anti-FLAG M2 agarose resin, washed with Buffer A and finally eluted with 200 ug/ml of FLAG peptide (Sigma) in Buffer A.

DNA substrates

The 3 kb linear dsDNA was produced by digestion of pUC19 plasmid with *EcoRI*. The resulting linear DNA was subsequently purified by standard phenol extraction and ethanol precipitation.

Scanning force microscopy (SFM)

For images of protein alone, approximately 3 nM of human MR(N) (wild-type or indicated mutants), with 1mM AMP-PNP as indicated, was incubated for 1 minute in 20 µl of protein storage buffer (25 mM Tris-HCl (pH8.0), 10% glycerol, 100 mM NaCl, 1 mM DTT). Experiments which reconstituted NBS1 with MR were done by incubating equimolar amounts of NBS1 and RAD50 for 1 minute to make 3 nM of MRN in 20 µl of protein storage buffer. For imaging, reactions were diluted 5-fold by adding 80 µl of deposition buffer (10 mM HEPES (pH 8.0), 20 mM $MgCl_2$) and deposited onto a freshly cleaved mica surface for 1 minute.

DNA-protein complexes for SFM imaging were formed by first incubating equimolar amounts of NBS1 and RAD50 together for 1 minute to reconstitute approximately 3 nM of MRN in 18 µl of protein storage buffer. Then 2 µl of 5 nM 3kb linear dsDNA was added to make a final concentration of 0.5 nM 3kb linear dsDNA and incubated for another minute. For binding reactions in the presence of ATP, 2 µl of 10 mM ATP and 2 µl of 5 nM 3kb linear dsDNA were added to make final concentrations of 1 mM ATP and 0.5 nM 3kb linear dsDNA. For imaging, reactions were diluted 5-fold by adding 80 µl deposition buffer and deposited onto a freshly cleaved mica surface for 1 minute.

For all samples; after absorbtion onto freshly cleaved mica for 1 minute, the mica was rinsed three times with MilliQ water and dried with filtered air. Samples were imaged in air at room temperature and humidity by tapping mode SFM using Nanoscope IV (Digital Instruments). Silicon Nanotips were from Digital Instruments (Nanoprobes). Images were collected at 2.5 µm x 2.5 µm and processed only by flattening to remove background slope.

RESULTS

Specific interfaces affect human Mre11-Rad50 (MR) architecture

We investigated the effect of changes in specific interfaces, of the human MRE11-RAD50 (MR) complex on architectural arrangement of the components, oligomerization, DNA binding and tethering. SFM images directly reveal the architecture of MR (wild-type and mutants) complexes with respect to the arrangement of the components. The relative distribution of different complex forms was determined for each protein variant, wild-type and mutant. For the wild-type, the most prevalent species were dimers linked by the globular head domain, as observed before (de Jager et al., 2001; de Jager et al., 2002; Moreno-Herrero et al., 2005; van der Linden et al., 2009) (hereafter referred to as head dimers) (Figure 1A).

An MRE11 dimer forms the center of the MR complex. Within the MR complex MRE11 also interacts with both RAD50 and NBS1. The organization of the MRE11 dimer is likely to effect the overall organization and function of the MR(N) complex. Therefore amino acids predicted to influence MRE11 dimerization were changed and the function of the resulting complex analysed. Crystal structures of *P. furiosus* Mre11 showed that the dimerization interface has a conserved 4-helix bundle that self-associates (Williams et al., 2008). Mutating the conserved leucine in the hydrophobic patch of the *P. furiosus* Mre11 dimer interface to a charged amino acid (Mre11-L61K or Mre11-L97D) prevents dimerization (Williams et al., 2008). For our studies, the equivalent leucine, L72, was

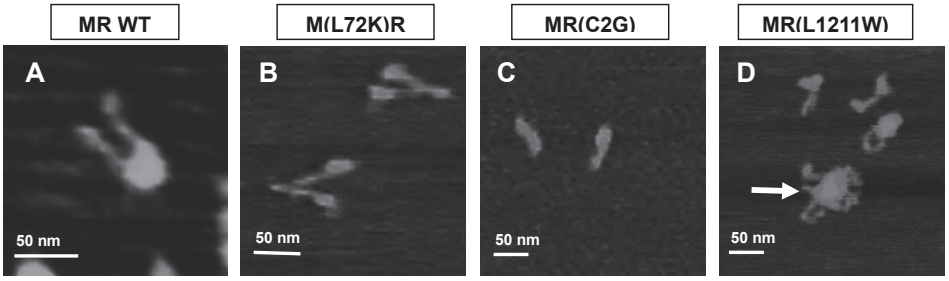

Figure 1. SFM analysis of the human Mre11-Rad50 (MR) complexes. Representative images of prevalent architectural forms observed by SFM (A) MR wild-type, globular domain linked dimer with respect to RAD50, (B) M(L72K)R, dimeric with respect to RAD50 but linked via the coiled-coil apexes, (C) MR(C2G), monomeric and (D) MR(L1211W), multimeric. An example of the MR(L1211W) multimer is indicated with a white arrow. Purified proteins were deposited onto freshly cleaved mica and imaged in air by tapping mode. Color represents height from 0 to 3 nm (dark to light).

changed to lysine in the human protein (MRE11 L72K) and MR(N) complexes including the mutant MRE11 were purified and characterized by SFM imaging. The M(L72K)R complexes largely resemble the wild-type MR architecture but differed in distribution of the different forms. The most prevalent forms for M(L72K)R was a dimer linked at the coiled-coil apex (hereafter referred to as hook dimers) (Figure 1B). This suggests that the leucine to lysine mutation in human MRE11 also perturbs dimer organization, causing weaker globular domain interactions and making association via the coiled-coil hooks more prominent.

Another protein-protein interface in the MR(N) complex involves the apparently dynamic association of the RAD50 coiled coil apexes via dimerization of their zinc hook domains. Crystal structures of *P. furiosus* Rad50 coiled-coil apex fragments showed that the conserved C-X-X-C motif of the Rad50 coiled-coils coordinates zinc in dimeric bridges (Hopfner et al., 2002). To interfere with this interaction of the coiled-coil apexes, the two cysteine residues in the zinc hook were changed to glycine (RAD50 C2G), and MR(N) complexes including mutant RAD50 were purified and characterized by SFM imaging. The most prevalent form of human MR(C2G) was a monomer (Figure 1C) though dimeric forms (both head and hook linked) were observed. This suggests that the C2G mutation weakens hook-hook interactions and that disturbing this interface also influences the interaction at the globular head domains. The overall arrangement as a dimeric complex appears weakened but not eliminated.

RAD50 also has a dimerization interface involving the globular ATPase domains, where ATP is bound and hydrolyzed at the active site created. The L1211W mutation in human RAD50 alters the ATPase active site and presumably ATP coordinated dimer interactions. Mutating the equivalent conserved leucine to a bulky tryptophan residue in *P. furiosus* Rad50 partially blocks the core cavity between the Walker A and Walker B halves, disturbing stable ATP-dependent dimerization (Unpublished data from R. Deshpande & T. Paull). The human MR(L1211W) binds and hydrolyzes ATP faster than the wild-type, preventing a stable ATP-bound state (Unpublished data R. Deshpande & T. Paull). SFM analysis of MR(L1211W) complexes revealed that the prevalent form of the human MR(L1211W) was multimeric (Figure 1D) suggesting that perturbing the ATPase active site increases ATP-independent globular head domain interactions, specifically in a way that enhanced inter-complex interactions.

Protein oligomerization stimulated by ATP or NBS1

The above observations indicated that disturbing protein interfaces (Mre11 dimerization, Rad50 hook and Rad50 ATPase core domain) affects the distribution of different protein architectures in distinct ways for each mutation. Components expected to influence the

architecture of the wild-type complex include NBS1 and ATP. We therefore investigated the effect of nucleotide binding and/or NBS1 addition on the observed architectures. A non-hydrolyzable ATP analog, AMP-PNP, was used to mimic the ATP-bound state of wild-type and mutant MR (Figures 2B, 2F, 2J and 2N). Compared to conditions without nucleotides (Figures 2A, 2E, 2I and 2M), we observed an increase in multimers and/or oligomers upon addition of AMP-PNP (Figures 2B, 2F, 2J and 2N). As clarification, we defined multimers as MR complexes containing up to 8 coiled coil arms protruding from a central globular accumulation. Larger multimerc MR complexes are referred to as oligomers. While all protein complexes generally formed more multimers and/or oligomers upon addition of AMP-PNP, M(L72K)R was the most dramatic, making the largest oligomers (Figure 2F). Interestingly, MR(L1211W) formed multimers but no oligomers even upon addition of AMP-PNP (Figure 2N). In parallel, we reconstituted the MRN complex (using equimolar amounts of NBS1 and RAD50) to determine the effect of NBS1 on protein architecture (Figures 2C, 2G, 2K and 2O). Compared to MR we observed that NBS1, similar to AMP-PNP, generally increased protein oligomerization although MR(L1211W)N clearly had the most oligomers. The fact that there was little effect of adding AMP-PNP to MR(L1211W) may indicate that nucleotides can no longer bind to this active site mutant. However upon adding NBS1, this form made the most oligomers, suggesting that NBS1 has a role in complex oligomerization. Adding AMP-PNP to complexes including NBS1 did not result in an additive increase of oligomers (Figures 2D, 2H, 2L and 2P). The prevalence of oligomers was quantified for the various conditions, as percentage of oligomers detected among observed protein complexes (Figure 2Q).

Effect of altered MR(N) interfaces on DNA binding

Our previous SFM studies have shown that MR(N) complexes bind DNA and can tether DNA molecules in large oligomeric complexes (de Jager et al., 2001; de Jager et al., 2002; van der Linden et al., 2009). In preliminary experiments, we compared the DNA-protein complexes formed by wild-type MRN in the absence and presence of AMP-PNP. The presence of AMP-PNP did not appear to make a significant difference in the DNA binding behavior of the wild-type MRN in this assay. Partial proteolysis of MRN indicated that ATP is in fact better at promoting conformational changes to the protein than AMP-PNP (Unpublished data from R. Deshpande). Consistent with this finding, the presence of ATP caused a significant change in the DNA binding behavior of wild-type MRN. We therefore compared the DNA-protein complexes formed by wild-type and mutant MRN, in the absence and presence of ATP. MRN bound to DNA as dimers, multimers or oligomers (For an example see Figure 3B) as well as in complexes tethering

DNA molecules (Figure 3A). Adding ATP increased the percentage of DNA bound by almost 2-fold (Examples of DNA bound complexes are shown in Figure 3C and 3D). The complex including an altered MRE11 interface, M(L72K)RN, bound to DNA as dimers, multimers or oligomers (For an example see Figure 3F) as well as in complexes tethering

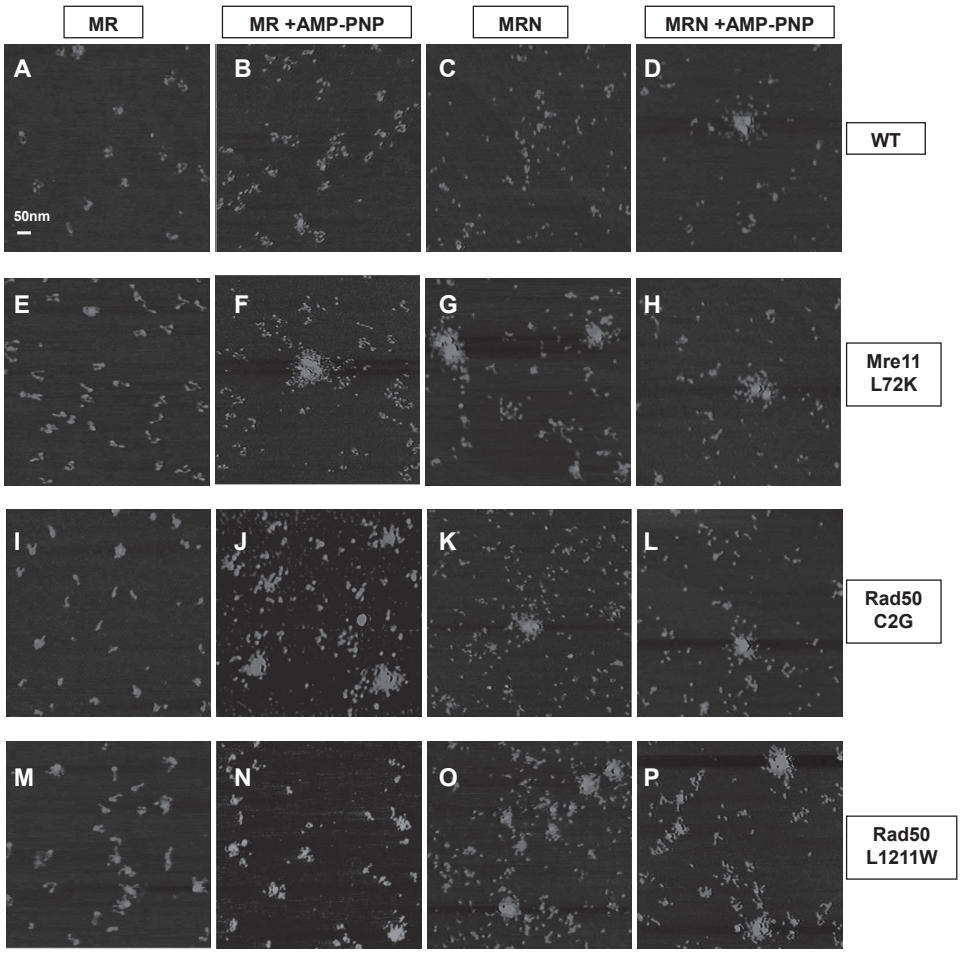

Figure 2. SFM analysis of MR(N) complexes without or with AMP-PNP. Representative images of the various MR(N) complex in the absence and presence of bound nucleotide; (A) MR (B) MR +AMP-PNP (C) MRN (D) MRN +AMP-PNP (E) M(L72K)R (F) M(L72K)R +AMP-PNP (G) M(L72K)RN (H) M(L72K)RN +AMP-PNP (I) MR(C2G) (J) MR(C2G) +AMP-PNP (K) MR(L1211W) (L) MR(L1211W) +AMP-PNP (M) MR(L1211W) (N) MR(L1211W) +AMP-PNP (O) MR(L1211W)N and (P) MR(L1211W) N +AMP-PNP. Purified proteins (with AMP-PNP as indicated) were deposited onto freshly cleaved mica and imaged in air by tapping mode SFM. Color represents height from 0 to 3 nm (dark to light).

DNA molecules (Figure 3E). This mutant made the largest DNA tethering complexes (Figure 3E), which were abolished in the presence of ATP. The lack of DNA tethering activity was not due to lack of DNA binding as the presence of ATP caused a 5-fold increase in the percentage of DNA bound by protein. The MR(C2G)N bound to DNA as monomers, dimers, multimers or oligomers (For an example see Figure 3H) but no DNA tethering was observed. Adding ATP only slightly recovered DNA tethering (Figure 3I) despite the 5-fold increase in the percentage of DNA bound by protein. Similarly, no DNA tethering was observed for MR(L1211W)N complexes, though dimers, multimers or oligomers still bound to DNA (For an example see Figure 3K). Adding ATP did not recover DNA tethering (Example of an oligomer-bound DNA is shown in Figure 3L).

The M(L72K)RN mutant was especially striking in that it bound less DNA than the wild-type but there were more DNA bound by oligomers and complexes in DNA tethers. Interestingly, ATP dramatically decreased MR(L72K)N oligomers bound to DNA with a corresponding decrease in DNA tethering. The MR(C2G)N mutant bound less DNA than the wild-type and showed no DNA tethering. In contrast, MR(L1211W)N complexes had a higher percentage of DNA bound compared to the wild-type which was largely decreased with ATP. Despite over a 10-fold increase of oligomerized MR(L1211W)N protein alone compared to the wild-type (Figure 2Q), there was no noticeable increase in oligomeric MR(L1211W)N complexes binding to DNA, with or without addition of ATP,

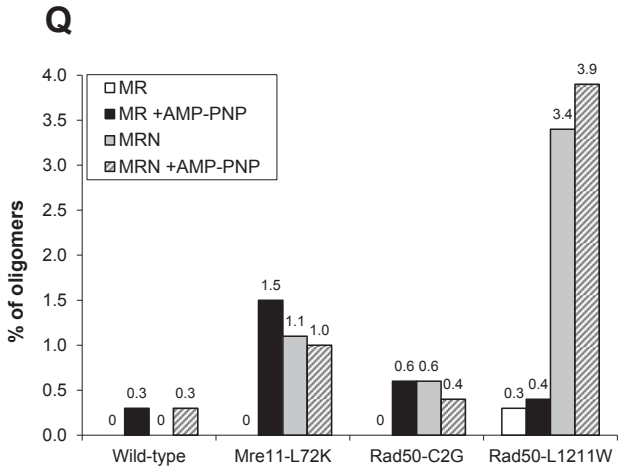

Figure 2. (*Continued*.) (Q) Quantification of MR(N) oligomers (wild-type and indicated mutants) without or in the presence of AMP-PNP. Between 1050 and 2250 protein molecules were counted for all conditions to calculate the percentage of oligomeric complexes.

compared to the wild-type. No DNA tethering was observed for this mutant, regardless of the presence or absence of ATP. These results are summarized in Table 1. The SFM studies we present here are to be combined with biochemical characterization carried out in the T.P. lab, where the mutants were created, for a complete analysis.

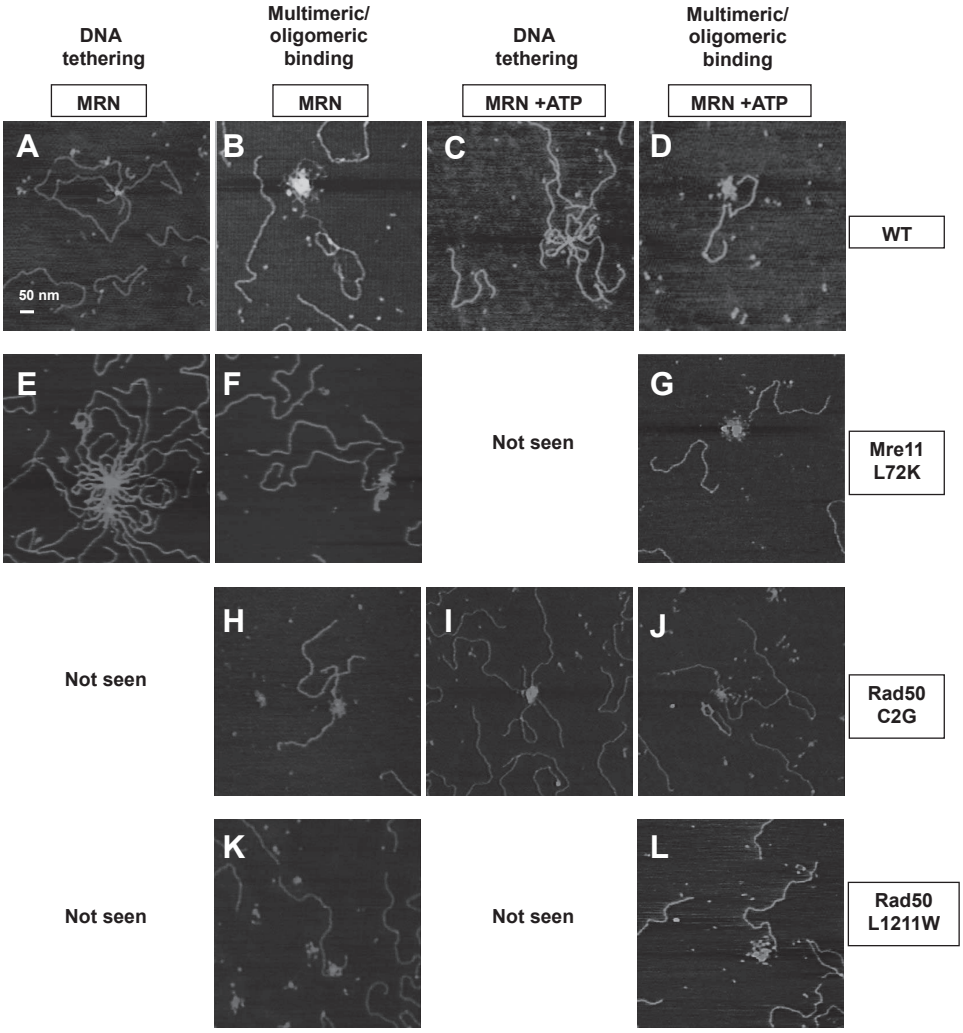

Figure 3. SFM analysis of MRN-DNA complexes without or with ATP. Representative images of RMN bound to 3 kb linear dsDNA with (A and B) MRN (C and D) MRN +ATP (E and F) M(L72K)RN (G) M(L72K)RN +ATP (H) MR(C2G)N (I) MR(C2G)N +ATP (J) MR(L1211W)N and (K) MR(L1211W)N +ATP. Purified proteins and DNA (with ATP as indicated) were deposited onto freshly cleaved mica and imaged in air by tapping mode SFM. Color represents height from 0 to 3 nm (dark to light).

Table 1. Summary of MR(N) (wild type and indicated mutants) complex characteristics.

		Wild-type	Mre11-L72K Mre11 interface	Rad50-C2G Hook	Rad50-L1211W Rad50 ATPase
% Oligomerized	MR	0	0	0	0.3
	MR +AMP-PNP	0.3	1.5	0.6	0.4
	MRN	0	1.1	0.6	3.4
	MRN +AMP-PNP	0.3	1.1	0.6	3.9
% DNA bound	MRN	39	12	5	73
	MRN +ATP	56	62	23	24
% Protein-bound DNA bound by oligomers	MRN	1.4	49	7	2
	MRN +ATP	7.5	3	6	3
% Protein-bound DNA in tethering complexes	MRN	5.6	58	0	0
	MRN +ATP	7.5	0	1	0
Prevalent form		**Head dimer**	**Hook dimer**	**Monomer**	**Multimer**

DISCUSSION

The role of NBS1 in protein structure and function

Although NBS1 is not necessary for the human MR to maintain its structure and DNA binding activities *in vitro*, adding NBS1 stimulates protein multimerization and/or oligomerization for all mutants (L72K, CG and L1211W) (Figure 2Q) although not for the wild-type. Recent crystal structures of the catalytic core of *S. pombe* Mre11 (residues 15 - 143) with Nbs1 (residues 474 - 531) revealed an equimolar (2:2) stoichiometry between these two components (Schiller et al., 2012). Nbs1 binds outside the Mre11 nuclease domain while one of the Nbs1 molecules additionally binds across the Mre11 dimer interface via a highly conserved asymmetric motif. Nbs1 binding to Mre11 potentially reorients the N-terminal region of Nbs1 in close vicinity to the Mre11 nuclease cleft which would place repair and checkpoint proteins interacting with the Nbs1 FHA/BRCT domains near the DNA (Schiller et al., 2012). However, the successful purification of human Rad50-Nbs1 (RN) complexes (van der Linden et al., 2009) indicates an additional interaction between Rad50 and Nbs1 that has not yet been structurally elucidated. Nbs1 binding clearly influences complex architecture, observed here as consistently increased oligomerization (compare Figures 2E, 2I, 2M with Figures 2G, 2K, 2O), which may facilitate DNA binding as multimeric and/or oligomeric complexes and in DNA tethering complexes. Our previous SFM study indicated the presence of two MRN species in which n for $M_2R_2N_n$ was 1.32 and 3.77 (van der Linden et al., 2009). The existence of the

latter high molecular weight MRN can be justified by the relative intensity of Coomassie staining bands on denatured polyacrylamide gels of purified MRN preparations where the NBS1 is up to 1.5 times more intense than the MRE11 band (van der Linden et al., 2009). It is possible that NBS1 promotes the association of already multimeric forms by interacting with itself and MR, this, could explain the existence of the high molecular weight $M_2R_2N_n$.

The importance of Mre11 dimerization in organizing protein architecture

Mre11 is a functional dimer with an overall inverted U-shape (Williams et al., 2008), where the DNA binding site on the convex side of the inverted U. Mre11 dimerization is clearly important for protein complex functions. Monomeric Mre11 has diminished DNA binding and introducing equivalent Mre11 mutations into yeast results in increased DNA damage sensitivity (Williams et al., 2008). Our results show that the MR complex including the MRE11 L72K mutant has decreased DNA binding compared to the -type (Table 1). Despite the reduced overall DNA binding of this mutant, protein associated with DNA was more often oligomeric. There was a corresponding increase in the percent of DNA bound by protein in tethering complexes compared to the wild-type (Table 1). Interestingly ATP largely decreased oligomeric DNA binding and abolished DNA tethering. The correlation with DNA binding by protein oligomers and DNA tethering is consistent throughout. This may indicate that ATP-independent MR complex oligomerization does not dependent on wild-type arrangement of Mre11 while ATP-dependent MR complex oligomerization is regulated by Mre11. Mre11 may have a role in organizing Rad50 in the MR complex and coordinating ATP binding with overall rearrangement to favour protein oligomerization and DNA tethering.

Role of zinc hook interface

Our results show that nucleotide induced oligomerization of the MR(C2G) is similar to the wild-type (Figure 2Q). Addition of NBS1 had a similar effect on oligomerization as did AMP-PNP. This mutant, however, had reduced DNA binding as well as abolished DNA tethering compared to the wild-type (Table 1). It is well established that DNA binding activities of the protein complex occur in the globular head domain. However studies on budding yeast show that deleting the zinc hook affects proper functions in both HR and NHEJ (Hohl et al., 2011; Hopfner et al., 2002; Wiltzius et al., 2001). It has been suggested that the zinc-mediated dimeric bridging at the hook domains connect sister chromatids and DNA ends in HR and NHEJ, respectively (Hopfner et al., 2002; Moreno-Herrero et al., 1998). Mutating the zinc hook most likely abolished zinc hook

interactions, which logically made it impossible to take part in DNA tethering via this interface. However interfering with the zinc hook domain also disturbed the arrangement of the complex in general, including decreased DNA binding via domains some 50 nm away in the globular domains. The minimal amount of DNA tethering observed may have been due to single oligomers associating with multiple DNAs, rather than the zinc hook association of different oligomers that are bound to different DNA molecules.

Crystal structures of *P. furiosus* MR with only the catalytic head of Rad50 with Mre11 show that the zinc hooks (and the whole length of the coiled coils) are not required for nucleotide-dependent conformational changes (Hopfner et al., 2001). However, the interesting converse situation that the complete coiled coils and associated zinc hooks may influence the arrangement at of the globular domains was not considered. Our data observing the complete complex and its response to added nucleotide and DNA binding activity by SFM suggests this can be the case. Considering that the same C2G mutation in *P. furiosus* disrupts Mre11 and Rad50 interactions (Hopfner et al., 2002), it appears that the hook domain can influence protein complex activities in the globular head domain as well the integrity of the protein complex. The zinc hooks are at the apex of the coiled coils connected to the Rad50 catalytic domains that undergo ATP-dependent rotations (Hopfner et al., 2000a) and rearrangement with the associated Mre11 dimer. It has been suggested that the disruption of the zinc hook alters the torsional strain applied through the coiled coils (Hohl et al., 2011), which may affect overall protein structure. The means of communication between the coiled-coiled apex and the distant globular head remains a fascinating mechanism to be elucidated.

Role of ATP binding on DNA organizational functions

The *P. furiosus* MR(L802W) mutant has increased ATPase activity and presumably does not maintain an ATP bound state (Unpublished data from R. Deshpande & T. Paull). Our results show that the equivalent human L1211W mutation has increased DNA binding compared to the wild-type. This DNA binding is decreased by the presence of ATP (Table 1). Interestingly, although this mutant had increased propensity to oligomerize (Figure 2Q) with Nbs1, the incidence of oligomeric complexes binding to DNA for the MR(L1221W) was not noticeably higher than the wild-type (Table 1). The L1211W mutation replaces a hydrophobic leucine with a bulky tryptophan residue in the Rad50 catalytic core, thereby affecting proper ATPase subdomain alignments (Unpublished data R. Deshpande & T. Paull). The dramatically decreased DNA binding we observed with ATP may indicate that this altered RAD50 interface also effects the MR complex as a whole, so that DNA binding sites are obscured. As well, MR(L1211W) was completely defective in DNA tethering. It is plausible to suggest that improper ATPase subdomain

rotation affects the accessibility of DNA binding sites at the globular domain and causes the coiled coils to take an orientation that disfavors DNA tethering.

CONCLUSIONS

The present study has shown that the protein interfaces within the MR(N) complex (i.e. Mre11 interface, zinc hook interface and Rad50 ATPase domain interface) influence the overall complex architecture and affect DNA binding and DNA tethering activities. DNA binding is promoted by MR(N) oligomerization and DNA bound oligomers promote DNA tethering. Additionally tethering via the zinc hooks required these to be available, thus not engaged in intra-complex associating. We can summarize our results so far with respect to these two elements of MR(N) complex architecture. This is admittedly simplistic but provides a framework for further structural and functional analysis. The Mre11 dimer interface may have roles regulating the associating of Rad50 in response to ATP binding. The Rad50 ATPase domain interface can be together or apart, with ATP binding and hydrolysis defining the closed and open state, respectively (Lammens et al., 2011; Lim et al., 2011; Williams et al., 2011). The ATP-bound Rad50 interface would typically be an intra-complex interaction if constrained by the Mre11 interface. Perhaps additional inter-complex interfaces are created in the ATP bound arrangement of MR(N). The zinc hook interface, for example, can potentially undergo both inter- and intra-complex interactions as shown by electron microscopy (EM) and scanning force microscopy (SFM) (Hopfner et al., 2002; Morenno-Herrero et al., 1998). DNA is tethered by inter-complex zinc hook interactions, which act as a molecular “velcro” to bring DNA substrates in close proximity. Considering that DNA tethering requires multimerized and/or oligomerized protein complexes, we have previously hypothesized that oligomerization is a prerequisite for DNA tethering. Figure 4 is a speculative model integrating the ATP-defined protein architecture with functions such as DNA binding and DNA tethering combined with the oligomerization which can be caused by ATP or Nbs1. We speculate that the ATP-induced conformational changes to the protein complex stimulate oligomerization. Oligomerization stimulates DNA binding which in turn favors a coiled coil orientation that can undergo DNA tethering. It is possible that DNA tethering is promoted by two conformational changes of the protein complex stimulated by DNA binding and ATP binding/hydrolysis. The presence of NBS1 similarly stimulates protein oligomerization which in turn stimulates DNA binding leading to DNA tethering. It would be necessary to combine high resolution single structure anslysis such as X-ray crystallography and SAXS with multimeric/oligomeric analysis such as SFM to fully understand the relationship/communication between protein conformation, ATP binding/hydrolysis and important functions such as DNA binding and DNA tethering.

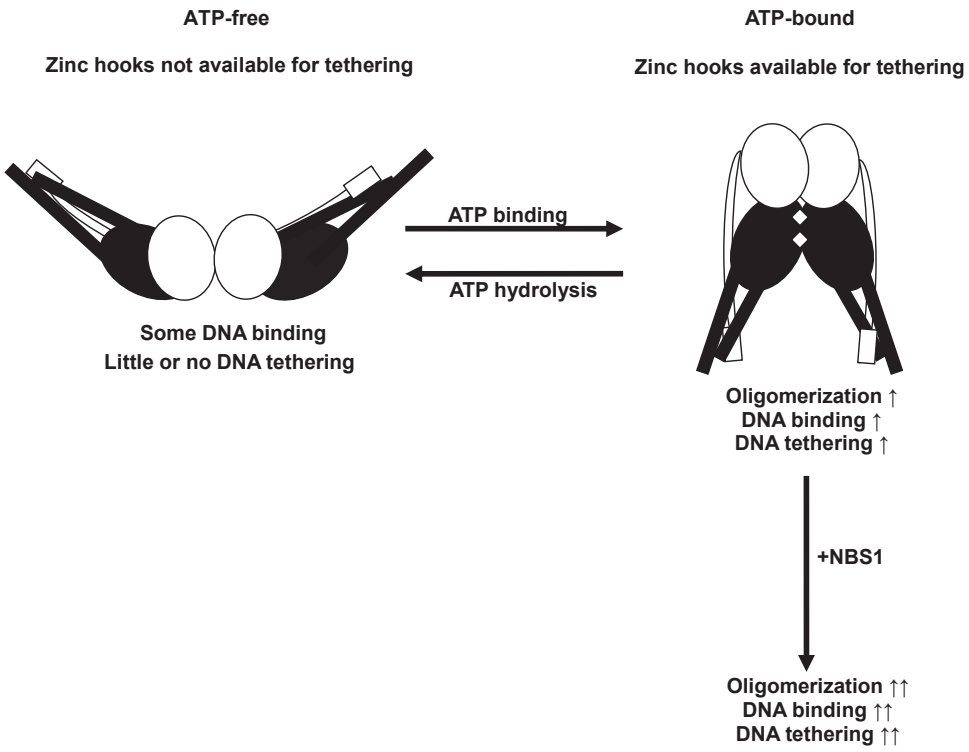

Figure 4. Schematic model of MR(N) without and with ATP and the functions speculated with each state. In the ATP-free "open" complex, the DNA binding sites of Mre11 are exposed and can bind to DNA (Mre11 is shown in white). The Rad50 ATP binding sites are facing outwards and away from one another, rendering it unlikely to bind DNA (Rad50 is shown in black). In this state the zinc hooks are not in the conformation that can undergo DNA tethering. In the ATP-bound "closed" complex, the Rad50 ATP-binding sites are dimerized, which can now bind DNA (position of DNA binding shown here as one possibility for illustration only). The ATP induced conformational change to the protein complex promotes DNA oligomerization which stimulates DNA binding. The zinc hooks are also in the conformation to undergo DNA tethering. NBS1 can further promote oligomerization by interacting with itself and MR, "bridging" together the components to form oligomers.

REFERENCES

Chen, S., Davies, A.A., Sagan, D., Ulrich, H.D. (2005). The RING finger ATPase Rad5p of *Saccharomyces cerevisiae* contributes to DNA double-strand break repair in a ubiquitin-independent manner. Nucleic Acids Res *33(18)*, 5878-5886.

Connelly, J.C., Kirkham, L.A., Leach, D.R. (1998). The SbcCD nuclease of Escherichia coli is a structural maintenance of chromosomes (SMC) family protein that cleaves hairpin DNA. Proc Natl Acad Sci USA *95(14)*, 7969-7974.

de Jager, M., van Noort, J., van Gent, D.C., Dekker, C., Kanaar, R., Wyman, C. (2001). Human Rad50/Mre11 is a flexible complex that can tether DNA ends. Mol Cell *8*, 1129-1135.

de Jager, M., Wyman, C., van Gent, D.C., Kanaar, R. (2002). DNA end-binding specificity of human Rad50/Mre11 is influenced by ATP. Nucleic Acids Res *30*, 4425-4431.

Falck, J., Coates, J., Jackson, S.P. (2005). Conserved modes of recruitment of ATM, ATR and DNA-PKcs to sites of DNA damage. Nature *434(7033)*, 605-611.

Hohl, M., Kwon, Y., Galvan, S.M., Sue, X., Tous, C., Aguilera, A., Sung, P., Petrini, J.H. (2011). The Rad50 coiled-coil domain is indispensable for Mre11 complex functions. Nat Struc Mol Biol *18(10)*, 1124-1131.

Hopfner, K.P., Karcher, A., Craig, L., Woo, T.T., Carney, J.P., Tainer, J.A. (2001). Structural biochemistry and interaction architecture of the DNA double-strand break repair Mre11 nuclease and Rad50-ATPase. Cell *105*, 473-485.

Hopfner, K.P., Karcher, A., Shin, D., Fairley, C., Tainer, J. A., Carney, J.P. (2000a). Mre11 and Rad50 from *Pyrococcus furiosus*: Cloning and biochemical characterization reveal an evolutionarily conserved multiprotein machine. J Bacteriol *182*, 6036-6041.

Hopfner, K.P., Karcher, A., Shin, D.S. et al. (2000b). Structural biology of Rad50 ATPase: ATP-driven conformational control in DNA double-strand break repair and the ABC ATPase superfamily. Cell *101*, 789-800.

Hopfner, K.P., Craig, L., Moncalian, G. et al. (2002). The Rad50 zinc-hook is a structure joining Mre11 complexes in DNA recombination and repair. Nature *418*, 562-566.

Lamarche, B.J., Orazio, N.I., Weitzman, M.D. (2010). The MRN complex in double-strand break repair and telomere maintenance. FEBS Lett *584(17)*, 3682-3695.

Lammens, K., Bemeleit, D.J., Möckel, C. et al. (2011). The Mre11:Rad50 structure shows an ATP-dependent molecular clamp in DNA double-strand break repair. Cell *145(1)*, 54-66.

Lee, J.H., Ghirlando, R., Bhaskara, V., Hoffmeyer, M.R., Gu, J., Paull, T.T. (2003). Regulation of Mre11/Rad50 by Nbs1: effects on nucleotide-dependent DNA binding and association with ataxia-telangiectasia-like disorder mutant complexes. J Biol Chem *278*, 45171-45181.

Lim, H.S., Kim, J.S., Park, Y.B., Gwon, G.H., Cho, Y. (2011). Crystal structure of the Mre11-Rad50-ATPγS complex: understanding the interplay between Mre11 and Rad50. Genes Dev *25(10)*, 1091-1104.

Maijka, J., Alford, B., Ausio, J., Finn, R.M., McMurray, C.T. (2012). ATP hydrolysis by RAD50 protein switches MRE11 enzyme from endonuclease to exonuclease. J Biol Chem *287(4)*, 2328-2341.

Mimitou, E.P., Symington, L.S. (2009). DNA end resection: many nucleases make light work. DNA Repair (Amst) *8(9)*, 983-995.

Moncalian, G., Lengsfeld, B., Bhaskara, V. et al. (2004). The Rad50 signature motif: essential to ATP binding and biological function. J Mol Biol *335*, 937-951.

Moreno-Herrero, F., de Jager, M., Dekker, N. H., Kanaar, R., Wyman, C., Dekker, C. (2005). Mesoscale conformational changes in the DNA-repair complex Rad50/Mre11/Nbs1 upon binding DNA. Nature *437*, 440-443.

Paull, T.T., Gellert, M. (1998). The 3‘ to 5‘ exonuclease activity of Mre11 facilitates repair of DNA double-strand breaks. Mol Cell *1*, 969-979.

Paull, T.T., Gellert, M. (1999). Nbs1 potentiates ATP-driven DNA unwinding and endonuclease cleavage by the Mre11/Rad50 complex. Genes Dev *13*, 1276-1288.

Schiller, C.B., Lammens, K. Guerini, I. et al. (2012). Structure of Mre11-Nbs1 complex yields insights into ataxia-telangiectasia-like disease mutations and DNA damage signaling. Nat Struct Mol Biol *19(7)*, 693-700.

Stracker, T.H., Petrini, J.H. (2011). The MRE11 complex: starting from the ends. Nat Rev Mol Cell Biol *12(2)*, 90-103.

Trujillo, K.M., Yuan, S.S., Lee, E.Y., Sung. P. (1998). Nuclease activities in a complex of human recombination and DNA repair factors Rad50, Mre11, and p95. J Biol Chem *273*, 21447-21450.

van der Linden, E. Sanchez, H., Kinoshita, E., Kanaar, R., Wyman, C. (2009). RAD50 and NBS1 form a stable complex functional in DNA binding and tethering. Nucleic Acids Res *37*, 1580-1588.

Williams, R.S., Moncalian, G., Williams, J.S. et al. (2008). Mre11 dimers coordinate DNA end bridging and nuclease processing in double-strand-break repair. Cell *135(1)*, 97-109.

Williams, G.J, Williams, R.S. Williams, J.S. et al. (2011). ABC ATPase signature helices in Rad50 link nucleotide state to Mre11 interface for DNA repair. Nat Struc Mol Biol *18(4)*, 423-431.

Wiltzius, J.J., Hohl, M., Fleming, J.C., Petrini, J.H. (2005). The Rad50 hook domain is a critical determinant of Mre11 complex functions. Nat Struct Mol Biol *12(5)*, 403-407.

You, Z., Chahwan, C., Bailis, J., Hunter, T., Russell, P. (2005). ATM activation and its recruitment to damaged DNA require binding to the C terminus of Nbs1. Mol Cell Biol *25*, 5363-5379.

CHAPTER 5

ATP influences DNA binding of the human Mre11-Rad50 complex

Eri Kinoshita[1], Eddy van der Linden[1], Sari van Rossum-Fikkert[1], Humberto Sanchez[1], Marijn van Loenhout[2], Cees Dekker[2] and Claire Wyman[1,3]

[1]Department of Cell Biology & Genetics, Cancer Genomics Center, Erasmus MC [2]Department of Bionanoscience, Kavli Institute of Nanoscience, Delft University of Technology, Delft, [3]Department of Radiation Oncology, Erasmus MC, The Netherlands

ABSTRACT

Many important biological processes are driven by ligand-induced conformational changes in proteins. In case of the Mre11-Rad50 (MR) genome maintenance complex ATP binding causes large conformation changes. Recent structural analyses showed that ATP binding and hydrolysis regulates the closed and open states of the protein complex, respectively. However, it is still unclear whether ATP influences MR functions such as DNA binding and DNA tethering. Using purified human MR, we observed that MR preferentially bound to single-stranded DNA over double-stranded DNA, regardless of the substrate length. SFM analysis indicated that the presence of ATP increased the number of oligomeric complexes. Additional SFM analysis with DNA indicated that the presence of ATP increases DNA binding. These results show that protein oligomerization correlates with DNA binding and DNA tethering.

INTRODUCTION

The Mre11-Rad50-Nbs1 (MRN) complex is activated early in double-strand break (DSB) repair and is involved in break recognition, DNA end processing and signaling for cell cycle arrest. All three genes are essential in mammals (Luo et al., 1999; Xiao & Weaver, 1997; Zhu et al., 2001). The biochemical functions of MRN include DNA binding by multiple subunits, tethering of DNA molecules through interactions between MRN complexes, incision of the DNA phosphodiester backbone through single-stranded (ssDNA) endonuclease and 3'- to 5'- exonuclease activities and ATP hydrolysis (Kinoshita et al., 2009; Lamarche et al., 2010; Stracker & Petrini, 2011).

The core Rad50 complex is heterotetrameric (M_2R_2) with the DNA binding sites of the Mre11 dimer close to the two Rad50 ATPase domains (de Jager et al., 2001; Lammens et al., 2011, Lim et al., 2011, Williams et al., 2011). Rad50 belongs to the structural maintenance of chromosomes (SMC) protein family characterized by Walker A and B nucleotide (NTP)-binding motifs at their N- and C-terminus, respectively (Hopfner et al., 2000a). These motifs are connected by a stretch of amino acid that forms an extended coiled coil. The intervening amino acids form a coiled coil that folds back onto itself making a very elongated structure with ATPase domains at one end and the hook or hinge domain at the other end. ATP binds where the Walker A and B motifs on one SMC/Rad50 subunit contact the highly conserved signature motif of the other subunit in the complex.

Structural studies of MR have revealed that Rad50 dimerization involves several specific molecular interactions that may be regulated by ATP. Structures of the isolated *P. furiosus* Rad50 ATPase domains showed that the signature motif is responsible for protein dimerization. The serine residue interacts with the γ-phosphate of the ATP molecule bound at the Walker motifs of the other subunit (Hopfner et al., 2000a). It is clear that ATP binding has an important role in regulating protein complex functions since mutating this conserved serine to arginine in the signature motif causes increased DNA damage sensitivity in *S. cerevisiae* and decreased ATP-dependent endonuclease activity of the human protein complex (Moncalian et al., 2004). The same mutation in the *P. furiosus* MR signature motif made it deficient in ATP-dependent dimerization (Hopfner et al., 2002). Crystal structures of *P. furiosus* Rad50 revealed that the ATPase domains and the N-terminal lobe is rotated by 30° relative to the C-terminal lobe when ATP is bound (Hopfner et al., 2001).

The question still remains as to how ATP influences the biochemical activities of MR. The existing data regarding this question is still ambiguous as some studies reported an ATP independent DNA binding (de Jager et al., 2001, van der Linden et al., 2009),

while others (Lee et al., 2003; Moncalian et al., 2004) observed a nucleotide and Nbs1 dependent DNA binding. SFM experiments (de Jager et al., 2001; de Jager et al., 2002) showed that MR bound and oligomerized internally and on ends of DNA but the effect of nucleotides on the DNA binding activities of MR oligomers was relatively subtle. We therefore investigated the DNA binding properties of the human MR complex and the effect of ATP on the interaction between MR and DNA. The MR complex did not require DNA ends for binding but clearly showed preferential binding to single-stranded DNA (ssDNA) over double-stranded DNA (dsDNA). Additionally, we observed by SFM that the presence of ATP increased the number of MR oligomers. Interestingly, ATP seemed to influence the percentage of DNA bound by oligomers as well as the percentage of DNA in tethering complexes. We propose that protein oligomerization, stimulated by ATP, leads to increased DNA binding that contributes to increased DNA tethering.

MATERIALS & METHODS

Protein expression and purification

Human MR was produced by infection of Sf9 cells in suspension culture with a baculovirus expressing both C-terminally 6-histidine tagged RAD50 and untagged MRE11. Cells were harvested after 72 hours. Infected cells were collected and flash frozen in liquid nitrogen. They were subsequently thawed on ice and resuspended in 100 ml of ice-cold buffer (50 mM Tris-HCl pH 8.0; 10% glycerol, 500 mM NaCl, 10 mM β-mercaptoethanol) and two EDTA-free protease inhibitor cocktail tablets (Roche). The cells were disrupted by 20 strokes of a type B pestle in a Dounce homogenizer and centrifuged for 1 hour at 100,000 g at 4°C. The soluble fraction was loaded onto 5 ml of Ni-NTA agarose beads (Qiagen) equilibrated with buffer (50 mM Tris-HCl pH 8.0; 10% glycerol, 500 mM NaCl, 1mM DTT). The column was washed with 10 column volumes of Buffer A (50mM Tris-HCl pH 8.0; 10% glycerol, 300 mM NaCl, 1mM DTT) containing 10 mM and then 40 mM imidazole. Proteins were eluted by 1 column volume each of Buffer A with 130 mM and then 200 mM imidazole. MR fractions were pooled, diluted two fold to lower the salt concentration to 150 mM NaCl and loaded onto a 1 ml HitrapQ column (GE Healthcare) equilibrated with Buffer B (50 mM Tris-HCl pH 8.0; 10% glycerol, 100 mM NaCl, 1 mM DTT). After washing the column with 5 column volumes of Buffer B, the proteins were eluted with a salt step of 600 mM NaCl in buffer (50 mM Tris-HCl pH 8.0; 10% glycerol, 1 mM DTT). Fractions including proteins of interest were pooled and loaded on a Superose 6 size exclusion column (GE Healthcare) equilibrated with Buffer A (200 mM NaCl). Fractions including proteins of interest were pooled and loaded onto a 1 ml MonoQ column equilibrated with Buffer B. The column was washed with 5 column volumes of Buffer B and the proteins were eluted with a salt gradient

from 100 mM to 600 mM NaCl in Buffer B. Relevant fractions were pooled and the protein concentration was determined by comparison to standard amounts on a Coomassie Blue stained gel (using a BSA standard). The protein was then aliquoted, flash frozen in liquid nitrogen and stored at -80°C.

ATPase assays

MR at 74 nM (calculated as a M_2R_2 dimer) were mixed with radiolabeled [γ^{32}P]ATP (1 mCi/mL) supplemented with non-labeled ATP to make concentrations of 1, 10, 20, 50, and 100 μM in a volume of 20 μl binding buffer (5% glycerol, 25 mM Tris-HCl, pH 7.5, 110 mM NaCl, 5 mM $MgCl_2$ and 1mM DTT). The reaction was incubated for 120 minutes at 37ºC. Aliquots were removed every 30 minutes and the reaction stopped by adding EDTA to 125 mM. Samples were analyzed by thin layer chromatography (Merck TLC plates), run in 0.7 M K_2HPO_4/0.4 M Boric acid and quantified by phosphorimaging.

DNA substrates

Short DNA substrates (90 nt ssDNA, 90 bp dsDNA, 45 bp +45 nt 5'- overhang and 45 bp +45 nt 3'- overhang) were used for non-denaturing polyacrylamide gel EMSA assays. Substrates in the 0.4 to 3 kb range were used for both agarose gel EMSA assays and SFM analysis. The 90 nt ssDNA (SK#3) had the following sequence: 5'- AF 532 - AAT TCT CAT TTT ACT TAC CGG ACG CTA TTA GCA GTG GCA GAT TGT ACT GAG AGT GCA CCA TAT GCG GTG TGA AAT ACC GCA CAG ATG CGT - 3'; the 90 bp dsDNA was made by annealing the 90 nt ssDNA to its complement 5'- ACG CAT CTG TGC GGT ATT TCA CAC CGC ATA TGG TGC ACT CTC AGT ACA ATC TGC CAC TGC TAA TAG CGT CCG GTA AGT AAA ATG AGA ATT - 3'; the 45 bp + 45 nt 5'-overhang and 45bp + 45 nt 3'-overhang were made by annealing the 90 nt ssDNA to its complement 5'- ACG CAT CTG TGC GGT ATT TCA CAC CGC ATA TGG TGC ACT CTC AGT - 3' and 5'- (phosphate) - ACA ATC TGC CAC TGC TAA TAG CGT CCG GTA AGT AAA ATG AGA ATT - 3', respectively. These oligonucleotides were all synthesized by Sigma. The 66 bp dsDNA was made by annealing the 5'- AF532 - AGA AAC TGG GCA TGT GGA GAC AGA GAA GAC TCT TGG GTT TCT GAT AGG CAC TGA CTC TCT CTG CCT-3' strand to its complement 5'-AGG CAG AGA GAG TCA GTG CCT ATC AGA AAC CCA AGA GTC TTC TCT GTC TCC ACA TGC CCA GTT TCT - 3' which were synthesized by Eurogenetec. The pBluescript II KS/SK (+) was used as the 3 kb supercoiled dsDNA. The 3 kb linear dsDNA was synthesized by treating this plasmid with *EcoRV*. The 1.5 kb dsDNA with a 500 nt 3'- overhang was made similarly as described by Ristic et al., 2003. Briefly, PCR products of pBluescript II KS/SK (+) plasmid amplified from sense primer 1 (5'- C(biotin) - GACTCACTATAGGGCGAATTG -'3) and antisense primer 1 (5'- (phosphate) ACAGCGGTAAGATCCTTGAGAG -'3) were bound to Dyna beads (Invitrogen).

This was treated with a saturating amount of lambda exonuclease (5 U/µg DNA) to digest the phosphorylated strand. The reaction was carried out at 37°C for 1 h and stopped by heat inactivation (95°C for 10 min). The resulting Dyna bead-bound ssDNA was hybridized to its antisense primer 2 (5'- ACTTCTGCGCTCGGCCCTTC -'3) and extended for 30 min at 37°C in a reaction containing Sequenase™ DNA polymerase Version 2.0 (Amersham), 40 mM Tris-HCl pH 7.5, 20 mM $MgCl_2$, 200 µM dNTPs and 50 mM NaCl. The resulting partially double stranded DNA was released from the beads by *EcoRV* digestion which created the final 1.5 kb dsDNA with the 500 nt 3'-overhang. The 400 bp linear dsDNA was made by first digesting the pBluescript II KS/SK (+) plasmid with *EcoRV* and subsequently with *NaeI.* If necessary, all substrates were subsequently purified by standard phenol extraction and ethanol precipitation protocols.

Electrophoretic mobility shift assays (EMSAs)

DNA binding experiments were done by incubating DNA and proteins at the indicated concentrations for 5 minutes at 25ºC in 20 µl of binding buffer (25 mM Tris–HCl, pH 7.5, 5% glycerol, 2% PEG-6000, 110 mM NaCl, 5 mM $MgCl_2$ and 1 mM DTT). Assays to find the effect of nucleotide cofactor on protein and DNA were done by incubating indicated substrate concentrations (see figures for details) for 5 minutes at 25ºC with the indicated protein concentration in binding buffer (5% glycerol, 25 mM Tris–HCl, pH 7.5, 110 mM NaCl, 5 mM $MgCl_2$, 1 mM DTT and 2% PEG-6000) in 18µl. Then 2µl of 1, 2.5, 5, 10 or 25 mM of AMP-PNP or ATP (as indicated in the figure) was added and incubated for another 5 minutes at 25ºC in a final volume of 20µl. The reaction products were separated on a 4.8% non-denaturing polyacrylamide gel for reactions if the DNA substrate up to 90 nt/bp and on a 0.7% agarose gel if the DNA substrate was in the 0.4 to 3 kb range, in all cases gels were run in 0.5 x TB buffer. All labeled DNA was visualized by scanning the gel with a 532 nm laser using an image analyzer (Typhoon 9200). The emission signal was recorded using a 555BP 20 nm filter. Unlabeled substrates were stained with ethidium bromide and scanned similarly using the Typhoon 9200. Data quantification was done with the ImageQuant 5.2 software from at least triplicate experiments.

Scanning force microscopy (SFM)

Sample preparation; proteins ± nucleotides ± DNA (in air)

MR (12 nM as M_2R_2), was incubated in 20 µl of protein storage buffer (50 mM Tris–HCl, pH 8.0, 10% glycerol, 300 mM NaCl, 1 mM DTT) for 1 minute at room temperature. Where indicated nucleotide was added as 1 mM ATP, DNA was added to 1 nM (fragment) 3 kb linear dsDNA in 20 µl and incubated, or both nucleotide and DNA were added. All binding reactions were incubated for 1 minute at room temperature. After incubation, the sample

was diluted 5-fold by adding 80 µl of deposition buffer (10 mM HEPES, pH8.0, 20 mM $MgCl_2$) and 50 µl was deposited onto freshly cleaved mica for 1 minute, washed 3 times with MilliQ water and dried with filtered air.

After deposition, all samples were imaged in air at room temperature and humidity by tapping mode SFM using a Nanoscope IV (Digital Instruments). Silicon Nanotips were from Digital Instruments (Nanoprobes). Images were collected at 2.5 µm x 2.5 µm and processed only by flattening to remove background slope. The total number of oligomers (defined as structures with at least 8 coiled coils protruding from a central accumulation) were counted from 15 randomly collected 2.5 µm x 2.5 µm fields.

Sample preparation; proteins ± nucleotides (in liquid)

35 nM 96 bp oligo was incubated with MR (4 nM (as M_2R_2) in storage buffer (20 mM Tris-HCl, pH 8.0, 100 mM NaCl, 10% glycerol, 0.1% Tween20, 1 mM DTT) for 5 minutes at 23°C. This was deposited onto freshly cleaved mica and mounted onto a liquid cell and imaged. Fifteen minutes later the buffer was exchanged by flushing the flow cell with 150 µl of imaging buffer (25 mM Tris-HCl; pH 8.0, 75 mM KCl, 3 mM $MgCl_2$) without or with 2 mM ATP. Samples were imaged in liquid at room temperature by tapping mode, operated at 9 kHz, using a Nanoscope IV (Digital Instruments). MSNL probes were from Veeco.

RESULTS

Characterization of ATPase activity of human MR

MR was produced in Sf9 insect cells using a baculovirus expression system. Figure 1 shows an SDS-PAGE analysis of the purified MR protein. The turnover rate of MR calculated from an ATPase assay as described previously (de Jager et al., 2002) was 0.044 min^{-1} $complex^{-1}$. This was similar to the previously reported turnover rate, indicating that the current preparation is functional in ATPase activity.

Characterization of human MR DNA-binding properties

Previous DNA-binding studies using purified human MRE11 indicated that this protein alone did not preferentially bind DNA ends but did have a preference for binding to ssDNA over dsDNA (de Jager et al., 2001). Additional DNA-binding studies using purified human MR showed that MR preferentially bound to ssDNA over dsDNA (de Jager et al., 2002). However, these experiments were performed with relatively short DNA substrates (50 nt / bp for MRE11 and 160 nt/bp for MR). Our previous SFM studies have clearly shown that MR makes large oligomers that bind to DNA substrates in the kbp length range. We therefore performed DNA binding experiments using short (up to 90 nt / bp) and long (in the kbp range) DNA substrates to investigate the effect of DNA length on MR binding.

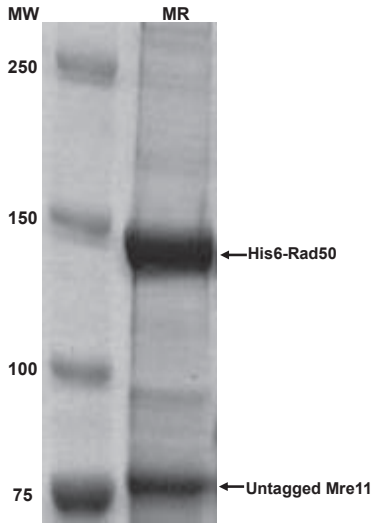

Figure 1. Purification of the human MR complex. Coomassie stained SDS-PAGE gel (6%) of the purified protein preparation. Lane 1, molecular weight marker (MW; molecular mass indicated in kilo-Daltons); Lane 2, MRE11-RAD50 complex (MR).

Human MR has been shown to bind to both linear and circular DNA (de Jager et al., 2001) via SFM imaging. However, no detailed analysis has been done on DNA binding properties on MR via gel shift assays. To test whether MR has a preference for DNA ends, MR was incubated with the same weight / bp amount of supercoiled 3 kb plasmid, 3 kb linear dsDNA, 3kb circular dsDNA or 400 bp linear dsDNA. Thus the shorter DNA has more ends per weight and the circular DNA had no ends. The binding of MR to each DNA substrate was quantified by calculating the portion of protein-bound DNA while varying the protein concentration. The protein concentration at which 50% of the DNA was bound for the supercoiled 3 kb plasmid, 3 kb linear dsDNA, 3 kb circular dsDNA and 400 bp linear dsDNA was 20, 30, 35 and 35 nM, respectively (Figures 2A and 2B). Thus MR bound to all of these dsDNA substrates about equally well. The lack of difference between circular and linear DNA shows there is no strong preference for MR binding to DNA ends. We therefore conclude that human MR does not require or preferentially bind to DNA ends.

While MR did not preferentially bind to DNA ends, the question as to whether MR preferentially bound to a specific substrate and whether substrate length affected DNA binding still remained. Our previous DNA binding experiments using MR showed that this complex bound to both ss- and dsDNA (de Jager et al., 2002). However, these assays

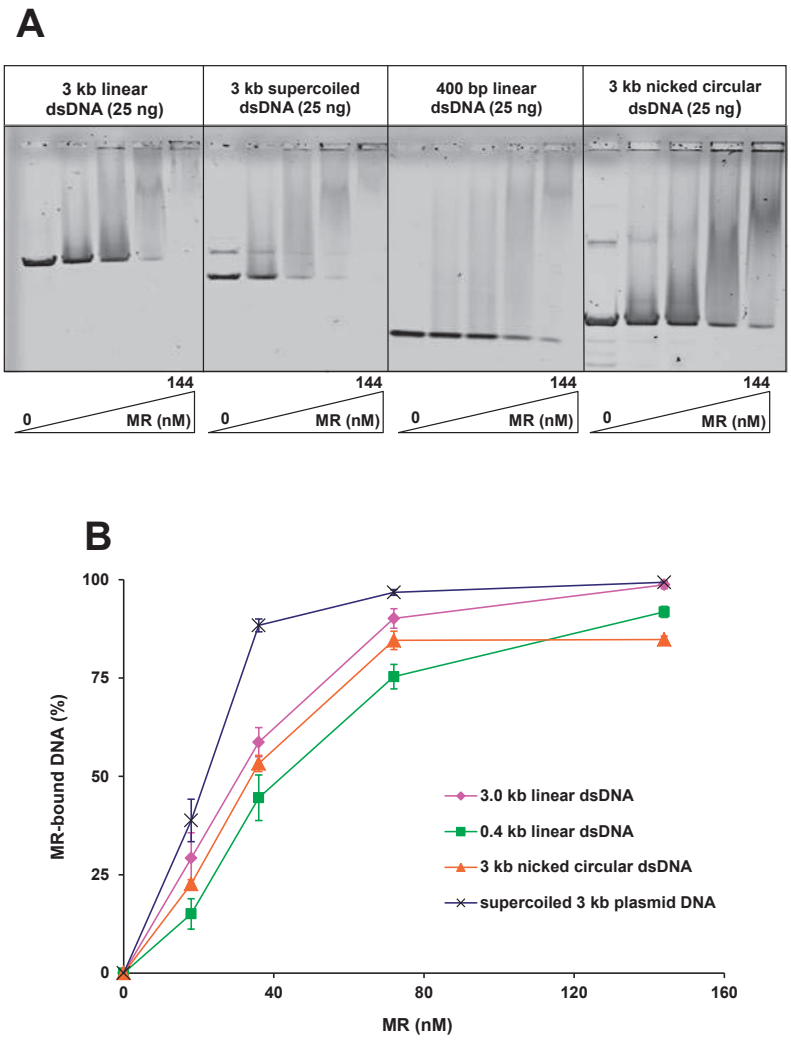

Figure 2. MR does not preferentially bind to DNA ends. (A) EMSA assay of MR with various substrates. 25 ng 3 kb linear dsDNA (0.63 nM), 25 ng 3 kb supercoiled dsDNA (0.63 nM), 25 ng 400 bp linear dsDNA (4.73 nM) or 25ng 3kb nicked circular dsDNA (0.63nM) was incubated with the indicated MR titrations. DNA concentrations are indicated in molar fragments. (B) Quantification of DNA binding by MR. The amount of free DNA plotted as percentage of total DNA in each lane, for increasing protein concentration. Error bars represent SEM of mean values of triplicate reactions.

were performed with only relatively short substrates, 160 nt / bp long. This may have eliminated the additional protein-protein interactions that occur when oligomeric MR binds to longer DNA, as observed by SFM. Considering that the MR complex promotes

DNA tethering which requires DNA-bound MR oligomers (de Jager et al., 2002, van der Linden et al., 2009), it would be logical to test the DNA binding activities of MR with longer substrates (in the kb range) where oligomeric MR can bind and compare this to

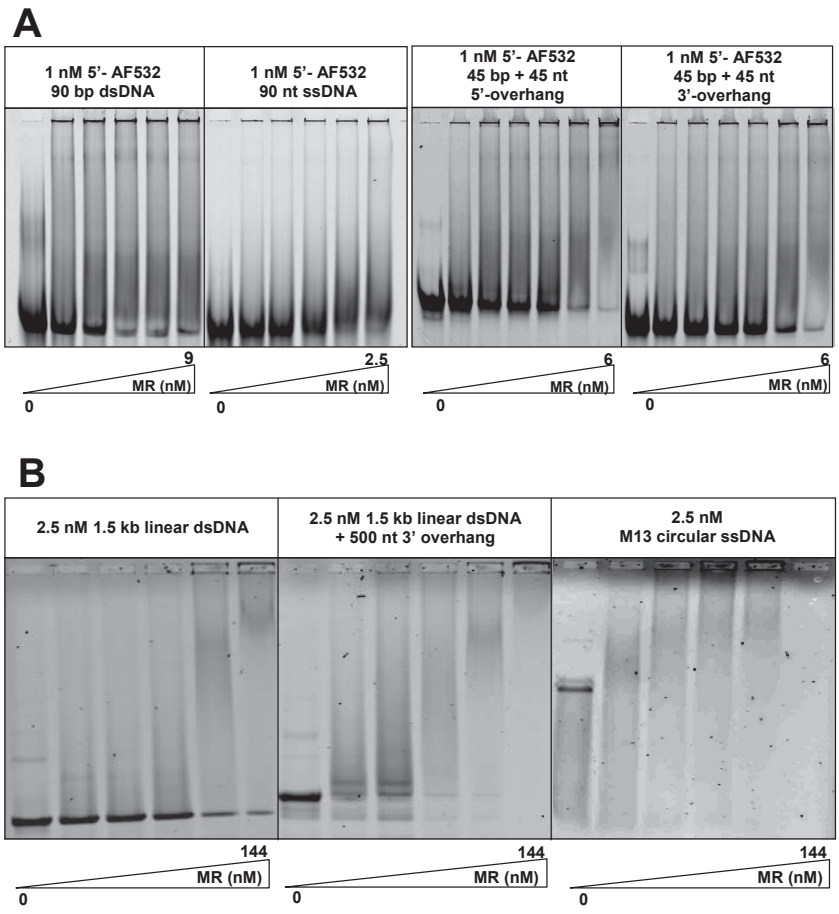

Figure 3. MR preferentially binds to ssDNA. EMSA assays of MR binding to various DNA substrates. All DNA concentrations are indicated as molar fragments. (A) 1 nM of 5'- Alexa Fluor 532 labeled 90 bp dsDNA, 90 nt ssDNA, 45 bp dsDNA with a 45 base 5'- overhang and 45 bp dsDNA with a 45 base 3'- overhang was incubated with the indicated MR titrations. (B) 2.5 nM 1.5 kb linear dsDNA (50 ng), 2.5 nM 1.5 kb dsDNA with a 500 base 3'- overhang (58 ng) and 2.5 nM M13 circular ssDNA (104 ng) was incubated with the indicated MR titrations. (C) Quantification of (A). The amount of free DNA and plotted against the amount of protein added. (D) Quantification of (B). The amount of free DNA and plotted against the amount of protein added. (E) Competitive DNA binding assay using 1 nM ssDNA (66 nt) and 1 nM dsDNA (66 bp) with the indicated MR titration. Error bars represent SEM of mean values of triplicate reactions.

short substrates which cannot accommodate oligomeric MR. We also investigated the relative binding of MR to different DNA structures, such as ssDNA, dsDNA, or ss-dsDNA junctions. We prepared 4 short substrates with the same sequence and length: 90 nt ssDNA, ss-ds DNA junction (45 bp + 45 nt 3'-overhang and 45 bp + 45 nt 5'-overhang) and 90 bp dsDNA. These short substrates had the purpose of minimizing additional protein-protein interactions that may occur when multiple protein complexes bind to a longer DNA

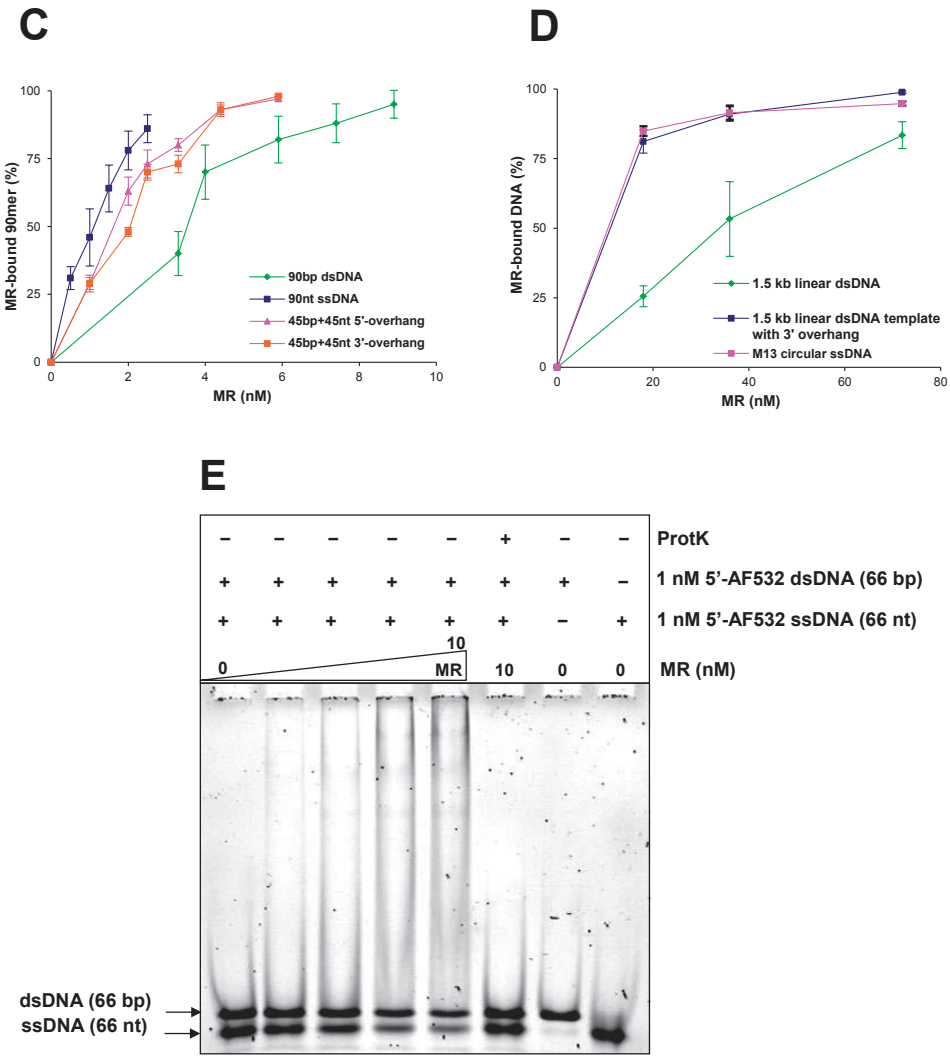

Figure 3. (*Continued*).

substrate, such as those in the kb range. These EMSAs were done with a constant DNA concentration (1 nM) with a protein concentration titration to enable comparison of MR binding to each substrate. MR bound to all substrates but with a clear order of preference: ss-, junction (the 5'- or 3'- overhang) and then dsDNA (Figure 3A and 3C). The protein concentration at which 50% of the DNA was bound for the ss-, 5'- overhang, 3'- overhang and dsDNA was 1, 2, 2 and 4 nM, respectively. This indicates an approximate 4-fold difference between the binding of MR to single compared to dsDNA. We then did EMSA assays using kb range substrates including ssDNA. MR also preferentially bound to ssDNA and junction containing DNA over dsDNA for the long substrates (Figure 3B and 3D). The protein concentration at which 50% of the substrate DNA was bound for the M13 circular ssDNA, 1.5kb dsDNA with a 3'- overhang and 1.5 kb linear dsDNA was 10, 10 and 30 nM respectively. There is approximately a 3-fold difference between MR binding to the ssDNA (as well as the junction DNA) compared to dsDNA. This indicates that MR consistently preferentially bound ssDNA over dsDNA regardless of the substrate length. Competition experiments in which both ss- and dsDNA were present simultaneously also showed that MR binds preferentially to ssDNA. Equal amounts (1 nM) of 66 nt ssDNA and 66 bp dsDNA were incubated with MR titrations (Figure 3E). We used these substrates as they were easily distinguishable on the non-denaturing PAGE gel (see first and last 2 lanes in Figure 3E) and the length (66 nt / bp) would prevent additional protein-protein interactions that may occur with substrates in the kb range. The ssDNA bound to MR first over the dsDNA and the protein concentration at which 50% of the substrate DNA was bound for the ssDNA and dsDNA was 2 and 4nM, respectively. We therefore conclude that MR binds to ssDNA preferentially over dsDNA.

ATP stimulates coiled-coil rearrangements causing DNA release

Recent structural studies indicate that the MR coiled coils undergo a dramatic conformational change in the presence of ATP. To obtain additional information on the conformation of the coiled coils in relation to DNA in the presence and absence of ATP, we used SFM imaging of MR in buffer with a short 96 bp oligo using a protein concentration at which the complexes were evenly distributed and not forming oligomeric complexes. We have previously shown that MR complexes bound to DNA have parallel coiled coils compared to open coiled coils in the absence of DNA but that ATP binding alone did not change coiled-coil arrangement when assayed by SFM imaging in buffer (Moreno-Herrero et al., 2005). We performed SFM imaging in buffer of MR +DNA in the absence (Figure 4A) and in the presence of 2 mM ATP (Figure 4B). Addition of ATP to MR +DNA deposited for SFM imaging in buffer resulted in an increase of bent coiled coils compared to parallel coiled coils in the absence of ATP, which we interpreted as MR releasing DNA in the presence of ATP. Following these findings,

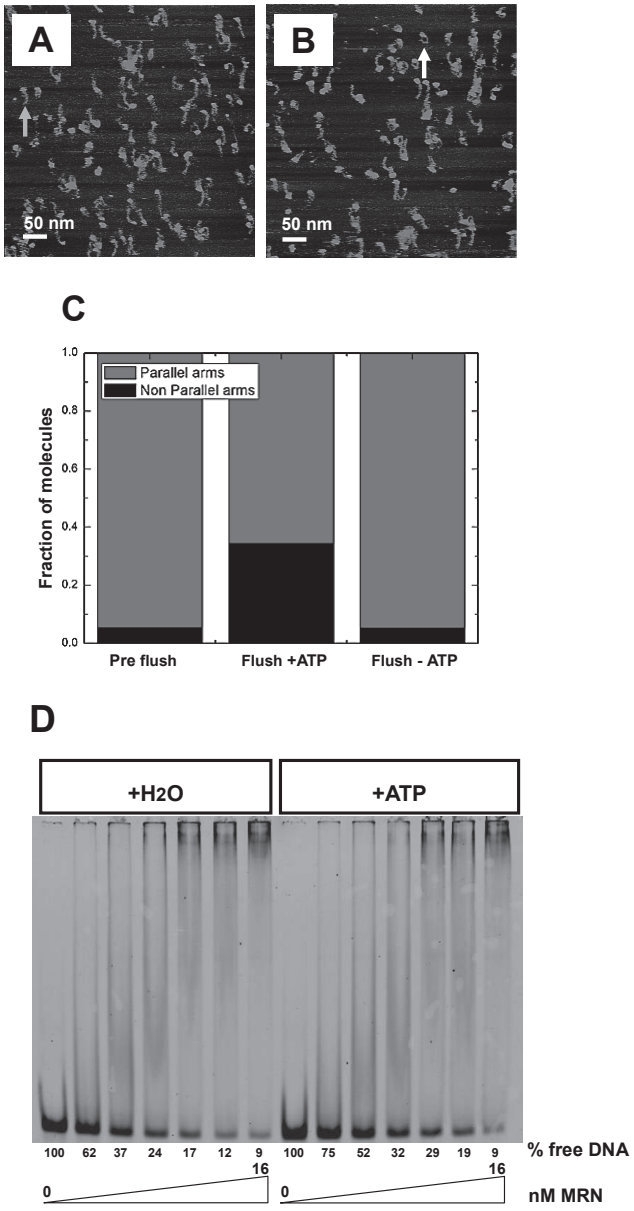

Figure 4. ATP stimulates coiled-coil rearrangements causing DNA release. (A and B) Representative SFM images of MR complexes in buffer; (A) without and (B) after addition of 2 mM ATP. Arrows indicate parallel (light gray arrow) and non-parallel coiled coils (white arrow). (C) Quantification of the fraction of MR complexes with parallel or non-parallel coiled coils. Number of MR complexes analyzed for before adding ATP (MR +DNA) = 376; Number of MR complexes analyzed after adding ATP (MR +DNA +ATP) = 198; Number of MR complexes analyzed for mock addition of ATP (MR +DNA) = 625.

we tested DNA binding under similar conditions by EMSA assays to biochemically assess this phenomenon. We used 1 nM 66 bp dsDNA (the concentration is indicated as a molar fragment) with a titration of 0 to 16 nM MRN (the approximate concentration range for 0 to 100% DNA binding) without or with ATP (Figure 4D). The addition of ATP had less effect on MRN release of DNA at protein concentrations at which 80% or more DNA was bound. We deposited the same binding reaction used for EMSA assays, with 4 nM and 16 nM MRN, onto a mica surface and scanned them by SFM in air to visualize the protein-DNA complex (data not shown). At 4 nM the protein was distributed as mainly dimeric and multimeric complexes while at 16 nM there was a clear increase of oligomeric complexes. These results combined indicate that ATP causes a release of DNA observed as a rearrangement of the coiled coils. However, it appears that for complexes formed at higher protein concentrations, this DNA release effect is less prominent and the EMSA assays suggest that MR as oligomers stays bound to DNA even in the presence of ATP.

ATP stimulates MR oligomerization and this affects DNA binding

Our SFM experiments with a relatively low concentration of MR (so that the protein complexes were mainly dimeric) clearly showed rearrangements to the MR coiled coils in the presence of ATP that indicate a DNA release (Figures 4A and 4B). However, in EMSA assays at higher protein concentrations we observed low mobility complexes that did not go away with ATP (Figure 4D). Preliminary SFM experiments indicated that these low mobility complexes observed in electrophoresis gels were most likely DNA bound by oligomeric complexes (data not shown). These results suggest that while ATP binding can cause DNA release from a single MR complex, other conformational changes associated with MR oligomerization also affect important functions such as DNA binding. To investigate whether ATP influenced

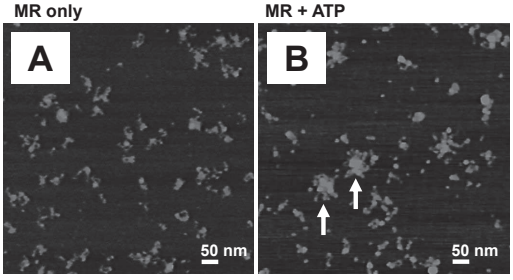

Figure 5. ATP stimulates MR oligomerization. (A and B) Representative SFM images of MR complexes; deposited after incubation (A) without and (B) with 1 mM ATP. Examples of oligomeric complexes are indicated with white arrows.

protein oligomerization, we visualized the proteins in the presence or absence of ATP by SFM (Figure 5A and 5B). The SFM images suggested that ATP stimulated oligomerization (Figure 5B, examples of oligomers are indicated with white arrows). As a preliminary estimate, the number of oligomers (defined as those with at least 8 coiled coils protruding from a central globular accumulation) was counted in a random selection of MR images consisting of 15 fields of 2.5 μm x 2.5 μm each. There were 11 and 24 oligomers present in these images for MR only and MR +ATP conditions, respectively.

Several studies have indicated that RAD50 (or parts of RAD50) have ATP-dependent DNA binding activities (Hopfner et al., 2000a; Raymond & Kleckner, 1993). We also used SFM imaging to study DNA binding with and without ATP, as this assay would enable characterizing MR oligomerization and DNA association via tethering as well as its DNA

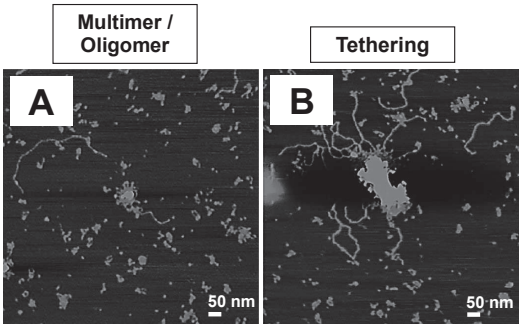

C

	Wild type	Percent (%)
% DNA bound	MR	64
	MR +ATP	73
% Protein-bound DNA bound by oligomers	MR +DNA	8.5
	MR +DNA +ATP	9.7
% Protein-bound DNA in tethering complexes	MR +DNA	6.8
	MR +DNA +ATP	8.6

Figure 6. ATP stimulates oligomeric DNA binding and DNA tethering. (A and B) Representative SFM images (in air) of protein-DNA complexes as indicated. The scale bar is 50 nm. Color represents height from 0 to 3 nm (dark to light). (C) A table summarizing the DNA binding properties of MR without and in the presence of ATP. Number of DNA molecules analyzed for MR +DNA = 184; Number of DNA molecules analyzed for MR +DNA +ATP = 239.

binding behavior. As expected, we observed oligomeric MR binding to DNA (Figure 6A) as well as DNA tethering complexes involving multiple DNA molecules (Figure 6B) similar to our previous studies (de Jager et al., 2001; de Jager et al., 2002; van der Linden et al., 2009). Interestingly, the presence of ATP increased the percentage of DNA bound by protein from 64% to 73%. Focusing solely on MR-bound DNA, the percentage of oligomeric MR bound to DNA increased from 8.5% to 9.7% and the percentage of MR-bound DNA involved in DNA tethering complexes increased from 6.8% to 8.6% in the presence of ATP (See Table in Figure 6C for an overview). Although these results are preliminary, based on the total number of molecules observed, the trend indicates that ATP-stimulated oligomerization, which in turn contributed to increased DNA binding and tethering. This suggestion will be the subject of further more extensive investigation.

DISCUSSION

The human Mre11-Rad50 (MR) complex is essential for various functions in DNA metabolism. This protein complex is evolutionarily conserved and functions in various aspects of genome metabolism involving DNA processing. This study characterized the DNA binding properties of human MR with both long and short DNA substrates. We observed that MR bound preferentially to ssDNA over dsDNA, regardless of the substrate length (Figures 3C and 3D). This observation is consistent with the importance of DNA flexibility in binding to Mre11 predicted from models based on X-ray crystallography. Crystal structures from *P. furiosus* Mre11 revealed an electropositive L-shaped DNA binding groove with two manganese ions at the nuclease active site. Modeling of DNA substrates into this L-shaped groove suggests that dsDNA substrates need to be rotated to position the phosphodiester backbone of the DNA close to the active site metal ions. In contrast, ssDNA, which is more flexible compared to dsDNA, could be positioned in close vicinity to the metal ions (Hopfner et al., 2001). A more recent study showed that different DNA structures bound in different ways to the Mre11 dimer (Williams et al., 2008) suggesting that blunt DNAs could be aligned when bound and that forked DNA would be positioned for nucleolytic processing of one strand. The existence of two DNA bound forms suggests others may be possible. Variation in the Mre11 dimer in the MR complex has been reported by both Lammens et al. (2011) and Lim et al. (2011) that could create different DNA interactions and control nuclease activity.

ATP binding causes large conformational rearrangements of the component proteins relative to each other in MR (Lammens et al., 2011; Lim et al., 2011; Williams et al., 2011). Our SFM studies showing return of the coiled coils to a conformation characteristic of the non-DNA bound form indicate that ATP induces DNA release from single MR complexes (Figures 4A, 4B and 4C). SFM of protein alone and protein bound to longer DNA revealed

increased protein oligomerization in the presence of ATP (Compare Figure 5A and 5B). ATP binding to Rad50 reorganizes the arrangement of Rad50 and Mre11 so that the ATP-bound Rad50 dimer physically blocks the Mre11 DNA binding sites. This reorganization is consistent with the differences observed in Mre11 nuclease activities on ssDNA in the presence and absence of ATP (Paull et al., 1999; Truijllo et al., 1998). Namely, the ATP-free and ATP-bound form of MR would have different accessibilities to the DNA binding sites of Mre11 that may contribute to differences in nuclease activities. Our data additionally suggest that MR oligomers have different or additional DNA binding sites that are still accessible in the presence of ATP.

The effect of ATP on MR interaction with DNA may be complex as multiple protein-protein and protein-DNA interfaces are involved. The MR globular domains can rearrange upon ATP binding. In the compact, ATP-bound "closed" conformation the Rad50 ATPase domain interface is engaged within the same complex and the accessibility of the Mre11 nuclease sites, an interface with DNA, is changed. It is possible that additional interfaces are exposed or created that would account for the changes we observe. ATP binding, for example, may create or expose a proposed DNA binding site on Rad50. The ATP-bound "closed" conformation may also expose interfaces that promote MR complex oligomerization. Oligomerization of MR bound to DNA is a feature that we have observed by SFM and correlates with important biochemical functions such as DNA binding and DNA tethering.

The effect of ATP on the interaction between MR and DNA is relatively subtle (See summary table in Figure 6C). The fact that MR-DNA complexes observed in SFM assays are not observed in EMSA assays at lower protein concentrations suggest that the interaction between MR and DNA and the intercomplex interactions between MR complexes are relatively weak or dynamic. This point is further supported by the fact that MR-DNA complexes are difficult to visualize in EMSAs and they are only prominent at relatively higher protein concentrations. The flexibility of the coiled coils also suggests that inter-complex coiled-coil interactions are dynamic. Interestingly, protein crosslinking between Rad50 domains indicate that ATP binding stabilizes the "closed" state of Rad50, however the crosslinking reaction was not overly efficient (Lammens et al., 2011). This may indicate that the Rad50 ATPase interface is dynamic and/or has variable conformations that make it difficult for the crosslinking reaction to be completed. In support of this possibility, SAXS analysis similarly indicated that ATPγS promotes the "closed" more compact conformation of the MR globular domains but a substantial amount of the population still had the "open" less compact conformation (Lammens et al., 2011). Recent SFM analysis in our lab using an MR(S1202R) mutant which does not bind ATP has shown that this mutant does not show ATP-dependent oligomerization

(Unpublished data from M. Grosbart). Additionally, the MR(E1232Q) mutant, which binds but does not hydrolyze ATP, also did not show ATP-dependent oligomerization (Unpublished data from M. Grosbart). However, this non-hydrolyzing mutant had an increased population of dimers with closed coiled coils. These results suggest that ATP-induced conformational changes in MR may involve two steps, requiring both the ATP binding and hydrolysis. We propose that ATP triggers MR oligomerization due to conformational changes to the globular head domain which together stimulates increased DNA binding and DNA tethering. The first step triggered by ATP binding may regulate the conformation of the globular head domain. The second step regulated by ATP hydrolysis may create or reveal an interface that is responsible for inter-complex interactions. The recent structural studies have used MR complexes with shortened or truncated coiled coils and currently there is no data regarding the effect of the conformational changes of the coiled-coils apex in relation to the whole protein complex. The fact that mutating the conserved second cysteine, in the CxxC motif, to glycine in the coiled-coils apex disrupted Mre11 and Rad50 interactions (Hopfner et al., 2002) also suggests the overall complex architecture is affected by the arrangement of the coiled coils, possibly including interaction between the apexes, although there is a possibility that the CxxC mutation might have resulted in misfolded, thus unstable complexes. Evidence suggests, however, that the zinc hook motif apparently has an important role in maintaining structural integrity and perhaps also regulating functions such DNA binding and tethering (Chapter 4 of this thesis). Whether the interactions between the Rad50 ATPase domains are dynamic and whether varying arrangements exist between these two globular domains remain important features of this multifunctional complex yet to be elucidated.

REFERENCES

de Jager, M., van Noort, J., van Gent, D.C., Dekker, C., Kanaar, R., Wyman, C. (2001). Human Rad50/Mre11 is a flexible complex that can tether DNA ends. Mol Cell *8*, 1129-1135.

de Jager, M., Wyman, C., van Gent, D.C., Kanaar, R. (2002). DNA end-binding specificity of human Rad50/Mre11 is influenced by ATP. Nucleic Acids Res *30*, 4425-4431.

Hopfner, K.P., Karcher, A., Craig, L., Woo, T.T., Carney, J.P., Tainer, J.A. (2001). Structural biochemistry and interaction architecture of the DNA double-strand break repair Mre11 nuclease and Rad50-ATPase. Cell *105*, 473-485.

Hopfner, K.P., Karcher, A., Shin, D., Fairley, C., Tainer, J. A., Carney, J.P. (2000a). Mre11 and Rad50 from *Pyrococcus furiosus*: Cloning and biochemical characterization reveal an evolutionarily conserved multiprotein machine. J Bacteriol *182*, 6036-6041.

Hopfner, K.P., Karcher, A., Shin, D.S. et al. (2000b). Structural biology of Rad50 ATPase: ATP-driven conformational control in DNA double-strand break repair and the ABC ATPase superfamily. Cell *101*, 789-800.

Hopfner, K.P., Craig, L., Moncalian, G. et al. (2002). The Rad50 zinc-hook is a structure joining Mre11 complexes in DNA recombination and repair. Nature *418*, 562-566.

Kinoshita, E., van der Linden, E., Sanchez, H., Wyman, C. (2009). RAD50, an SMC family member with multiple roles in DNA break repair: how does ATP affect function? Chromosome Research *17*, 277-288.

Lamarche, B.J., Orazio, N.I., Weitzman, M.D. (2010). The MRN complex in Double-Strand Break Repair and Telomere Maintenance. FEBS Lett *584(17)*, 3682-3695.

Lammens, K., Bemeleit, D.J., Möckel, C. et al. (2011). The Mre11:Rad50 structure shows an ATP-dependent molecular clamp in DNA double-strand break repair. Cell *145(1)*, 54-66.

Lee, J.H., Ghirlando, R., Bhaskara, V., Hoffmeyer, M.R., Gu, J., Paull, T.T. (2003). Regulation of Mre11/Rad50 by Nbs1: effects on nucleotide-dependent DNA binding and association with ataxia-telangiectasia-like disorder mutant complexes. J Biol Chem *278*, 45171-45181.

Lim, H.S., Kim, J.S., Park, Y.B., Gwon, G.H., Cho, Y. (2011). Crystal structure of the Mre11-Rad50-ATPγS complex: understanding the interplay between Mre11 and Rad50. Genes Dev *25(10)*, 1091-1104.

Luo, G., Yao, M.S., Bender, C.F. et al. (1999). Disruption of mRad50 causes embryonic stem cell lethality, abnormal embryonic development, sensitivity to ionizing radiation. Proc Natl Acad Sci USA *96*, 7376-7381.

Moncalian, G., Lengsfeld, B., Bhaskara, V. et al. (2004). The Rad50 signature motif: essential to ATP binding and biological function. J Mol Biol *335*, 937-951.

Paull, T.T., Gellert, M. (1999). Nbs1 potentiates ATP-driven DNA unwinding and endonuclease cleavage by the Mre11/Rad50 complex. Genes Dev *13*, 1276-1288.

Raymond, W.E., Kleckner, N. (1993). RAD50 protein of *S. cerevisiae* exhibits ATP-dependent DNA binding. Nucleic Acids Res *21*, 3851-3856.

Stracker, T.H., Petrini, J.H. (2011). The MRE11 complex: starting from the ends. Nat Rev Mol Cell Biol *12(2)*, 90-103.

Trujillo, K.M., Yuan, S.S., Lee, E.Y., Sung. P. (1998). Nuclease activities in a complex of human recombination and DNA repair factors Rad50, Mre11, and p95. J Biol Chem *273*, 21447-21450.

van der Linden, E. Sanchez, H., Kinoshita, E., Kanaar, R., Wyman, C. (2009). RAD50 and NBS1 form a stable complex functional in DNA binding and tethering. Nucleic Acids Res *37*, 1580-1588.

Williams, R.S., Moncalian, G., Williams, J.S. et al. (2008). Mre11 dimers coordinate DNA end bridging and nuclease processing in double-strand-break repair. Cell *135(1)*, 97-109.

Williams, G.J, Williams, R.S. Williams, J.S. et al. (2011). ABC ATPase signature helices in Rad50 link nucleotide state to Mre11 interface for DNA repair. Nat Struc Mol Biol *18(4)*, 423-431.

Xiao, Y., Weaver, D.T. (1997). Conditional gene targeted deletion by Cre recombinase demonstrates the requirement for the double-strand break repair Mre11 protein in murine embryonic stem cells. Nucleic Acids Res *25*, 2985-2991.

Zhu, J., Petersen, S., Tessarollo, L., Nussenzweig, A. (2001). Targeted disruption of the Nijmegen breakage syndrome gene NBS1 leads to early embryonic lethality in mice. Curr Biol *11*, 105-109.

ADDENDUM

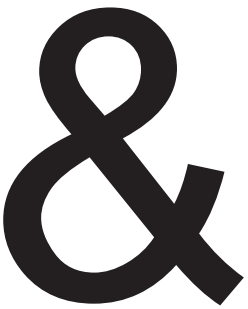

List of abbreviations

Summary

Nederlandse samenvatting

Portfolio

Curriculum vitae

List of publications

LIST OF ABBREVIATIONS

ADP	adenosine 5'-diphosphate
AMP-PNP	adenosine 5'-(β,γ-imido)-triphosphate
AT	ataxia telangiectasia
ATLD	ataxia telangiectasia – like disorder
ATM	ataxia telangiectasia mutated
ATP	adenosine 5'-triphosphate
bp	basepair
CXXC	(cysteine – any amino acid – any amino acid - cysteine)
DNA	deoxyribonucleic acid
DSB	double-strand break
dsDNA	double-stranded DNA
EM	electron microscopy
EMSA	electrophoretic mobility shift assay
HLH	helix-loop-helix
HR	homologous recombination
kb	kilo basepairs (1000 basepairs)
KD	dissociation constant
MR	Mre11-Rad50 protein complex
MRN	Mre11-Rad50-Nbs1protein complex
NBD	nucleotide-binding domain
Nbs1	Nijmegen breakage syndrome protein
NHEJ	nonhomologous end-joining
nt	nucleotide
SAXS	small-angle X-ray scattering
SFM	scanning force microscopy (also called atomic force microscopy)
SMC	structural maintainance of chromosomes
ssDNA	single-stranded DNA

SUMMARY

DNA double-strand breaks (DSBs), which can be caused by both internal and external factors, are a threat to genomic stability. Persistent DSBs can cause cell-cycle checkpoint arrest, ultimately leading to cell death. Improper repair can cause rearrangements in the genome, which in multicellular organisms are a common precursor to cancer. Organisms have, therefore, developed distinct pathways to repair these breaks to avoid losing genetic information. The two main DSB DNA repair mechanisms are non-homologous end-joining (NHEJ) and homologous recombination (HR). The type of repair mechanism utilized depends on the structure of the broken DNA, requiring a set of proteins with specialized functions which repair the broken ends. The Mre11-Rad50-Nbs1 (MRN) complex, the subject of study in this thesis, is an essential component activated early in DSB repair pathways.

Chapter 1 describes the mechanism of non-homologous end joining (NHEJ) and homologous recombination (HR). It also defines the known functions of the MRN complex that is involved in several distinct steps in DSB repair. These functions include break recognition, DNA end processing and signalling for cell cycle arrest. All DSB repair functions of MRN involve interactions with DNA that require at least Rad50 and Mre11. The associated Nbs1 (also known as nibrin) or Xrs2 proteins (MRN or MRX complexes), in mammalian and yeast cells, respectively, link the Mre11-Rad50 complex to cell-cycle checkpoint activation. The chapter further discusses the ATP-dependent activities of the protein complex as well as an update on the structure recently revealed by X-ray crystallography and SAXS analysis.

Chapter 2 investigates the biochemical activities of human RAD50 alone. While there are various studies on the ATP-dependent activities of MRN (as summarized in Chapter 1), there was limited information regarding the biochemistry of only Rad50. Only one study showed that the full-length Rad50 from *S. cerevisiae* had ATP-dependent DNA binding activities. The results in this thesis chapter indicate that human RAD50 binds ATP, undergoes ATP-dependent conformational changes as well as having ATPase activities. Interestingly, neither human RAD50 nor MRE11 alone can make DNA tethers, a well-established mechanistic function of this protein complex. This suggests that MRE11 plays a role in maintaining the structure of the protein complex and participates in reinforcing proper alignment of the coiled coils in the ATP-bound state.

Chapter 3 focuses on the varying stable complexes formed by different combinations of MRE11, RAD50 and NBS1. Previous studies by SFM showed that the MR complex did not require Nbs1 to make a functional complex. The MR complex has been shown to bind

to various DNA substrates and promote DNA tethering. The present study succeeded in purifying stable MR, MRN and RN complexes, all of which maintain known functions such as DNA binding and DNA tethering. While it is well established that MRE11 is a DNA binding protein, the results from this chapter suggests that its presence is not strictly required for DNA binding activities of the protein complex. Purified RN complexes, in fact, show increased DNA binding and DNA tethering activities compared to MR and MRN complexes. SFM-based volume analysis of the purified complexes suggests that the individual subunits can form different stable complexes with varying stoichiometries which may be relevant in defining the functions of this versatile protein machinery.

Chapter 4 focuses on understanding the relationship between arrangement of proteins in the complex and function (i.e. DNA binding and DNA tethering). The combination of techniques such as electron microscopy (EM), scanning force microscopy (SFM), X-ray crystallography as well as SAXS analysis have shown that the basic structure of the Rad50 complex is a hetero-tetramer with two molecules of Mre11 and two molecules of Rad50 (M2R2). Interestingly, there is evidence that the arrangement of the protein components is important and influence functions such as DNA binding. In this chapter, point mutations disrupting important interfaces such as MRE11 dimerization (L72K), zinc hook dimerization (C2G) and a stable ATP-bound state (L1211W) are compared with the wild-type. These mutants showed altered complex architecture and DNA binding activities compared to the wild-type. The results indicate not only that complex architecture is linked to function but also that the various interfaces in this multifunctional protein complex have specific functional roles controlling MR(N) activity in DSB repair.

Chapter 5 discusses the potential role of the ATPase cycle of the MRN complex in relation to DNA binding and DNA tethering. X-ray crystallography and SAXS analysis suggested that ATP binding is associated with the engaged state of the two RAD50 ATPase domains and ATP hydrolysis is associated with its dissociated state, referred to as “closed” and “open” states, respectively. (Lammens et al., 2011, Lim et al., 2011, Williams et al., 2011). This thesis chapter indicated that while ATP stimulates MR oligomerization, the effect of ATP on DNA binding and tethering activities of MR is relatively subtle. The fact that MR-DNA complexes observed in SFM assays are not observed in EMSA assays at lower protein concentrations suggest that the interaction between MR and DNA and the inter-complex interactions between MR coiled coils are relatively weak or transient. Results from Chapter 4 indicated a link between complex architecture and function but currently the data clarifying the relation between the conformation of the coiled coils and the whole protein complex is limited. Unpublished data from our laboratory (using ATP-binding and ATP-hydrolysis

mutants) indicated that ATP-induced changes in MR may be a two-step process requiring both ATP binding and hydrolysis to trigger conformational changes to the globular head domain and to the coiled coils, respectively.

SAMENVATTING VAN HET PROEFSCHRIFT

Dubbelstrengs breuken (DSB) in het DNA, die veroorzaakt kunnen worden door zowel externe als interne factoren, zijn een gevaar voor genoomstabiliteit. Niet-gerepareerde DSB kunnen leiden tot het stoppen van de celdeling en het afsterven van cellen. Het onjuist repareren van DSB kan leiden tot veranderingen in het genoom, wat in meercellige organismen uiteindelijk kan leiden tot het ontstaan van kanker. Organismen hebben daarom reparatiemechanismes ontwikkeld om deze breuken te herstellen om verlies van genetische informatie tegen te gaan. Niet homologe end-joining (NHEJ) en homologe recombinatie (HR) zijn de twee voornaamste mechanismes. Welke route wordt genomen, hangt af van de structuur van het gebroken stuk DNA en vereist een set gespecialiseerde eiwitten om het gebroken eind te repareren. Het Mre11-Rad50-Nbs1 (MRN) complex, het onderwerp van dit proefschrift, is een essentiële component gedurende de eerste stappen in DSB reparatie.

Hoofdstuk 1 beschrijft het mechanisme van NHEJ en HR. Het definieert ook de reeds bekende functies van MRN complex in de verschillende stappen van het DSB herstel mechanisme. Deze functies omvatten onder andere de detectie van de breuk, de resectie van het DNA uiteinde en het signaleren naar het celcyclus apparaat om de celdeling te pauzeren. Bij alle DNA herstel functies van MRN zijn in ieder geval interacties van Rad50 en Mre11 met het DNA nodig. Het Nbs1 (ook bekend als Nibrin) of Xrs2 eiwit (in MRN of MRX complexen) zorgt in zoogdier- en, respectivelijk, gistcellen voor de activatie van de celcyclus controle. Het hoofdstuk beschrijft verder ATP-afhankelijke activiteiten van het eiwitcomplex en bespreekt de recent beschreven kristalstructuur en SAXS (kleine hoekverstrooiing van röntgenstraling) analyses.

Hoofdstuk 2 beschrijft onderzoek naar de biochemische activiteiten van het afzonderlijke RAD50 eiwit. Er zijn meerdere studies gedaan naar de ATP-afhankelijke activiteiten van MRN (zie hoofdstuk 1), maar over de biochemie van RAD50 afzonderlijk is weinig bekend. Slechts één studie liet ATP-afhankelijke DNA-binding zien voor Rad50 uit *S. cerevisiae*. De resultaten in dit hoofdstuk laten zien dat het geïsoleerde RAD50 eiwit ATPase activiteit heeft en bij ATP-binding van conformatie verandert. Interessant genoeg kunnen RAD50 of MRE11 afzonderlijk geen DNA moleculen bij elkaar brengen (tethering), wat wel een belangrijke functie van het eiwit complex is. Dit suggereert dat MRE11 een belangrijke rol speelt in het onderhouden van de structuur van het complex en de juiste houding versterkt van de spiraalvormige “armen” van RAD50 in de ATP-gebonden staat.

Hoofdstuk 3 bespreekt de verschillende stabiele complexen, die gevormd worden door verschillende combinaties van MRE11, RAD50 en NBS1. Eerdere scanning force microscopie (SFM) studies lieten zien dat het MR complex functioneel is zonder NBS1. Het MR complex kan verschillende DNA substraten binden en DNA moleculen bij elkaar brengen. Voor het huidige onderzoek zijn MR, MRN en RN gezuiverd en is vastgesteld dat de basis functies, zoals DNA binding en DNA tethering, functioneel zijn. Terwijl er vastgesteld is dat MRE11 een DNA bindende eiwit is, blijkt uit de resultaten in dit hoofdstuk dat MRE11 niet strikt noodzakelijk is voor DNA binding door het eiwitcomplex. Gezuiverd RN laat zelfs een betere DNA binding en tethering zien dan MR of MRN complexen. Volume analyse van de SFM data suggereert dat de gezuiverde eiwitten stabiele complexen vormen van verschillende stoichiometrie, welke relevant kunnen zijn voor de verschillende functies van dit veelzijdige complex.

Hoofdstuk 4 richt zich op het begrijpen hoe veranderingen in de vorm van het complex de functie beïnvloeden (bij DNA binding en tethering). De combinatie van verschillende technieken, zoals elektronen microscopie, scanning force microscopie, Röntgen diffractie kristallografie en SAXS, laten zien dat de basisstructuur van RAD50 een hetero-tetrameer is met twee MRE11 en twee RAD50 moleculen (M_2R_2). Interessant genoeg is er bewijs dat de vorm van het complex belangrijk en bepalend is voor bepaalde functies zoals DNA binding. Dit hoofdstuk vergelijkt verschillende mutaties in belangrijke gebieden van het complex, zoals MRE11 dimerisatie (L72K), zink haak dimerisatie (C2G) en een stabiele ATP gebonden staat (L1211W), met het normale eiwit. Deze mutanten laten een verandering in de architectuur van het complex en DNA-bindings activiteit zien vergeleken met het normale complex. Deze resultaten bevestigen dat de vorm van het complex de functie beïnvloed, maar ook dat onderlinge contactgebieden tussen de eiwitten in het complex een specifieke rol spelen in de activiteit van MR(N) tijdens DSB reparatie.

Hoofdstuk 5 bespreekt de mogelijke rol van de ATP cyclus van het MRN complex in relatie tot DNA binding en DNA tethering. Röntgen diffractie kristallografie en small-angle X-ray scattering (SAXS) analyse suggereren dat ATP binding zorgt voor een associatie (gesloten staat) en ATP hydrolyse zorgt voor een dissociatie (open staat) van het complex (Lammens et al., 2011, Lim et al., 2011, Williams et al., 2011). Dit hoofdstuk laat zien dat hoewel ATP de vorming van oligomeren stimuleert, het effect op DNA binding en tethering relatief subtiel is. Het feit dat MR-DNA complexen, die we met SFM zien, niet worden waargenomen in een EMSA analyse met lage eiwitconcentratie, geeft aan dat de interactie tussen DNA en MR en tussen de MR complexen onderling, via de spiraalvormige armen, zwak of kortstondig zijn. De resultaten van hoofdstuk 4 laten duidelijk een relatie zien tussen de architectuur van

het MR complex en functies, echter de huidige data kan de relatie tussen de conformatie van de spiraalvormige armen en die van het volledige complex onvoldoende verklaren. Uit nog niet gepubliceerde data uit ons lab (met gebruik van ATP-binding- en ATP-hydrolyse mutanten) zijn er aanwijzingen dat het een twee-staps proces is, waarbij zowel ATP-binding als hydrolyse nodig is om conformatie veranderingen te bewerkstelligen van respectievelijk het bolvormige hoofddomein en van de spiraalvormige armen.

PORTFOLIO

Name:	Eri Kinoshita
PhD period:	March 2008 - September 2012
Erasmus MC Department:	Cell Biology & Genetics
Promoter:	Prof. dr. C. Wyman
Research School:	MGC

Research skills

Safe laboratory techniques (Winter 2009)

Radiation course 5B (Winter 2009)

In-depth courses

Cell and Developmental Biology (CDB) (Spring 2010)

Epigenetic regulation (January 21-22, 2010)

Technology facilities (February 9-11, 2011)

Reading and discussing scientific literature (Winter 2011)

Seminars and workshops

Department weekly work discussion (2008, 2009, 2010, 2011, 2012)

Department journal club (2008, 2009, 2010, 2011, 2012)

Genetics cluster weekly work discussion (2008, 2009, 2010, 2011, 2012)

Medical Genetics Center (MGC) promovendi workshop (2008, 2009, 2010)

The 9th Structural Cell Biology of DNA Repair Machines (SBDR) workshop, Berkeley, CA, USA (March 18-20, 2010)

Conferences

Annual Dutch Meeting on Molecular and Cellular Biophysics, Veldhoven, The Netherlands (2008, 2009, 2010)

NWO-CW meeting in Protein Research, Nucleic Acids and Lipids & Biomembranes, Veldhoven, The Netherlands (2010, 2011)

CURRICULUM VITAE

Personal details

Name:	Eri Kinoshita
Date of birth:	July 7th, 1982
Place of birth:	Kawasaki, Japan

Education

2005 – 2007	Master of Science, specialization in Molecular Plant Biotechnology Leiden University, The Netherlands
2001 - 2005	Bachelor of Arts, interdisciplinary major in Biology and Psychology International Christian University, Mitaka, Japan

Scientific background

2008 – 2012	PhD research in the Department of Cell Biology and Genetics Erasmus MC, Rotterdam, The Netherlands
2006 – 2007	MSc thesis internship in the Department of Biology Leiden University, The Netherlands
2004 – 2005	Bachelor thesis internship National Institute of Agrobiological Sciences, Tsukuba, Japan

LIST OF PUBLICATIONS

Lee, J.H., Mand, M.R., **Kinoshita, E.**, Yang, S.H., Wyman, C., Paull, T.T. (2013). ATM kinase activity is regulated by ATP-driven conformational changes in the MRN complex. The Journal of Biological Chemistry *288(18)*, 12840-12851.

Nimonkar, A.V., Genschel, J., **Kinoshita, E.**, Polaczek, P., Campbell, J.L., Wyman, C., Modrich, P., Kowalczykowski, S.C. (2011). BLM-DNA2-RPA-MRN and EXO1-BLM-RPA-MRN constitute two DNA end resection machineries for human DNA break repair. Genes & Development *25(4)*, 350-362.

Kinoshita, E., van der Linden, E., Sanchez, H., Wyman, C. (2009). Rad50, an SMC family member with multiple roles in DNA break repair: how does ATP affect function? Chromosome Research *17(2)*, 277-288.

van der Linden, E., Sanchez, H**., Kinoshita, E.**, Kanaar, R., Wyman, C. (2009). RAD50 and NBS1 form a stable complex functional in DNA binding and tethering. Nucleic Acids Research *37(5)*, 1580-1588.

Kumagai, K., **Kinoshita, E.**, Ridge, R.W., Kouchi, H. (2006). RNAi knockdown of ENOD40s leads to significant suppression of nodule formation in *Lotus japonicus*. Plant and Cell Physiology *47*, 1102-1111.